



Fuel Cell Auxiliary Power Study

Volume 1: RASER Task Order 5

*Audie Mak and John Meier
Honeywell Engines, Systems & Services, Phoenix, Arizona*

NASA STI Program . . . in Profile

Since its founding, NASA has been dedicated to the advancement of aeronautics and space science. The NASA Scientific and Technical Information (STI) program plays a key part in helping NASA maintain this important role.

The NASA STI Program operates under the auspices of the Agency Chief Information Officer. It collects, organizes, provides for archiving, and disseminates NASA's STI. The NASA STI program provides access to the NASA Aeronautics and Space Database and its public interface, the NASA Technical Reports Server, thus providing one of the largest collections of aeronautical and space science STI in the world. Results are published in both non-NASA channels and by NASA in the NASA STI Report Series, which includes the following report types:

- **TECHNICAL PUBLICATION.** Reports of completed research or a major significant phase of research that present the results of NASA programs and include extensive data or theoretical analysis. Includes compilations of significant scientific and technical data and information deemed to be of continuing reference value. NASA counterpart of peer-reviewed formal professional papers but has less stringent limitations on manuscript length and extent of graphic presentations.
- **TECHNICAL MEMORANDUM.** Scientific and technical findings that are preliminary or of specialized interest, e.g., quick release reports, working papers, and bibliographies that contain minimal annotation. Does not contain extensive analysis.
- **CONTRACTOR REPORT.** Scientific and technical findings by NASA-sponsored contractors and grantees.

- **CONFERENCE PUBLICATION.** Collected papers from scientific and technical conferences, symposia, seminars, or other meetings sponsored or cosponsored by NASA.
- **SPECIAL PUBLICATION.** Scientific, technical, or historical information from NASA programs, projects, and missions, often concerned with subjects having substantial public interest.
- **TECHNICAL TRANSLATION.** English-language translations of foreign scientific and technical material pertinent to NASA's mission.

Specialized services also include creating custom thesauri, building customized databases, organizing and publishing research results.

For more information about the NASA STI program, see the following:

- Access the NASA STI program home page at <http://www.sti.nasa.gov>
- E-mail your question via the Internet to help@sti.nasa.gov
- Fax your question to the NASA STI Help Desk at 301-621-0134
- Telephone the NASA STI Help Desk at 301-621-0390
- Write to:
NASA STI Help Desk
NASA Center for AeroSpace Information
7115 Standard Drive
Hanover, MD 21076-1320



Fuel Cell Auxiliary Power Study

Volume 1: RASER Task Order 5

Audie Mak and John Meier
Honeywell Engines, Systems & Services, Phoenix, Arizona

Prepared under Contracts NAS3-01136

National Aeronautics and
Space Administration

Glenn Research Center
Cleveland, Ohio 44135

This report contains preliminary findings,
subject to revision as analysis proceeds.

Trade names and trademarks are used in this report for identification
only. Their usage does not constitute an official endorsement,
either expressed or implied, by the National Aeronautics and
Space Administration.

This work was sponsored by the Fundamental Aeronautics Program
at the NASA Glenn Research Center.

Level of Review: This material has been technically reviewed by NASA technical management.

Available from

NASA Center for Aerospace Information
7115 Standard Drive
Hanover, MD 21076-1320

National Technical Information Service
5285 Port Royal Road
Springfield, VA 22161

Available electronically at <http://gltrs.grc.nasa.gov>

ACKNOWLEDGEMENTS

This study, to evaluate the feasibility of fuel cell auxiliary power for regional jet applications, was sponsored by the NASA Glenn Research Center under RASER Program Task Order No. 5, Amendment No. 3. Several parties and individuals from various agencies have contributed to the results and conclusions of the study, as listed below:

NASA GLENN RESEARCH CENTER – Cleveland, OH

James Walker, PRV
Lisa Kohout, RPC
Serene Farmer, RXC
Josh Freeh, PBP

HONEYWELL INTERNATIONAL, INC.

Air Frame Systems – Des Plaines, IL

Amber Arzadon
Mark Kaiser

Air Frame Systems – Torrance, CA

Joe Borghese
Kathrine Clarke

Engines, Systems & Accessories – Tempe, AZ

Peter Zeiner

Engines, Systems & Services Laboratory – Morristown, NJ

James Guiheen
Steve Sund

Engines, Systems & Services – Propulsion Engineering, Phoenix, AZ

Philip Chow
Jochen Deman
Jerrod Hofferth
Fred Klaass
Terrel Kuhn
Audie Mak, Project Engineer
Ray McGinley
John Meier, Program Manager
Jack Rowse
Jeff Turner

NATIONAL FUEL CELL RESEARCH CENTER (NFCRC) – U. of California – Irvine, Irvine, CA

Jack Brouwer

PHOENIX ANALYSIS AND DESIGN TECHNOLOGIES (PADT) – Phoenix, AZ

Steve Beekman
Dan McGuinness

PRECISION COMBUSTION, INC. (PCI) – North Haven, CT

Subir Roychoudhury

EXECUTIVE SUMMARY AND CONCLUSION

EXECUTIVE SUMMARY

This study, sponsored by the National Aeronautics and Space Administration Glenn Research Center (NASA–GRC), Cleveland, OH under the Revolutionary AeroSpace Engine Research (RASER) Program Task Order 5 (Contract No. NAS3-01136) evaluated the feasibility of a hybrid solid oxide fuel cell (SOFC) auxiliary power unit (APU) and the impact in a 90-passenger More-Electric Regional Jet application. The study established realistic hybrid SOFC APU system weight and system efficiencies, and evaluated the impact on the aircraft total weight, fuel burn, and emissions from the main engine and the APU during cruise, landing and take-off (LTO) cycle, and at the gate.

A range of SOFC system power outputs between 116 to 185 kW has been established to meet the aircraft minimum and maximum power requirements on the ground and at cruise. Electric power output from the SOFC system is supplied from the SOFC stack and turbogenerator to the aircraft electrical bus, and estimated power included losses from the DC/DC converter and rectifier.

The study projects the use of year 2010 – 2015 SOFC stack technology with assumed power densities of 0.56/1.0/1.4 kW/kg, consistent with future technology assessed by the National Fuel Cell Research Center (NFCRC) and NASA GRC. A 70 percent SOFC stack fuel utilization based on hydrogen (H₂) and carbon monoxide (CO) input into the stack anode was used in the study for reduced system weight. A comparison to an increase in fuel utilization to 0.85 is also presented for a case study in Appendix A.

The Balance-Of-Plant estimates in this study employed realistic technology, including auto-thermal jet fuel reformer with anode re-circulation, a catalytic combustor for burning off excessive H₂ and CO exiting the stack, a motor-assisted turbocompressor capable of ground and cruise altitude operation, a heat exchanger for energy recuperation and temperature control, and a DC/DC converter and rectifier for stable electric supply.

Inlet losses were included in determining the SOFC system cycle efficiencies. Available SOFC system exhaust thrust was not included in the system efficiency, but is accounted for in the aircraft fuel burn calculation. The study compared both ambient and cabin air for the air supply to the SOFC system.

The results of the study show that, although the use of cabin air has higher system efficiency, the aircraft fuel burn calculation shows practically the same results with ~0.2 percent delta, favoring the use of ambient air when accounting for total aircraft exhaust thrust. This is due to the additional ambient ram air supplied to the SOFC system, which is then compressed, heated, and expanded before exiting the aircraft as SOFC thrust, along with the cabin air exhaust thrust.

Weight

- SOFC APU Weights: ~487 to 1,151 lb (~2.0X to 4.5X weight of baseline model conventional APU), depending on the duty cycle and stack power density

Efficiency

- SOFC APU Cruise System Efficiency: ~45 to 48% (Competitive with the main engine bleed and extraction)
- SOFC APU Ground System Efficiency: ~32 to 36% (Improvement compared to the baseline conventional APU system efficiency of ~9 to 13%)
- Increase in SOFC stack fuel utilization from 0.70 to 0.85 could increase the SOFC APU system efficiency by ~2 to 3%, but would also increase the SOFC APU system weight by ~3 to 6%, depending on the stack power density. The impact on the aircraft total fuel burn is expected to be similar.

Fuel Burn

- SOFC APU In-Flight Fuel Burn Reduction: ~0.4 to 1.6% (24 to 235 lb) of total aircraft fuel burn (5,594 to 14,380 lb) depending on design and mission range of 500/1,000/1,500 nmi
- SOFC APU Ground Fuel Burn Reduction: ~66 to 78% (184 to 174 lb) over baseline conventional APU (278 to 224 lb) on ground, depending on operation limited by SOFC thermal fatigue characteristic
- SOFC APU Total Fuel Burn Reduction: Can be up to ~3% (420 lb out of 14,380 lb) of total aircraft fuel burn per mission, including both air and ground operation.

Emissions

- SOFC APU Cruise NO_x Reduction: Similar to cruise fuel burn reduction, which is ~0.4 to 1.6% (<1.0 kg out of 65 kg) depending on the mission range. In-flight CO impact is ±0.3% (<0.01 kg out of 4 kg)
- SOFC APU Landing and Takeoff (LTO, excluding terminal gate operation) NO_x Impact: ±3% (<0.15 kg out of 4.92 kg). LTO CO reduction is ~53% (~0.36 kg out of 0.67 kg)
- SOFC APU has 100% NO_x reduction (0.9 kg) and possible 92% CO reduction (0.7 kg) over the baseline conventional APU at the gate, depending on operation limited by SOFC stack thermal fatigue characteristic.
- SOFC Landing and Take-Off Cycle, including 60 minutes of terminal gate operation can have possible 15% NO_x reduction (4.79 kg out of 5.64 kg), and 72% CO reduction (0.35 kg out of 1.29 kg).

CONCLUSION

Although the SOFC APU may be heavier than the current conventional APU, its weight disadvantage can be offset by fuel savings in the higher SOFC APU system efficiencies against the main engine bleed and extraction during cruise. The higher SOFC APU system efficiency compared to the conventional APU on the ground can also provide considerable fuel saving and emissions reduction, particularly at the gate, but is limited by the fuel cell stack thermal fatigue characteristic.

TABLE OF CONTENTS

	<u>Page</u>
ACKNOWLEDGEMENTS.....	v
EXECUTIVE SUMMARY AND CONCLUSION.....	vi
1. INTRODUCTION.....	1
1.1 Study Objectives.....	1
2. TECHNICAL SUMMARY.....	2
2.1 Part I – Power Definition and Characterization of Aircraft Systems.....	3
2.1.1 Task 1.1 – Aircraft Power Definition and Characterization.....	3
2.2 Part II – Fuel Cell Power System.....	11
2.2.1 Task 2.1 – Estimation of Current and Future Fuel Cell Performance.....	11
2.2.2 Task 2.2 – Applicability of Fuel Cell Power System.....	18
2.2.3 SOFC APU Component Descriptions.....	18
2.2.4 Heat Exchangers.....	19
2.2.5 Hydrocarbon Fuel Processing – Desulfurization And Reformation.....	20
2.3 Additional Fuel Cell APU Components – Descriptions.....	32
2.3.1 DC/DC Converter.....	32
2.3.2 Turbine.....	32
2.3.3 Generator/Rectifier/Bearings.....	33
2.4 Task 2.3 – Fuel Cell Power System Architecture Concepts.....	33
2.4.1 SOFC APU System Architecture.....	33
2.4.2 SOFC APU System Modeling.....	36
2.5 SOFC APU System Performance.....	43
2.5.1 SOFC APU System Power, Efficiency, Mass, Power, and Energy Density.....	77
2.6 Task 2.4 – Evaluation of Fuel Cell Powered Architecture.....	87
2.6.1 Aircraft Value Function/Index Evaluation.....	87
2.6.2 Aircraft Fuel Burn Analysis.....	88
2.6.3 Aircraft Emissions Analysis.....	92
2.7 Task 2.5 – Identification of Technology Gaps.....	96
2.7.1 Desulfurization.....	96
2.7.2 Reformer Technology.....	98
2.7.3 Effects of Aircraft Attitude.....	98
2.7.4 Combustion System Technology.....	98
2.7.5 Water Management and Utilization.....	99
2.7.6 Stack Materials and Architectures.....	100
2.7.7 Air Management System Technology.....	102
2.7.8 SOFC Technology Gaps and Road Map.....	103
APPENDIX A.....	105
SOFC APU CASE STUDY WITH INCREASED STACK FUEL UTILIZATION.....	105
ACRONYMS AND ABBREVIATIONS.....	109
REFERENCES.....	115

LIST OF FIGURES

	<u>Page</u>
Figure 1. Sample Mission Profile.	7
Figure 2. Sulfur Removal Systems For Aerospace Fuel Cell Applications.....	23
Figure 3. Reformer Gas Composition.....	27
Figure 4. Flowchart of Reformer Algorithm.....	28
Figure 5. SOFC APU System Architecture – Option 1.....	33
Figure 6. SOFC APU System Architecture – Option 2.....	34
Figure 7. SOFC APU System Architecture – Option 3.....	34
Figure 8. Consolidated SOFC APU System Architecture.....	35
Figure 9. SOFC APU Model Sample Main Cycle Sheet.....	40
Figure 10. Sample SOFC APU System Schematic with Component Output Data.....	41
Figure 11. Sample SOFC Stack and Reformer Schematic.....	42
Figure 12. SOFC Stack Performance On Ground Versus In-Flight Cruise.....	45
Figure 13. SOFC APU System 1, Case 1(a) Performance Results.....	48
Figure 14. SOFC APU System 1, Case 1(b) Performance Results.....	49
Figure 15. SOFC APU System 1, Case 1(c) Performance Results.....	50
Figure 16. SOFC APU System 1, Case 1(d) Performance Results.....	51
Figure 17. SOFC APU System 1, Case 2(a) Performance Results.....	53
Figure 18. SOFC APU System 1, Case 2(b) Performance Results.....	54
Figure 19. SOFC APU System 1, Case 2(c) Performance Results.....	55
Figure 20. SOFC APU System 2, Case 3(a) Performance Results.....	57
Figure 21. SOFC APU System 2, Case 3(b) Performance Results.....	58
Figure 22. SOFC APU System 2, Case 3(c) Performance Results.....	59
Figure 23. SOFC APU System 2, Case 3(d) Performance Results.....	60
Figure 24. SOFC APU System 2, Case 4(a) Performance Results.....	62
Figure 25. SOFC APU System 2, Case 4(b) Performance Results.....	63
Figure 26. SOFC APU System 2, Case 4(c) Performance Results.....	64
Figure 27. SOFC APU System 1, Case 5(a) Performance Results.....	66
Figure 28. SOFC APU System 1, Case 5(b) Performance Results.....	67
Figure 29. SOFC APU System 1, Case 6(a) Performance Results.....	69
Figure 30. SOFC APU System 1, Case 6(b) Performance Results.....	70
Figure 31. SOFC APU System 1, Case 6(c) Performance Results.....	71
Figure 32. SOFC APU System 1, Case 6(d) Performance Results.....	72
Figure 33. SOFC APU System 1, Case 7(a) Performance Results.....	74
Figure 34. SOFC APU System 1, Case 7(b) Performance Results.....	75
Figure 35. SOFC APU System 1, Case 7(c) Performance Results.....	76
Figure 36. Sample SOFC APU Model Incorporating Estimated Mass and Volume Values.....	78
Figure 37. Value Index Calculator (Excel Spreadsheet).....	87
Figure 38. Regional Jet Mission Profile for Fuel Burn Evaluation.....	89
Figure 39. SOFC Performance Schematic with 0.85 Stack Fuel Utilization (System 1, Case 2b).....	105

LIST OF TABLES

	<u>Page</u>
Table 1. Regional Jet 90-PAX Mission Summary.....	3
Table 2. Estimated Regional Jet Mission Load Profile.....	4
Table 3. SOFC Stack Output Parameters.....	18
Table 4. Comparison of Sulfur Removal Processes.....	21
Table 5. Fuel Reforming Process Comparison.....	25
Table 6. Catalytic Combustor Characteristics.....	32
Table 7. SOFC Stack Characteristics.....	37
Table 8. Reformer Characteristics.....	38
Table 9. Catalytic Combustor Characteristics.....	38
Table 10. Heat Exchanger Characteristics.....	38
Table 11. Turbomachinery Characteristics.....	38
Table 12. Electrical Components and Other Characteristics.....	38
Table 13. SOFC APU Model Input Parameters.....	39
Table 14. SOFC APU Model Output Parameters.....	39
Table 15. Sample SOFC APU Component Output Data Tabulation.....	42
Table 16. Sample SOFC APU System Performance Output Data Tabulation.....	43
Table 17. Summary of SOFC APU System Case Studies.....	44
Table 18. Summary of SOFC APU Performance Model Cases and Output Data.....	46
Table 19. SOFC APU System 1, Case 1 Performance Results Summary.....	47
Table 20. SOFC APU System 1, Case 2 Performance Results Summary.....	52
Table 21. SOFC APU System 2, Case 3 Performance Summary.....	56
Table 22. SOFC APU System 2, Case 4 Performance Summary.....	61
Table 23. SOFC APU System 1, Case 5 Performance Summary.....	65
Table 24. SOFC APU System 1, Case 6 Performance Summary.....	68
Table 25. SOFC APU System 1, Case 7 Performance Summary.....	73
Table 26. Estimated SOFC APU System and Component Weight Distribution.....	78
Table 27. Estimated SOFC APU System Mass, Power, and System Efficiency.....	79
Table 28. Power Density Comparison of Baseline Gas Turbine APU Vs. SOFC APU.....	79
Table 29. Estimated SOFC Stack/APU System Characteristics (Cases 1, 2, 5, 6, and 7 – Ambient Air).....	80
Table 30. SOFC Stack/APU System Characteristics (Cases 3 and 4 – Cabin Air).....	80
Table 31. SOFC APU Performance Summary. (System 1, Case 1 – Ambient Air).....	81
Table 32. SOFC APU Performance Summary. (System 1, Case 2 – Ambient Air).....	82
Table 33. SOFC APU Performance Summary. (System 2, Case 3 – Cabin Air).....	83
Table 34. SOFC APU Performance Summary. (System 2, Case 4 – Cabin Air).....	84
Table 35. SOFC APU Performance Summary. (System 1, Case 5 – Ambient Air).....	85
Table 36. SOFC APU Performance Summary. (System 1, Cases 6 and 7 – Ambient Air).....	86
Table 37. Aircraft TOGW-Based Value Index.....	88
Table 38. SOFC APU System Estimated Weight Summary.....	89
Table 39. SOFC APU Fuel Burn Comparison With Baseline Main Engine (Without SOFC Weight Impact).....	90
Table 40. SOFC APU Cruise Fuel Burn Summary (With SOFC Weight Impact).....	91

LIST OF TABLES (Contd)

	<u>Page</u>
Table 41. SOFC APU Versus Baseline Gas Turbine APU Ground/Gate Fuel Burn Comparison.	92
Table 42. Estimated Emissions.	93
Table 43. Estimated SOFC APU Cruise Emissions.....	93
Table 44. Landing and Takeoff (LTO) Cycle (EPA Definition).	94
Table 45. SOFC APU LTO Cycle Emissions Calculations (Gate Operation Excluded).....	94
Table 46. SOFC APU On-Ground/Gate Emissions Calculations.....	95
Table 47. Landing and Takeoff (LTO) Cycle Emissions Including 60 Minutes Gate Operation.	96
Table 48. SOFC Technology Gaps and Technology Road Map.	103
Table 49. SOFC Mass and Volume With 0.85 Fuel Utilization for System 1, Case 2b.....	106
Table 50. SOFC APU System Performance Comparison, 0.70 vs. 0.85 Fuel Utilization.	107
Table 51. SOFC APU System Weight Comparison, 0.70 vs. 0.85 Fuel Utilization.....	107

**NASA RASER TASK ORDER NO. 5
FUEL CELL AUXILIARY POWER STUDY
FINAL REPORT
(VOLUME I – NON-PROPRIETARY VERSION)**

1. INTRODUCTION

This Final Report, prepared and submitted by Honeywell Engines, Systems & Services (Honeywell) Phoenix, AZ, a unit of Honeywell International Inc. presents the technical results and conclusions in the Fuel Cell Auxiliary Power Study Project, performed under Contract No. NAS3-01136, Task Order No. 5, Amendment No. 3, conducted by Honeywell for the NASA Glenn Research Center (NASA – GRC), Cleveland, OH 44135. This final Report was prepared in accordance with the terms of the Task Order.

Under Task Order 5, Honeywell integrated the efforts of the team members from three Honeywell Aerospace Enterprises under Honeywell Engines, Systems & Services (ES&S) Business Unit:

- Propulsion Systems Enterprise (PSE)
- Airframe Systems (AFS)
- Engine Systems & Accessories (ESA)

This team was supported by two Honeywell Laboratories, located in Morristown, NJ and Des Plaines, IL. Aircraft characteristics and power requirement were established utilizing limited support from a regional jet aircraft original equipment manufacturer (OEM). Honeywell worked with the National Fuel Cell Research Center (NFCRC) at the University of California in Irvine in establishing the Solid Oxide Fuel Cell (SOFC) stack characteristics, and with Phoenix Analysis and Design Technologies (PADT), Phoenix, AZ in creating the SOFC auxiliary power unit (APU) systems architecture and performance modeling with balance-of-plant components. The SOFC system was integrated into the aircraft system for impact analysis on weight, efficiency, fuel burn and emissions.

1.1 Study Objectives

The original study objective was to evaluate airborne applications in both inhabited and uninhabited aircraft for power generation devices; and initially addressed three aircraft systems: Uninhabited Air Vehicle (UAV), Regional Jet, and Commercial Air Transport. In addition, both Proton Exchange Membrane (PEM) and Solid Oxide (SOFC) fuel cells were considered. However, early in the study, NASA decided to focus on one application, namely, the Regional Jet. Thus, the refined objective of this study was to evaluate the feasibility of a SOFC Auxiliary Power Unit (APU) for Regional Jet applications, and the impact of its weight and efficiency on the aircraft mission fuel burn and emissions. The study was divided into two main parts:

Part I – Power Definition and Characterization for Aircraft System, including evaluation of performance and identification of enabling technologies for more-electric aircraft (MEA) architecture.

Part II – Fuel Cell Power System (Up to 180 kW) Study to include estimation of current and future fuel cell performance, generation of fuel cell power system concepts, fuel cell power system integration into a Regional Jet aircraft, evaluation of performance of the system(s), and identification of enabling technologies.

2. TECHNICAL SUMMARY

This technical summary covers information and results from Part I/Task 1.1 and Part II/Tasks 2.1, 2.2, 2.3, 2.4, and 2.5.

Part II/Task 1.1 established the baseline aircraft characteristics and mission load profiles for a Regional Jet. Information on a representative Regional Jet was established, incorporating “More-Electric-Aircraft” (MEA) architecture. The Value Function characterizing Take-Off Gross Weight (TOGW) has also been established.

Part II/Task 2.1 established current and future performance/characteristics of a typical SOFC stack for Regional Jet ground and altitude cruise conditions, including power density, specific power, fuel efficiency, input/output constituencies, start-up and transient response time, weight, and size. A computer model for the SOFC was created, and was integrated with balance-of-plant components for system level modeling. Stack weight, size, start-up and response was projected based upon future year 2015 capability.

Part II/Task 2.2 assessed the balance-of-plant requirement for the SOFC APU. Sizing of the fuel cell stack, fuel process system, air handling system, as well as thermal management systems were identified and integrated into a conceptual fuel cell power system. The fuel process system was established using on-ground desulfurization and on-board reformation. Turbocompressor characteristics were scaled and integrated into the air handling system. Heat exchangers were modified and sized for the thermal management system. Component sizing and system integration was established.

Part II/Task 2.3 generated the SOFC APU architecture and cycle performance, based on the Regional Jet mission load profile established in Part I/Task 1.1.

Part II/Task 2.4 evaluated the impact of the SOFC APU weight and system efficiencies on the Regional Jet aircraft weight, mission fuel burn, and emissions during the Cruise, Landing and Take-Off (LTO) cycle, and during on-ground operations at the terminal.

Part II/Task 2.5 identified the technology gap(s) for an SOFC APU in Regional Jet application and outlines potential research and development options in mitigating requirements for future operations.

2.1 Part I – Power Definition and Characterization of Aircraft Systems

During Part I, the baseline aircraft characteristics, mission, pneumatic and electric load profile required for SOFC APU sizing and for aircraft fuel burn / emissions analysis were established.

2.1.1 Task 1.1 – Aircraft Power Definition and Characterization

The Regional Jet characteristics and mission load profile are discussed in this section.

2.1.1.1 Regional Jet Characteristics

Table 1 lists the initial data and information Honeywell developed that was representative of a typical 90-passenger (90-PAX) Regional Jet design and mission.

Table 1. Regional Jet 90-PAX Mission Summary.

	Time (min)	Powerset	Altitude	Velocity	Distance (nmi)	Fuel Burn (lbs)																																																	
Startup, Warmup, Taxi	10	idle	0	0	0	304																																																	
Takeoff	1	TKO	0	0	0	203																																																	
Climb	19	MCL	0 - 35Kft	250 KCAS	125	2179																																																	
Cruise	175	as req'd	35Kft	0.77 Mn	1290	10951																																																	
Descent	23	as req'd	35Kft - 0	350 KTAS	134	710																																																	
Reserve Climb	6	MCL	0 - 20Kft	250 KCAS	38	947																																																	
Reserve Cruise	9	as req'd	20Kft	0.70 Mn	62	621																																																	
Reserve Descent	20	as req'd	20Kft - 0	300 KTAS	100	730																																																	
Reserve Loiter	30	as req'd	5Kft	210 KTAS	n/a	1412																																																	
Land, Taxi, Shutdown	10	idle	0	0	0	312																																																	
<table> <tr> <td>TOGW</td> <td colspan="6">80,500 lbs.</td> </tr> <tr> <td>OWE</td> <td colspan="6">47,500 lbs.</td> </tr> <tr> <td>Payload (86 pax)</td> <td colspan="6">14,620 lbs.</td> </tr> <tr> <td>Fuel</td> <td colspan="6">18369</td> </tr> <tr> <td>Block Dist.</td> <td colspan="3">1549 Nmi.</td> <td>BFL</td> <td colspan="2">6,111 ft</td> </tr> <tr> <td>Block Fuel</td> <td colspan="3">15166 lbs.</td> <td>Decision Speed</td> <td colspan="2">133 KTAS</td> </tr> <tr> <td>Block Time</td> <td colspan="3">3:58 Hrs:Min</td> <td>Decision Point</td> <td colspan="2">3,535 ft</td> </tr> </table>							TOGW	80,500 lbs.						OWE	47,500 lbs.						Payload (86 pax)	14,620 lbs.						Fuel	18369						Block Dist.	1549 Nmi.			BFL	6,111 ft		Block Fuel	15166 lbs.			Decision Speed	133 KTAS		Block Time	3:58 Hrs:Min			Decision Point	3,535 ft	
TOGW	80,500 lbs.																																																						
OWE	47,500 lbs.																																																						
Payload (86 pax)	14,620 lbs.																																																						
Fuel	18369																																																						
Block Dist.	1549 Nmi.			BFL	6,111 ft																																																		
Block Fuel	15166 lbs.			Decision Speed	133 KTAS																																																		
Block Time	3:58 Hrs:Min			Decision Point	3,535 ft																																																		

Table 2 represents an estimated Regional Jet mission load profile, based on More-Electric Aircraft (MEA) architecture. The Fuel Cell APU vs. main engine generator power split was determined as follows:

- Solid Oxide Fuel Cell (SOFC) APU power
 - Ground Load
 - Main Engine Start (MES)
 - In-Flight Environmental Control System (ECS), wing de-ice, and one-engine-out back-up power
- Main Engine Generator Power
 - On-Board Inert Gas Generator (OBIGG)
 - Fuel Tank Pump
 - Flight Controls
 - Non-Essential Loads
 - Essential (ESS) Loads
 - Galley
 - Electric Motor Pump (EMP)

In addition to the power splits shown in Table 2, the study also considered having the SOFC APU handle the total auxiliary power on ground and during Cruise.

Table 2. Estimated Regional Jet Mission Load Profile.

	Flight Segment	ECS CACTCS	OBIGGS	FUEL PUMPS	FLIGHT CONTROL	28VDC ESSL	28VDC non-ESSL	115VAC ESSL	115VAC non-ESSL	GALLEY	EMP	WING DE-ICE	ENGINE START	FCAPU POWER	Engine Generator	Duration minutes
Ground Op	Gate APU Loading	63.86	0.00	0.00	2.05	0.00	1.33	0.00	21.11	19.10	0.00	0.00	0.00	107.45	0.00	As Req'd
	Engine Start	0.00	0.00	0.00	2.05	5.56	4.89	5.86	23.27	14.10	16.78	0.00	112.82	185.31	0.00	25 sec per engine
	Taxi, flap deploy	63.86	5.43	10.00	9.09	5.00	5.82	5.24	15.86	13.94	16.78	22.83	0.00	86.68	87.16	10
Take-off	Lift-off + climb	63.86	5.43	10.00	2.05	4.22	5.56	5.62	31.53	13.30	22.44	22.83	0.00	86.68	100.15	1
Climb	Hi-lift and Flap stow	79.52	5.43	10.00	11.14	4.22	5.60	5.62	27.98	13.30	22.40	22.83	0.00	102.34	105.69	19
Cruise	35,000 ft	84.34	3.26	10.00	2.05	4.11	5.44	5.56	30.70	12.95	5.56	0.00	0.00	84.34	79.62	175
Approach	Approach & Landing	79.52	5.43	10.00	2.05	4.22	5.56	5.62	25.48	7.09	22.44	22.83	0.00	102.34	87.89	20
	Flap deploy	63.86	5.43	10.00	11.14	4.22	5.56	5.62	25.48	7.09	22.44	22.83	0.00	86.68	96.99	3
Emergency	Go-around again Emergency	0.00	5.43	10.00	2.05	4.78	0.00	23.40	0.00	0.00	5.56	0.00	0.00	0.00	RAT	As Req'd
Ground Op	Taxi - in	63.86	3.26	10.00	9.09	4.96	5.82	5.64	18.89	13.94	16.80	0.00	0.00	63.86	88.40	10
	Ground Maintenance	0.00	0.00	0.00	0.00	3.89	3.78	4.28	12.36	12.16	16.78	0.00	0.00	0.00	External Pwr	As Req'd

Minimum Load

	Flight Segment	ECS CACTCS	OBIGGS	FUEL PUMPS	FLIGHT CONTROL	28VDC ESSL	28VDC non-ESSL	115VAC ESSL	115VAC non-ESSL	GALLEY	EMP	WING DE-ICE	ENGINE START	FCAPU POWER	Engine Generator	Duration minutes
Ground Op	Gate APU Loading	63.86	0.00	0.00	0.00	0.00	0.72	0.00	11.43	10.24	0.00	0.00	0.00	86.26	0.00	As Req'd
	Engine Start	0.00	0.00	0.00	0.00	3.12	0.00	0.13	0.00	0.00	0.00	0.00	112.82	116.08	0.00	25 sec per engine
	Taxi, flap deploy	63.86	0.00	0.00	5.05	2.76	3.23	0.16	5.57	7.74	9.33	22.83	0.00	86.68	33.83	10
Take-off	Lift-off + climb	63.86	0.00	0.00	1.14	2.34	3.11	0.78	14.43	7.39	12.44	22.83	0.00	86.68	41.64	1
Climb	Hi-lift and Flap stow	79.52	0.00	0.00	6.18	2.34	3.11	0.78	9.50	7.39	12.44	22.83	0.00	102.34	41.75	19
Cruise	35,000 ft	84.34	0.00	0.00	1.14	2.28	3.03	0.81	14.00	7.19	3.11	0.00	0.00	84.34	31.56	175
Approach	Approach & Landing	79.52	0.00	0.00	1.14	2.34	3.09	0.78	11.09	3.94	12.44	22.83	0.00	102.34	34.82	20
	Flap deploy	63.86	0.00	0.00	6.18	2.34	3.09	0.78	6.16	3.94	12.44	22.83	0.00	86.68	34.93	3
Emergency	Go-around again Emergency	0.00	0.00	0.00	1.14	2.63	0.00	10.37	0.00	0.00	3.11	0.00	0.00	0.00	RAT	As Req'd
Ground Op	Taxi - in	63.86	0.00	0.00	5.05	2.76	3.23	0.16	5.57	7.74	9.33	0.00	0.00	63.86	33.83	10
	Ground Maintenance	0.00	0.00	0.00	0.00	2.19	2.08	0.19	4.78	6.76	9.33	0.00	0.00	0.00	External Pwr	As Req'd

MEA Architecture	SOFC Load <input type="text" value=""/>	Main Engine Generator <input type="text" value=""/>
-------------------------	--	--

2.1.1.2 Incorporation of Fuel Cell Into System Model

The ultimate goal was to incorporate the fuel cell system into the aircraft system model and evaluate performance deltas. This required expertise from other areas. Specifically, the following assumptions and approach were used in the analysis:

- 1) Aircraft (A/C) weight impact due to on-board system hardware must be defined. No matter what system is used, if it is intended to be loaded on the aircraft it must be roughly sized to account for the weight impact. The information was refined as systems were explored in finer detail.
- 2) A/C drag impact due to on-board system hardware must be defined. A fuel cell can either be carried on-board or slung under the wing in a pod. Again, a rough sizing and drag count due to surface and frontal area was initially used, and this assumption was traded off as the study progressed.
- 3) A/C mission impact due to on-board fuel cell was assessed. The fuel cell horsepower load on the aircraft was scheduled as a function of the flight segment. This load appeared as an installation loss to the engine. The weight on the aircraft as a function of the mission profile was also scheduled. The fuel cell used onboard fuel and potentially had a need for hydrogen conversion. These effects impacted the aircraft performance transiently as the mission was “flown”.

- 4) Next, “How the mission is run” was assumed. The initial approach was to assume that the Maximum Takeoff Gross Weight (MTOGW) of the aircraft was fixed, and there was no additional payload capability. With this approach, fuel must be offloaded to balance the additional weight of the fuel cell system. This is the most conservative method. Then by “flying” the aircraft over the defined mission profiles, the tradeoff of a fuel cell system was evaluated.
- 5) Finally, the results were compared and contrasted against the baseline.

2.1.1.3 Value Functions (Based on TOGW)

This section describes the derivation process for the Value Functions, based upon the aircraft Takeoff Gross Weight (TOGW).

Value Indices Of The System By Itself

To represent the value of the system, two system “quality” parameters have been chosen:

- (a) The power-to-weight ratio = P/W
- (b) The overall system efficiency = η

With this, the Value Index (VI) is defined as shown:

$$VI = P/W \cdot \eta \quad \text{[Eq. 1]}$$

In most cases, the better system yields the higher value of the VI. However, it is more revealing to also consider the operational scenario (i.e., mission) of the system.

Since the power generating system evaluated herein is an element of an air vehicle system, it appears appropriate to define a mission-specific weight w_{Sm} as a value index. Again, this index is based on the system “quality” parameters of power-to-weight ratio and efficiency. The Value Index VI is defined as:

$$VI_2 = w_{Sm} = \frac{1}{(P/W)_{pgs}} + \frac{\tau_m}{HV_F \cdot \eta} \quad \text{[Eq. 2]}$$

Or:

$$VI_2 = w_{Sm} = (W/P)_{pgs} + \tau_m \cdot SFC_F \quad \text{[Eq. 3]}$$

Where:

HV_F = Heating Value of Fuel

w_{sm} = Power Generating System (pgs) Weight

P_R = System Power

SFC_F = Specific Fuel Consumption at mission power based on fuel used by the system.

τ_m = Operating or Mission Time.

This value index represents the total specific system mission weight; i.e., the weight of the system itself plus the weight of the energy carrier for one unit of rated power and a given mission duration.

Value Function Related to the Total Aircraft System

The aircraft take-off gross weight (TOGW) for a specific mission has been chosen to reflect the value of the secondary power generating system relative to the total aircraft system. The TOGW is a function of the mission with the power generating system, and its energy carrier weight as independent variables.

The aircraft and mission cost as well as the propulsion energy consumption are all direct functions of the TOGW.

Value Function Derivation:

$$\text{TOGW} = W_o = W_P + W_E + W_F \quad \text{[Eq. 4]}$$

Where:

W_P = weight of payload, which for these purposes is defined as the weight of the mission equipment (W_{ME}) plus the weight of the fuel (W_{F2}) carried as supply for the secondary power generating system.

Then:

$$W_P = W_{ME} + W_{F2} = W_{ME} + \sum^i SFC_{2i} \cdot \tau_{M2i} \cdot P_{2i} \quad \text{[Eq. 5]}$$

Where:

SFC_{2i} = SFC of secondary power system at P_{2i} (for fuel used by this system).

τ_{M2i} = Mission time segment at P_{2i}

P_{2i} = Secondary power generated during a mission segment (i).

W_E = Empty weight of the aircraft, which for these purposes is defined as the empty weight without the secondary power system (W'_E), plus the weight of the secondary power system (W_2).

Then:

$$W_E = W'_E + \left(\frac{W_2}{P_{2R}} \right) \cdot P_{2R} \quad [\text{Eq. 6}]$$

Where:

$\left(\frac{W_2}{P_{2R}} \right)$ is the weight-to-power ratio (a quality factor), and
 P_{2R} is the rated power of the secondary power system.

With this, the takeoff weight of the aircraft can be expressed as:

$$W_O = \frac{W_{ME} + W'_E + \left(\frac{W_2}{P_{2R}} \right) \cdot P_{2R} + \sum^i SFC_{2i} \cdot \tau_{M2i} \cdot P_{2i}}{1 - \left(\frac{W_F}{W_O} \right)} \quad [\text{Eq. 7}]$$

$\left(\frac{W_F}{W_O} \right)$ is the fuel fraction of the aircraft that will now be derived for a specified mission profile, as shown in Figure 1.

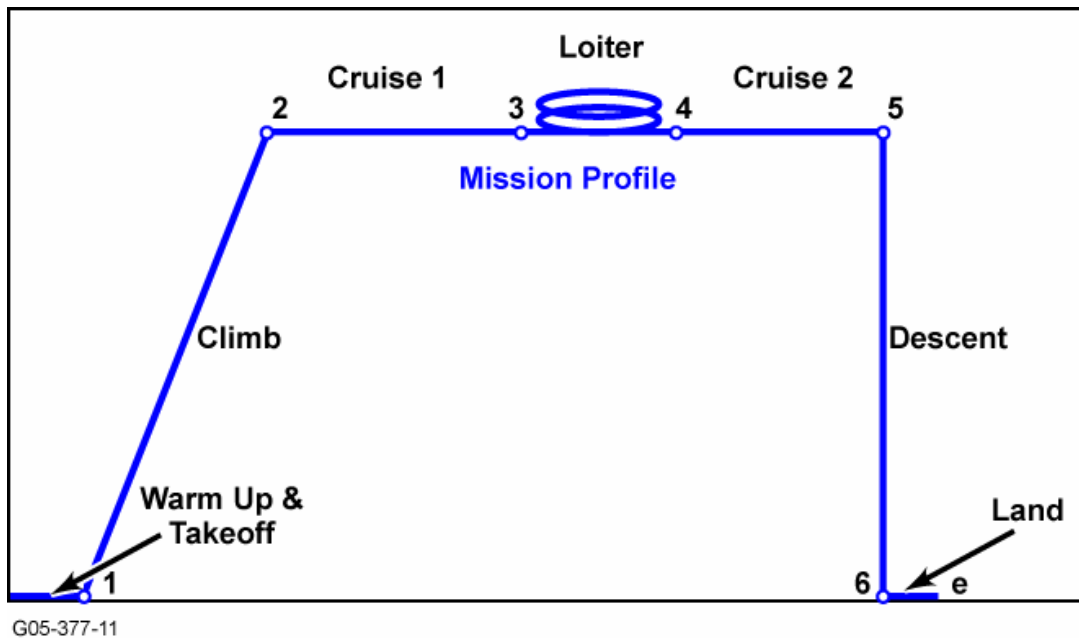


Figure 1. Sample Mission Profile (Typical Military Example).

The total fuel consumed by the propulsion system is calculated as:

$$W_F = W_O - W_e \quad \text{[Eq. 8]}$$

Or:

$$\frac{W_F}{W_O} = 1 - \frac{W_e}{W_O} \quad \text{[Eq. 9]}$$

Where:

W_e = Mission end weight.

Since the aircraft must carry more than the mission fuel (i.e., a fuel reserve plus fuel that cannot be pumped out of the tank), a factor k is applied to account for this.

Then:

$$\frac{W_F}{W_O} = k \left(1 - \frac{W_e}{W_O} \right) \quad \text{[Eq. 10]}$$

The term $\frac{W_e}{W_O}$ is broken down into the fuel fractions of each mission leg:

$$\frac{W_e}{W_O} = \frac{W_1}{W_0} \cdot \frac{W_2}{W_1} \cdot \frac{W_3}{W_2} \cdot \frac{W_4}{W_3} \cdot \frac{W_5}{W_4} \cdot \frac{W_6}{W_5} \cdot \frac{W_e}{W_6} \quad \text{[Eq. 11]}$$

$\frac{W_1}{W_0}$ = Warm-Up/Takeoff leg. A constant value could be assigned to it (≈ 0.97).

$\frac{W_2}{W_1}$ = Climb leg. A constant could be assigned to it also (≈ 0.98).

$\frac{W_3}{W_2}$ = First Cruise leg. Its value is obtained from the Breguet range equation:

$$\frac{W_3}{W_2} = e - \left[\frac{R_c \cdot SFC_c}{V_c \cdot (L/D)_c} \right]_1 \quad \text{[Eq. 12]}$$

Where:

R_c = Cruise Range

SFC_c = Cruise Specific Fuel Consumption, which is Thrust Specific Fuel Consumption (TSFC) for a jet engine, and

$(L/D)_c$ = Lift-to-Drag ratio at Cruise.

$\frac{W_4}{W_3}$ = Loiter leg. Its value is obtained from the Breguet endurance equation:

$$\frac{W_4}{W_3} = e^{-\frac{T_e \cdot SFC_e}{(L/D)_e}} \quad \text{[Eq. 13]}$$

Where:

T_e = Loiter time.

$\frac{W_5}{W_4}$ = Second Cruise leg. Its value is obtained like: $\frac{W_3}{W_2}$.

$\frac{W_6}{W_5}$ = Descent leg. It is proposed to include the Descent leg in the Second Cruise leg.

Then:

$$\frac{W_6}{W_5} = 1.$$

$\frac{W_e}{W_6}$ = Landing leg. A constant value is proposed (≈ 0.995).

Relative to the SFC values appearing in the above expressions, it has to be noted that if the secondary power is produced by a power takeoff from the propulsion engine, the given SFC includes this power takeoff and:

$$\sum^i SFC_{2i} \cdot \tau_{M2i} \cdot P_{2i} = 0. \quad [\text{Eq. 14}]$$

The difference in SFC with power takeoff and without power takeoff (propulsive power only) yields the fuel consumption for the takeoff power.

In case of independently generated secondary power, the given SFC is related to propulsive power only and:

$$\sum^i SFC_{2i} \cdot \tau_{M2i} \cdot P_{2i} \neq 0. \quad [\text{Eq. 15}]$$

In compact form, the takeoff weight-based value function W_o can now be expressed as:

$$W_o = \frac{\sum W_{EP}}{(1-k) + kF} \quad [\text{Eq. 16}]$$

With the definitions:

$$\sum W_{EP} = W_{ME} + W'e + \left(\frac{W_2}{P_{2R}} \right) \cdot P_{2R} + \sum^i SFC_{2i} \cdot \tau_{M2i} \cdot P_{2i} \quad [\text{Eq. 17}]$$

and:

$$F = \alpha \cdot e - \left[\left(\frac{R \cdot SFC}{V \cdot (L/D)} \right)_{C1} + \left(\frac{T \cdot SFC}{(L/D)} \right)_e + \left(\frac{R \cdot SFC}{V \cdot (L/D)} \right)_{C2} \right] \quad [\text{Eq. 18}]$$

The takeoff weight-based value function W_o contains the secondary power generating system and the mission energy carrier weight as independent variables.

The exact solution of this function has to be iterative, since the parameters SFC , V , and L/D are dependent upon W_o .

The above equation for the takeoff weight-based value function can also be used for tradeoff studies (e.g., W_o versus payload, or W_o versus range).

2.2 Part II – Fuel Cell Power System

Part II/Tasks 2.1 through 2.4 established the SOFC APU system characteristics and analyzed the impact on a typical Regional Jet application.

- **Task 2.1** established SOFC stack performance, modeled with current year 2005 and projected 2015 technology.
- **Task 2.2** matched the balance-of-plant characteristics with the SOFC stack design and mission load requirements.
- **Task 2.3** incorporated the SOFC stack with balance-of-plant components to model the SOFC APU performance. The estimated SOFC APU system and component weights were established.
- **Task 2.4** integrated the SOFC APU into the regional jet aircraft for mission analysis.
- **Task 2.5** identified technology gaps.

2.2.1 Task 2.1 – Estimation of Current and Future Fuel Cell Performance

A zero-dimensional model was used to represent the solid oxide fuel cell (SOFC). This higher-level model was used in lieu of a detailed and time-consuming representation of flow-field geometry, manifold, and the like. Six chemical constituents (H_2 , CO, CO_2 , O_2 , N_2 , and H_2O) are tracked from inlet to outlet for both the anode and cathode streams. Electrochemical and water-gas-shift (WGS) equilibrium reactions were represented via a standard molar exchange. Anode fuel utilization was fixed at a constant 70 percent in the SOFC system and aircraft mission analysis. An increase in fuel utilization to 85 percent was also assessed (shown in Appendix A) to evaluate the impact on weight and efficiency.

Losses to the model included a 5-percent linear pressure drop and heat loss to ambient via natural convection. Both year 2005 and predicted 2015 polarization curves, stack materials, and number of cells/stack could be implemented. Stack geometry was modeled using a simple algorithm to calculate volume and mass. Fuel cell system efficiency was calculated to determine heat addition to the outlet streams. Enthalpy calculations were made to equate the anode and cathode exit stream temperatures during an iterative loop. The fuel cell operating temperature was defined as the average between the inlet and exit stream temperatures. Constraints on model performance included a fuel cell operating temperature range of $850^{\circ}C \pm 75^{\circ}C$ and a temperature differential (ΔT) between the inlet and exit stream temperatures of less than $150^{\circ}C$.

2.2.1.1 Solid Oxide Fuel Cell Stack Computer Model

This section describes the algorithms used to predict the performance of an SOFC fuel cell stack.

Algorithm Description

The SOFC algorithm is comprised of the following thirteen steps:

- 1) Define constants
- 2) Load input parameters
- 3) Load model parameters
- 4) Calculate Cell Voltage (Polarization Function)

- 5) Calculate Electric Power and Heat generated
- 6) Calculate Inlet Flow Requirements
- 7) Calculate Total Input Enthalpy
- 8) Chemical Processing
- 9) Calculate Outlet Enthalpy Goal
- 10) Calculate pressure loss through cell
- 11) Calculate anode gas equilibrium at estimated outlet temperature
- 12) Iterate over steps 9 through 11 to find outlet temperature
- 13) Print out final outlet conditions.

1. Define Constants

The constants for the algorithm were defined as follows:

Parameter	Value	Units	Description
F	96485.34	C/mol	Faraday's number
R	8.314	J/mol-K	Universal gas constant
n	2	---	Number of electrons exchanged
g	9.81	m ² /s	Acceleration due to gravity

2. Load Input Parameters

Input parameters were loaded, as follows:

Parameter	Units	Description
N	---	Stack geometry, number of cells
A	cm ²	Stack geometry, active area (cm ²), expressed as L x W
St_c	---	Oxidant flowrate, cathode stoichiometric ratio
St_a	---	Fuel flowrate, anode stoichiometric ratio
U	---	Fuel flowrate, anode utilization
i	A	FC current demand (A)
q_{loss}	kW	FC heat loss (kW) - from loss function
V_{fc}	V/cell	FC polarization voltage (V/cell) – from polarization function
η_{fc}	---	FC efficiency – from polarization function

3. Load Model Parameters

Model parameters were loaded, as follows:

Parameter	Units	Description
T_{ci}	°C	Inlet temperature, cathode
T_{ai}	°C	Inlet temperature, anode
p_{ci}	psia	Inlet pressure, cathode
p_{ai}	psia	Inlet pressure, anode
$y_{ai}(1-6)$	moles/mole	Anode constituents: $y_{ai}(1)$ – mole fraction of H ₂ in anode inlet $y_{ai}(2)$ – mole fraction of CO in anode inlet $y_{ai}(3)$ – mole fraction of CO ₂ in anode inlet $y_{ai}(4)$ – mole fraction of O ₂ in anode inlet $y_{ai}(5)$ – mole fraction of N ₂ in anode inlet $y_{ai}(6)$ – mole fraction of H ₂ O in anode inlet
$y_{ci}(1-6)$	moles/mole	Cathode constituents: $y_{ci}(1)$ – mole fraction of H ₂ in cathode inlet $y_{ci}(2)$ – mole fraction of CO in cathode inlet $y_{ci}(3)$ – mole fraction of CO ₂ in cathode inlet $y_{ci}(4)$ – mole fraction of O ₂ in cathode inlet $y_{ci}(5)$ – mole fraction of N ₂ in cathode inlet $y_{ci}(6)$ – mole fraction of H ₂ O in cathode inlet

4. Calculate Cell Voltage (Polarization Function)

The polarization function is calculated in a separate Excel Visual Basic subroutine called fc_volt3c. Taken from the work of J. Brouwer,⁽¹⁾ the fc_volt3c subroutine performs the following calculations:

Equations used for fuel cell electrical calculations (polarization function):

Nernst Calculation:

$$\Delta G_{H_2O} = -247.891 + 0.0472357 \cdot T(K) + 0.00000413425 \cdot T(K)^2$$

$$V_{Nernst} = -\frac{\Delta G_{H_2O}}{nF} + \frac{RT}{nF} \ln \left(\frac{ppH_2^{ai} \cdot (ppO_2^{ci})^{\frac{1}{2}}}{ppH_2O^{ao}} \right) \quad [\text{Eq. 19}]$$

Note that SOFC stacks, operating in the 800 to 900°C range (and producing gaseous water), will typically have Nernst voltages of 0.91 to 0.96 V/cell.⁽²⁾

* References given in parentheses () are listed in a separate section at the conclusion of this report.

Activation Term:

$$i_o = 0.00755 \cdot e^{0.011 \cdot T(C)} \cdot \left(1 + \frac{\ln(p_{ao})}{2.7183}\right)$$
$$V_{activ} = \frac{RT}{cnF} \ln\left(\frac{i_{cd}}{i_o}\right)$$
[Eq. 20]

Ohmic Term:

$$r_{eff} = f(\text{geometry, materials})$$
$$V_{ohm} = i_{cd} \cdot r_{eff}$$
[Eq. 21]

Concentration Term:

$$i_{leak} = 800$$
$$V_{conc} = -\frac{RT}{nF} \ln\left(1 - \frac{i_{cd}}{i_{leak}}\right)$$
[Eq. 22]

The above equations represent year 2005 polarization curve performance. Year 2015 predictions (represented by the primed values below) make adjustments to two parameters in the activation and ohmic loss terms, viz.:

$$i_o' = 6 \cdot i_o$$
$$r_{eff}' = \frac{r_{eff}}{2}$$
[Eq. 23]

5. Calculate Electric Power and Heat Generated

Once the fuel cell (FC) polarization operating point has been defined, the FC voltage can be used to calculate overall stack voltage, power, efficiency, and heat loss, viz.:

$$V_{tot} = V_{fc} \cdot N \quad \text{(Total FC Voltage)} \quad \text{[Eq. 24]}$$

$$i_{cd} = \frac{i}{A} \quad \text{(FC Current Density)} \quad \text{[Eq. 25]}$$

$$P_{fc} = V_{tot} \cdot i$$
$$q_{tot} = \frac{P_{fc}}{\eta_{fc}} \quad \text{(FC Electrical Power and Heat)} \quad \text{[Eq. 26]}$$

$$q_{gen} = q_{tot} - P_{fc}$$

$$\eta_{fc} = 0.83 \cdot \left(\frac{V_{fc}}{V_{Nernst}}\right) \quad \text{(FC Efficiency)}^{(3)} \quad \text{[Eq. 27]}$$

6. Calculate Inlet Flow Requirements

The required mass flow of the anode and cathode are dictated by the specified FC current, the number of cells, the stoichiometric ratio (and utilization), and the corresponding mole fractions of oxidant and fuel in the input streams, viz.:

$$Q_{ai} = \frac{i \cdot St_a \cdot \left(\frac{1}{U}\right)}{n \cdot F \cdot y_{ai,H_2}} \cdot 24.465 \cdot N$$
$$\dot{m}_{ai} = Q_{ai} \cdot \rho_{ai} \quad \text{[Eq. 28]}$$
$$Q_{ci} = \frac{i \cdot St_c}{2n \cdot F \cdot y_{ci,O_2}} \cdot 24.465 \cdot N$$
$$\dot{m}_{ci} = Q_{ci} \cdot \rho_{ci}$$

Note that St_a is set to 1.0 in the model, and fuel flowrate is adjusted via fuel utilization.

Other constituent information, such as mass fraction, partial pressure, and molar flowrates are calculated using molar mass, and mole fraction information. The following constituents are tracked in the FC module for both the anode and cathode streams:

- H₂
- CO
- CO₂
- O₂
- N₂
- H₂O

7. Calculate Total Input Enthalpy

The enthalpy calculations for the input streams are performed using enthalpy, $h(T)$ relations for each constituent using the JANAF thermochemical tables.⁽⁴⁾ From this, a total input enthalpy can be calculated, viz.:

$$h_i = h_{ai} + h_{ci} \quad \text{[Eq. 28]}$$

8. Chemical Processing

Perform the chemical “processing” of constituents to model the FC production of water on the anode. This involves a mole exchange: 1 mol of hydrogen is “consumed” on the anode side, while a corresponding 1 mol of water is produced. Likewise, 0.5 mol of oxygen is consumed on the cathode side to complete the reaction. This results in a first-pass outlet stream composition, which will later be modified by the water gas shift (WGS) reaction (see below).

9. Calculate Outlet Enthalpy Goal

Establish the outlet enthalpy goal, taking into account the generated heat of the fuel cell and the losses to the surroundings:

$$\begin{aligned} q_{add} &= h_{gen} - q_{loss} \\ h_o &= h_i + q_{add} \end{aligned} \quad \text{[Eq. 29]}$$

To calculate heat loss, q_{loss} , from the fuel cell to the ambient surroundings, an additional function is used. Here, the fuel cell geometry (number of cells, active area size, etc.) is used to calculate an overall stack surface area. Insulation is assumed to cover this entire area. Forced airflow is assumed to be absent around the fuel cell, so calculations are made for heat transfer via natural convection. A surface temperature for the insulation is assumed before entering an iteration loop. Within the loop, a series of calculations are made. To start, Rayleigh numbers for both the vertical and horizontal walls of the stack are calculated, viz.:

$$Ra_L = \frac{g \cdot \beta \cdot (T_s - T_{amb}) \cdot L^3}{\alpha \cdot \nu} \quad \text{[Eq. 30]}$$

Where: g is gravity;

β , α , and ν are standard fluid properties for air (as a function of temperature);

L is the specific characteristic length;

T_s is the fuel cell surface temperature, and

T_{amb} is the ambient temperature.

From this, Nusselt numbers can be calculated using empirical relations from Incropera and Dewitt:⁽⁵⁾

$$Nu_{vert} = 0.68 + \left(\frac{0.67 \cdot Ra_{vert}^{1/4}}{\left[1 + \left(\frac{0.492}{Pr} \right)^{9/16} \right]^{4/9}} \right) \quad \text{[Eq. 31]}$$

$$\begin{aligned} Nu_{upper} &= 0.54 \cdot Ra_{hori}^{1/4} \\ Nu_{lower} &= 0.27 \cdot Ra_{hori}^{1/4} \end{aligned} \quad \text{[Eq. 32]}$$

From these, characteristic heat transfer coefficients can be calculated using:

$$h = \frac{Nu \cdot k}{L}, \quad \text{[Eq. 33]}$$

And the appropriate vertical and/or horizontal Nu and L values, and thermal conductivity, k , for the insulation. Finally, a set of calculations are performed to ultimately match the heat loss through the insulation (via conduction) with the heat loss to ambient (via natural convection):

$$q = \frac{k \cdot A}{L} (T_{fc} - T_s)$$

$$q = hA \cdot (T_s - T_{amb})$$
[Eq. 34]

When these are matched, the surface temperature equilibrium point has been reached and the final q_{loss} term can be calculated and returned to the main SOFC module.

10. Calculate Pressure Loss Through Stack

Calculate the pressure loss through the fuel cell as a function of mass flow. A simple linear model is developed using a reference pressure loss of 5 percent at a reference mass flow. Both the anode and cathode experience the same loss, using the cathode flow rate as the reference, viz.:

$$\Delta p = \Delta p_{ref} \cdot \left(\frac{\dot{m}_i}{\dot{m}_{ref}} \right)$$

$$p_o = p_i \cdot (1 - \Delta p)$$
[Eq. 35]

11. Calculate Anode Gas Equilibrium at Estimated Outlet Temperature

Equilibrium among the six species tracked is assumed to be only due to the water gas shift:



The change in moles of H₂, CO, CO₂, and H₂O are calculated in a separate Excel VBA function call WGS_equil which, given the temperature and number of moles of H₂, CO, CO₂, and H₂O returns x_react, the number of moles of H₂ and CO₂ created and H₂O and CO consumed.

12. Iterate to Find Outlet Temperature

Iterate for final temperature of anode/cathode streams by constraining both outlet temperatures to be identical. In essence, determine the percentage split of available energy (q_{add}) being added to the anode vs. the cathode such that the resulting temperatures are identical. During the looping structure, the following tasks are performed:

- Water gas shift (WGS) equilibrium reaction at (guessed) final temperature
- Recalculation of molar flowrates, constituent mole fractions, anode/cathode enthalpies, etc.
- Calculation of anode and cathode exit temperatures using enthalpies and mole fractions.
- Comparison of anode and cathode exit temperatures (convergence check) and readjustment of percentage split of available energy if needed.

13. Print Out Final Outlet Conditions

A printout of final outlet conditions, temperatures, etc. includes the terms listed in Table 3.

Table 3. SOFC Stack Output Parameters.

Parameter	Units	Description
P_{fc}	kW	FC output electrical power
T_{fc}	°C	FC bulk operating temperature, constrained to average of inlet and exit stream temperatures
T_{co}	°C	Outlet temperature, cathode
T_{ao}	°C	Outlet temperature, anode
P_{co}	psia	Outlet pressure, cathode
P_{ao}	psia	Outlet pressure, anode
$y_{ao}(1-6)$	Mole fractions	Anode constituents
$y_{co}(1-6)$	Mole fractions	Cathode constituents
ΔT_{o-i}	°C	Inlet to Exit temperature difference across FC, constrained to be 200°C max, 150°C or less, ideal

2.2.2 Task 2.2 – Applicability of Fuel Cell Power System

2.2.2.1 System Architecture Description

This section describes the component characteristics and system architecture development leading to the consolidated SOFC APU architecture (shown later in Figure 8). The compressor provides air for both the reformer and fuel cell stack. Waste heat from the turbine exhaust is used to heat the compressor discharge air in Heat Exchanger HX1. The compressor discharge air is further heated using the heat in the stack discharge flow through Heat Exchanger HX2. The air is then divided; part going to the SOFC stack cathode and a small portion going to the reformer. A series of streams enter the reformer where they are processed to generate hydrogen fuel for the stack. This includes Jet-A fuel, heated compressor discharge air, a percentage of stack anode discharge flow, and liquid water (if necessary to prevent coking). The reformer discharge and the stack cathode air are brought to a common temperature in Heat Exchanger HX3. Using the air and fuel, the stack generates electricity and heat. The electric power is sent through the DC/DC converter and delivered to the aircraft bus.

The stack anode discharge is divided – part is recycled to the reformer and the remainder passes through Heat Exchanger HX2. The anode and cathode discharge streams are then sent to the catalytic combustor where the hydrogen and carbon monoxide are oxidized. The combustor discharges to the turbine, which shares a common shaft with the compressor. Excess shaft power is used to run a generator that adds its output to the aircraft bus. Finally, the turbine exhaust air passes through Heat Exchanger HX1 and is discharged to ambient.

2.2.3 SOFC APU Component Descriptions

2.2.3.1 Compressor

Inlet air for the APU is compressed, providing high-pressure/high-flow air to both the fuel cell and reformer. Two air sources were considered in this study: ambient air and cabin air. The compressor shares the same mechanical drive shafting as the turbine, drawing power from the turbine for its operation. A scaled compressor performance map is used to determine efficiency values at various pressure and flow conditions. Preliminary values used in the model were 78 to 81 percent efficiency at a pressure ratio (PR) = 3.2 to 5. An inlet recovery factor of 0.9 was also used. For the final design, matching between the compressor and turbine will need to be considered.

2.2.4 Heat Exchangers

Reverse-flow heat exchangers HX1 and HX2 are used to redistribute heat from the turbine and stack discharge streams to the stack and reformer input streams. Parallel-flow heat exchanger HX3 is used to balance the stack input stream temperatures (cathode air and anode fuel). HX1 and HX2 include a 5-percent heat loss, while HX3 has no heat loss. All of the heat exchangers are also modeled with a 5-percent pressure loss through each pass. Thermal management of the APU system is very sensitive to heat exchanger placement and performance. For this study, fixed effectiveness values (HX1 = 0.65, HX2 = 0.70) were used.

A detailed description of the modeling of the reverse heat exchangers is given in the following discussion, based on the approach in the textbook by Kreith.⁽⁶⁾

$$\text{If: } \dot{m} C_p^* \Big|_{hot} \leq \dot{m} C_p^* \Big|_{cold} \quad [\text{Eq. 37}]$$

$$\text{Then: } \eta = \frac{\dot{m}_{cold} C_p^* (T_{cold,out} - T_{cold,in})}{\dot{m}_{hot} C_p^* (T_{hot,in} - T_{cold,in})} = \frac{\dot{m}_{cold}^* (H_{cold,out} - H_{cold,in})}{\dot{m}_{hot}^* (H_{hot,in} - H_{cold,in})} \quad [\text{Eq. 38}]$$

Solving for enthalpy per unit mass at cold side out:

$$H_{cold,out} = H_{cold,in} + \frac{\eta \dot{m}_{hot}^* (H_{hot,in} - H_{cold,in})}{\dot{m}_{cold}^*} \quad [\text{Eq. 39}]$$

$$\text{Then: } \Delta H_{cold} = \eta \left(\frac{\dot{m}_{hot}^*}{\dot{m}_{cold}^*} \right) (H_{hot,in} - H_{cold,in}) \quad [\text{Eq. 40}]$$

$$\text{And: } \Delta H_{hot,out} = \Delta H_{cold,out} \left(\frac{\dot{m}_{cold}^*}{\dot{m}_{hot}^*} \right) \quad [\text{Eq. 41}]$$

$$\text{Similarly, if: } \dot{m} C_p^* \Big|_{cold} \geq \dot{m} C_p^* \Big|_{hot} \quad [\text{Eq. 42}]$$

$$\text{Then: } \eta = \frac{\dot{m}_{hot}^* C_p^* (T_{hot,in} - T_{hot,out})}{\dot{m}_{cold}^* C_p^* (T_{hot,in} - T_{cold,in})} = \frac{\dot{m}_{hot}^* (H_{hot,in} - H_{hot,out})}{\dot{m}_{cold}^* (H_{hot,in} - H_{cold,in})} \quad [\text{Eq. 43}]$$

Solving for enthalpy per unit mass at hot side out:

$$H_{hot,out} = H_{hot,in} - \frac{\eta \dot{m}_{cold}^* (H_{hot,in} - H_{cold,in})}{\dot{m}_{hot}^*} \quad [\text{Eq. 44}]$$

Then:
$$\Delta H_{hot} = \eta \left(\frac{m_{hcold}^*}{m_{hot}^*} \right) (H_{hot,in} - H_{cold,in})$$
 [Eq. 45]

And:
$$\Delta H_{cold,out} = \Delta H_{hot,out} \left(\frac{m_{hot}^*}{m_{cold}^*} \right)$$
 [Eq. 46]

To account for heat loss:

$$\Delta H_{hot} = \Delta H_{hot}^* (1. - hlf)$$
 [Eq. 47]

$$\Delta H_{cold} = \Delta H_{cold}^* (1. - hlf)$$
 [Eq. 48]

Where:
$$hlf = \frac{heat_lost}{total_heat_transferred}$$
 [Eq. 49]

The heat exchanger effectiveness will now be somewhat less than the input value.

2.2.5 Hydrocarbon Fuel Processing – Desulfurization And Reformation

Significant advances in fuel processing technologies are required for fuel cells to meet the needs of future high energy density aerospace systems. For fuel cells to find widespread usage without significant changes in fuel distribution infrastructure, standard logistic liquid fuels (such as JP fuel and diesel) need to be processed in order to:

- 1) Convert logistic fuel constituent hydrocarbons to hydrogen and carbon oxides, and
- 2) Remove undesirable species, particularly sulfur.

2.2.5.1 Desulfurization Technology

2.2.5.1.1 Poisoning Effect Of Sulfur Compounds On SOFC

SOFC stacks are highly sensitive to sulfur poisoning. It is essential that sulfur contamination be reduced to, at least, <10 ppm concentrations in the reformat fuel feed. Onboard fuel reformer and hydrogen storage technologies were studied, and the results are discussed in Appendix A. The targeted direction for the SOFC system includes using reformed jet fuel, which typically contains 200 to 1,600 ppmw of sulfur that will poison current fuel cell stacks. SOFC anodes are typically Ni-YSZ cermets (nickel-yttria-stabilized zirconia ceramic-metal), which demonstrate a decrease in performance in the presence of 1 to 2 ppm^(7, 8) and 50 ppb⁽⁸⁾ of H₂S at 1,000°C and 800°C, respectively. Therefore, in order to achieve and maintain optimum fuel cell performance the SOFC fuel processing system needs to include an onboard and/or ground-based desulfurization system. Sulfur-tolerant SOFC anodes are currently being developed.

2.2.5.1.2 Background

Concepts for removing sulfur in aircraft applications differ significantly than their ground-based counterparts in the need to minimize both weight and size of the removal technology. Typical filtration based technology must undergo a redesign to maximize removal efficiency, usually at the expense of lifetime. Additionally, the sulfur removal technology must be compatible with both the reformer technology that it will support and the needs of the aircraft.

Sulfur removal is typically accomplished using one of the following four possible methods:

1. Catalytic Hydrodesulfurization (HDS) – This process is usually conducted at the plant level, as high pressure and temperatures are usually needed to run this process. Hydrogen is added to the hydrocarbon feed and organosulfur compounds are converted into hydrogen sulfide (H₂S) and olefins. Hydrogen sulfide is then removed from the remaining process as a gaseous contaminant. The thiophenic compounds present in jet fuel pose a particular desulfurization challenge in that they require partial or full hydrogenation (or isomerization) of the aromatic system prior to sulfur removal. This requires the consumption of hydrogen, as well as forcing conditions such as high temperatures and pressures. The downsides of this technology: while HDS is a mature technology, excess energy is required due to the high temperatures and pressures (Table 4). Additionally, the hydrogen required for hydrogenation of the aromatic thiophenes results in parasitic loss.

Table 4. Comparison of Sulfur Removal Processes.

No.	Process	Pros	Cons
1	Hydrodesulfurization (HDS)	<ul style="list-style-type: none"> – Mature technology – Good catalyst activity – Good catalyst lifetimes – Regenerable 	<ul style="list-style-type: none"> – High Temperature and Pressure (T and P) – H₂ consumption – High energy consumption
2	Adsorption	<ul style="list-style-type: none"> – Low P and T – Does not consume H₂ – Regenerable 	<ul style="list-style-type: none"> – Low capacities – High residence times
3	Oxidation	<ul style="list-style-type: none"> – Low P and T 	<ul style="list-style-type: none"> – Stability issues – Requires oxidant feed stream

2. Adsorptive Desulfurization – Sulfur-containing organic compounds are adsorbed on specific media (some regenerable) at low or slightly elevated temperatures and pressures. Current technology for high-concentration sulfur removal in a hydrocarbon feed typically requires the use of a metal or metal alloy, such as nickel or zinc compounds; whereas, high-concentration sulfur removal in the reformat gas typically requires the use of a pelletized sorbent, such as RVS-1 developed by DOE (METC).⁽⁹⁾ The downsides of this technology: Current removal technology is immature but being rapidly developed. Adsorptive technology requires little energy but does require large amounts of adsorptive material to sulfur, as generally adsorption ranges from 15 mg/g (S/ads). Additionally, the rate of removal is slower than would be necessary for on-demand feeding of a reformer.

3. Oxidative Desulfurization – Through the addition of an oxidant such as peroxides, the sulfur-containing organic compound is oxidized to remove the sulfur compounds. The downsides of this technology: Sulfur removal requires an additional feed that must be kept within the required area of conversion. Should this be onboard, an additional feed tank would be necessary. Additionally, peroxide stability is an issue, especially when combined with an organic. Temperature and pressures vary in this process, as shown in Table 5.

4. Biodesulfurization – Use of biological processes to remove sulfur within the feed. This process is immature and not feasible at this time and will not be discussed further.

Logistic fuels, such as JP-8 or Jet-A, typically have sulfur concentrations between 200 to 1,600 ppmw,^(10, 11) with a total sulfur limit of 3,000 ppmw. The sulfur contained in jet fuel typically consists of refractory organosulfur compounds such as alkyl-substituted benzothiophenes and dibenzothiophenes. Unfortunately, these sulfur compounds are significantly more difficult to remove from fuel than thiols or sulfides. Since sulfur can be removed either prior to, or after the reformer, multiple options exist for its removal.

2.2.5.1.3 Pre-Reformer Fuel Desulfurization Technology

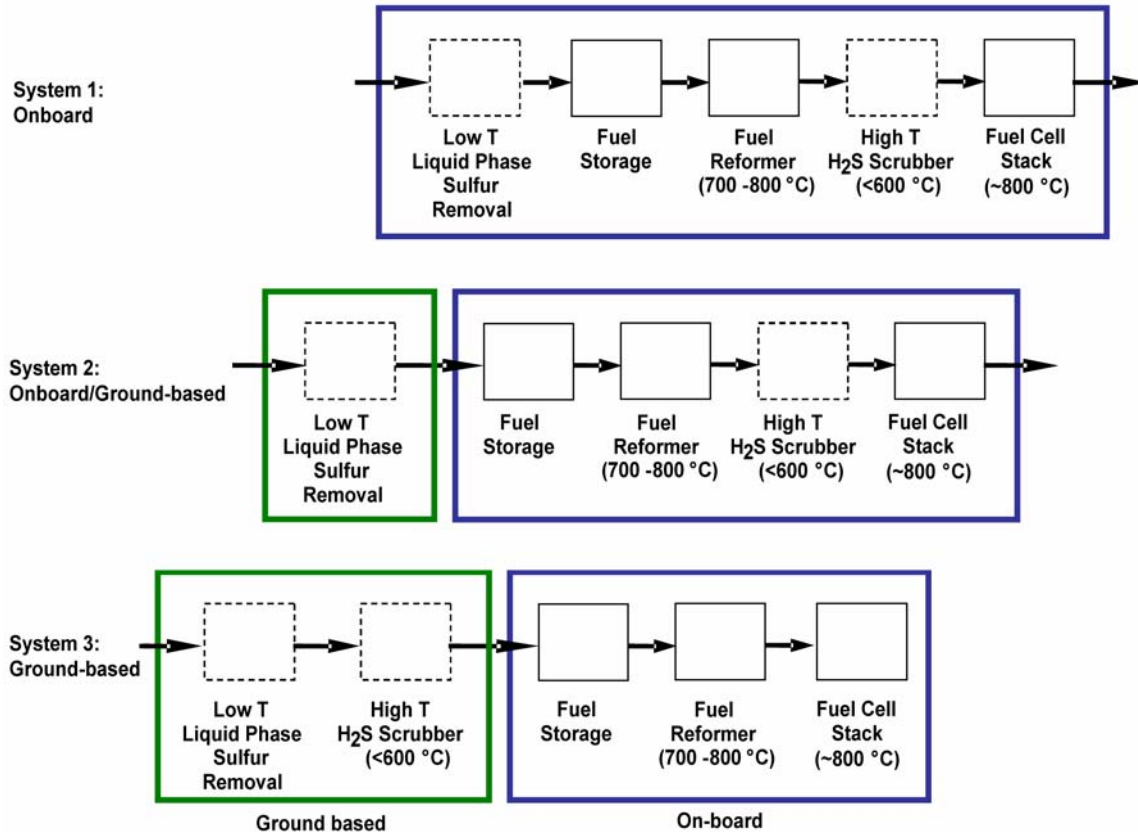
A primary, ground-based adsorbent sulfur removal system has been targeted to reduce the weight and size of the onboard fuel processing system. Phillips Petroleum (now ConocoPhillips) has commercialized an adsorptive desulfurization process called S-Zorb, which can reduce the sulfur level in gasoline and diesel fuel down to 10 ppm or less.⁽¹²⁾ The S-Zorb adsorbent retains the sulfur on adsorbent and releases the hydrocarbon portion back to the fuel stream. However, the process consumes hydrogen and operates at high temperatures (340 to 430°C) and pressures (100 to 500 psig). Liquid-phase adsorbents which operate at low temperatures and pressures include metal compounds, supported metals,⁽¹³⁾ transition metal ion-exchanged zeolites,⁽¹⁴⁾ and mixed metal oxides.⁽¹⁵⁾ Unlike the S-Zorb process, these adsorbents do not consume hydrogen and typically have sulfur capacities between 1 to 25 mg S/g adsorbent. Unfortunately, the adsorbents that demonstrate relatively high capacities tend to require long regeneration times. In addition, for liquid-phase sulfur removal, residence times on the order of minutes to hours are needed to reduce sulfur concentrations to acceptable levels (<10 ppm); therefore, kinetic and mass transfer limitations need to be addressed to reduce the residence times.

2.2.5.1.4 Post-Reformer H₂S Removal

Organosulfur compounds processed through a reformer are converted into H₂S (or SO_x), which can then be removed using a high-temperature adsorbent. This would increase the fuel stack lifetime and mitigate any deficiencies associated with the ground-based desulfurization unit. Metal oxides, such as ZnO, FeO, and CuO,⁽¹⁶⁾ are typically used as gas-phase H₂S adsorbents.⁽¹⁷⁾ Researchers at the U.S. Department of Energy National Energy Technology Laboratory (DOE-NETL) have developed a regenerable ZnO-based H₂S adsorbent, RVS-1, which has been commercialized by Süd-Chemie Inc.⁽¹¹⁾ The adsorbent operates over a wide temperature range (260 to 600°C) and can be regenerated using oxygen at ~480°C. The RVS-1 adsorbent demonstrates a sulfur capacity of 17-20 wt% and can maintain H₂S levels below 5 ppm. Gas diffusion limitations and high catalyst weights are often alleviated by using monolithic structures which demonstrate better performance than extrudates.^(18, 19, 20) Higher sulfur capacities are observed with gas-phase adsorbents than with typical liquid-phase adsorbents; however, a penalty is paid for removing sulfur in the gas phase, as long regeneration times and reduced reactivity in the presence of high steam concentrations result in limited applications with fuel cells.⁽²¹⁾

2.2.5.1.5 Possible Technology For Desulfurization

Adsorbent-based desulfurization is the preferred choice for fuel cell application due to the low operating temperatures, minimal energy input, and lack of H₂ consumption. There are three main desulfurization systems that can be envisioned: 1) onboard desulfurization, 2) liquid-phase, ground-based adsorbent system combined with an onboard H₂S scrubber, and 3) entirely ground-based system (see Figure 2).



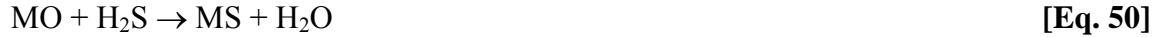
	Advantages	Disadvantages
System 1	<ul style="list-style-type: none"> - One fuel tank - Standard refueling 	<ul style="list-style-type: none"> - High system weight - Poor capacity with current adsorbents
System 2	<ul style="list-style-type: none"> - Majority of the system weight moved onto the ground 	<ul style="list-style-type: none"> - Moderate system weight - Separate fuel tank for APU
System 3	<ul style="list-style-type: none"> - No added system weight 	<ul style="list-style-type: none"> - Best conducted at refinery level - Separate fuel tank

G05-377-20

Figure 2. Sulfur Removal Systems For Aerospace Fuel Cell Applications.

Unfortunately, System 1, an entirely onboard sulfur removal system, would add significant weight and complexity to the onboard fuel processing system. Our original targeted direction for sulfur removal involved System 2, a tandem ground-based/onboard system. Our original approach removed significant weight from the aircraft by conducting the primary desulfurization on the ground using a low-temperature, liquid-phase adsorbent. Placing the primary desulfurization system on the ground would reduce the weight of the fuel processing system; however, onboard desulfurization would likely be required to remove trace levels of sulfur compounds which remain in the jet fuel.

Any organosulfur compounds that survive the primary, ground-based desulfurization process and are fed to the reformer will be converted into H₂S (or SO_x). An onboard, adsorbent-based filter located between the reformer and the fuel cell stack would then scrub the reformat gas free of H₂S. Unfortunately, commercial H₂S adsorbents (typically metal oxides, such as ZnO)^(22, 23) operate best at temperatures below 600°C [Eq. 50].



At higher temperatures (and in reducing conditions) these metal oxides suffer from low structural stability and consequently decreased reactivity. Therefore, inserting an H₂S adsorbent (at 250 to 600°C) between the reformer (at ~800°C) and the fuel stack (at ~800°C) would require heat exchangers for thermal integration. Promising, high-temperature H₂S adsorbents, such as CeO_n and MnO, need to be further developed to reduce the weight of an onboard desulfurization unit.

With the current desulfurization technology, our targeted direction has been revised to an entirely ground-based desulfurization system. SOFC anodes are sensitive to 1 ppm of H₂S; therefore, a ground-based desulfurization system would require reducing jet fuel sulfur levels to <10 ppmw. Reducing sulfur levels from 200 to 1,200 ppmw down to 10 ppmw is non-trivial. In order to avoid placing a small refinery at each airport processing unit, the best option currently involves removing sulfur at the fuel supplier's refinery. High-capacity liquid- and gas-phase adsorbents, which operate over a range of temperatures, need to be developed to make onsite (airport) and onboard desulfurization more feasible. In addition, adsorbent regeneration and potential improvements in addressing mass transfer issues need to be addressed to reduce the weight and size of the system.

Ground-based sulfur removal was selected to minimize system weight and complexity. Since sulfur contaminants present in both the fuel stream and reformat gas will poison the reformer catalyst and fuel cell stack, our model assumed that the fuel feed was desulfurized on the ground and that the APU fuel feed was sulfur-free.

2.2.5.2 Fuel Reforming Technology

The conversion of logistic liquid fuels to a hydrogen and carbon dioxide (H₂ and CO) gas phase mixture is accomplished via fuel reforming, using three typical processes: Steam Reforming (SR), Partial Oxidation (POX), and Autothermal Reforming (ATR). Steam reforming involves a reaction between water and the hydrocarbon fuel to produce H₂ and CO [Eq. 51].



The steam reforming catalyst also promotes the reaction of CO and H₂O to form CO₂ to reduce CO levels via the Water Gas Shift (WGS) reaction [Eq. 51].

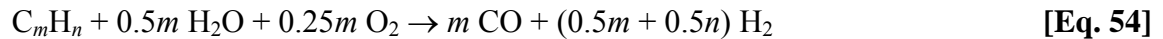


Due to the endothermic nature of the combined steam reforming (SR) and WGS reactions, additional energy is required to maintain feed temperatures, and a water feed must be available for the system to operate. Although, once running, the water vapor in the fuel cell exhaust can be recycled to the reformer feed, the parasitic energy and weight requirements makes this process an unlikely candidate for use in an onboard aircraft power system. The water and energy from the fuel cell exhaust can potentially be reclaimed and used more efficiently for heating, drinking and several other purposes.

POX is an exothermic process which utilizes an oxygen reactant stream to facilitate the reformation process and form H₂ and CO [Eq. 53].



Catalytic partial oxidation (CPOX) is a similar technology to POX involving the use of a catalyst to reduce the energy requirements of the reformer system. Both technologies are attractive because they permit more specific tailoring of the output gas composition based on the level of oxygen co-fed to the reformer, while minimizing weight and volume. Additionally, in previous studies, CPOX has demonstrated tolerance to sulfur laden feeds and a high degree of feed conversion, which enables a process based on the downstream gas phase removal of sulfur compounds. ATR is virtually a thermoneutral process [Eq. 54] that provides a greater efficiency, requiring only minimal energy input during starting, to initially heat feed gases, and no additional energy input once the catalytic process reaches thermal equilibrium.



The advantages and disadvantages of all three fuel reforming processes are shown in Table 5. For fuel cell application, ATR and CPOX are preferred over SR due to their faster dynamic response and start-up times, compactness, and minimal (CPOX) to moderate (ATR) water consumption.

Table 5. Fuel Reforming Process Comparison.

Process	Advantages	Disadvantages
Steam Reforming (SR)	<ul style="list-style-type: none"> – Stationary process is well developed – Not diluted by N₂ – Higher hydrogen concentrations 	<ul style="list-style-type: none"> – Endothermic (external heating required) – Water required – Slow dynamic response and start-up time (vs. CPOX and ATR)
Catalytic Partial Oxidation (CPOX)	<ul style="list-style-type: none"> – Fast dynamic response and start-up time (vs. SR) – Compact 	<ul style="list-style-type: none"> – Localized overheating can lead to catalyst sintering – Diluted by N₂ due to air feed
Autothermal Reforming (ATR)	<ul style="list-style-type: none"> – Fast dynamic response and start-up time (vs. SR) – Compact 	<ul style="list-style-type: none"> – Some water required – Diluted by N₂ due to air feed

Regardless of the reforming method selected, some amount of CO will be present in the reformat gas. SOFCs can use CO as a fuel, either through direct oxidation of CO to CO₂ [Eq. 55] or via WGS [Eq. 52].



2.2.5.2.1 Targeted Direction for Fuel Reformation (SOFC)

Solid oxide fuel cells can use CO as a fuel, which makes hydrogen generation via fuel reformation a practical option for SOFC systems. Due to the lack of hydrogen infrastructure and the higher power density of liquid hydrocarbon fuels than hydrogen, onboard reformation is currently a reasonable option for SOFC systems. This advantage comes at a slight cost, since the addition of a reformer to the fuel cell system is accompanied by added system weight and a parasitic energy loss. Autothermal and partial oxidation (both catalytic and non-catalytic) reformation are preferred because they require less water than steam reformation and a water tank can often be eliminated by recycling the water vapor present in the fuel cell exhaust to the reformer feed.

An autothermal reformer will require a water management system; however, any waste heat generated by the high temperature SOFC and reformer (exothermic CPOX) can be used to drive the endothermic steam reforming, which can lead to an increase in efficiency. The reformer can be evaluated from a systems integration point-of-view in order to determine which reformer results in the most effective APU. Most reformers demonstrate a turndown ratio of 5-6 to 1.

2.2.5.2.2 Problems Associated with Carbon Formation

Carbon (coke) formation typically occurs in the reformer and fuel vaporizer, according to [Eq. 56 - 58]. Carbon deposited on the catalyst surface results in catalyst deactivation and decreased reformer performance. In addition, carbon formation in the vaporizer can result in blockage of the fuel flow path. Coking is particularly problematic with the reformation of higher molecular weight hydrocarbon fuels such as diesel and jet fuel, as aromatic compounds and sulfur contaminants increase the tendency for carbon formation.⁽²⁴⁾ An adiabatic pre-reformer can be used to avoid carbon formation by converting the high molecular weight hydrocarbons to lower molecular weight hydrocarbons at lower temperatures where coking is unfavorable; however, weight will added to the system.⁽²⁵⁾ As an alternative method, carbon formation can be minimized by carefully controlling the reformer conditions including increasing the steam, hydrogen, or CO concentrations and ensuring uniform fuel, water, and air stream mixing. Unfortunately, it is difficult to avoid carbon formation during the startup period, which suffers from low steam concentrations.



2.2.5.2.3 Selected Reformer Characteristics

Auto-Thermal Reformation (ATR) was selected over Catalytic Partial Oxidation (CPOX) and Steam Reformation (SR) for the study for the following reasons:

- Minimum water requirement
- Water reduces coking and increases system lifetime
- Anode tail gas recycling eliminates the need for a water tank
- Minimizes reactor size and weight

Operating temperature range of model: 870 to 950°C

- Minimize hydrocarbon breakthrough (CH_4)
- Precision combustion
 - Average exit temperature: $\sim 800^\circ\text{C}$
 - Max operating temperature: ~ 1150 to 1200°C

Reformer gas composition:

- Based on thermodynamic modeling (Gibbs free energy minimization)
- Reformate gas compositions were compared to literature values and found to be consistent with experimental data (see Figure 3).

Reformer component sizing was based on estimates from commercial sources and mass and volume models developed at NASA-Glenn Research Center.⁽²⁶⁾

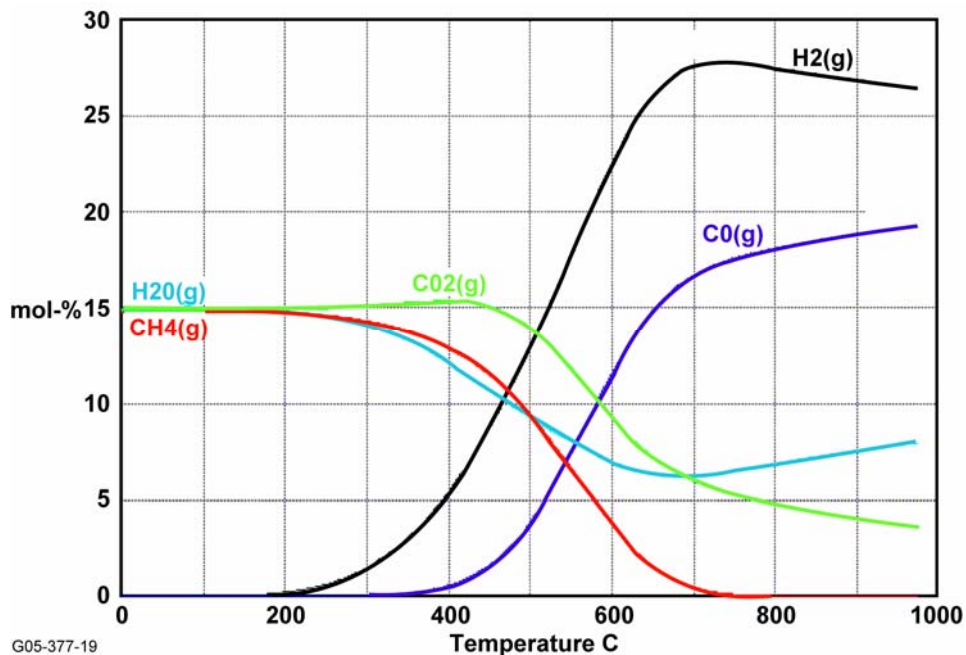


Figure 3. Reformer Gas Composition.

2.2.5.3 Reformer Algorithm

The following paragraphs describe the algorithm used to predict the performance of the reformer. The process is shown schematically in Figure 4.

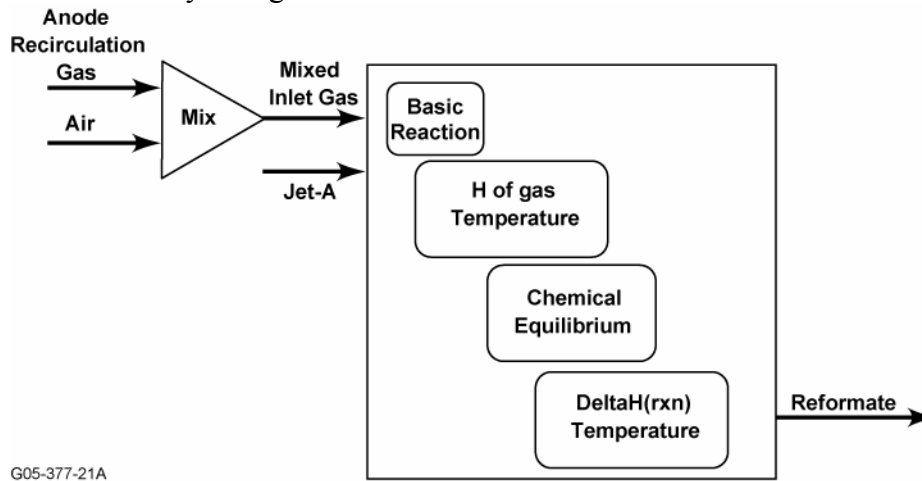


Figure 4. Flowchart of Reformer Algorithm.

2.2.5.3.1 Reformer Algorithm Description

The reformer process is modeled by the following ten steps:

- 1) Mix air and anode recirculation
- 2) Calculate Jet-A flow
- 3) React O_2 with Jet-A to form only H_2 , CO, and CO_2
- 4) Bring the rest of the equation left-hand side (LHS) to the right-hand side (RHS)
- 5) Find chemical equilibrium of products at inlet mix temperature
- 6) Calculate delta heat of reaction
- 7) Calculate sum of H of reactants
- 8) Calculate temperature of products
- 9) Find chemical equilibrium of products at exit temperature
- 10) Adjust temperature for delta heat of reaction of equilibrium shift.

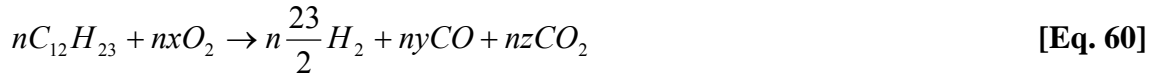
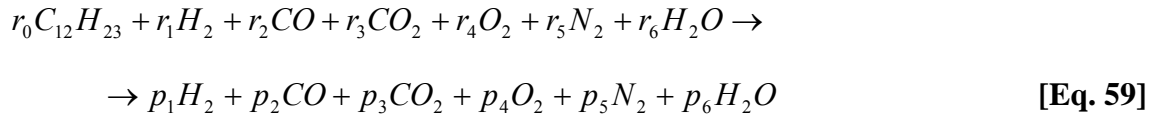
1. Mix Air and Anode Recirculation Gas

- a) Add species mass flows
- b) Calculate total mass flow of mixed flow
- c) Calculate temperature of mixed flow

2. Calculate Jet-A Flow

- a) Set O_2/C
- b) If $O_2/C < 0.5$, insufficient O_2 to react with all C leading to soot
- c) If $O_2/C > 1.0$, after reacting with C, O_2 remains to oxidize H_2 to H_2O – uses up FC fuel
- d) Set $O_2 = 0.5$.

3. React O₂ With Jet-A to Form Only H₂, CO, and CO₂ [Eq. 59 - 61]:

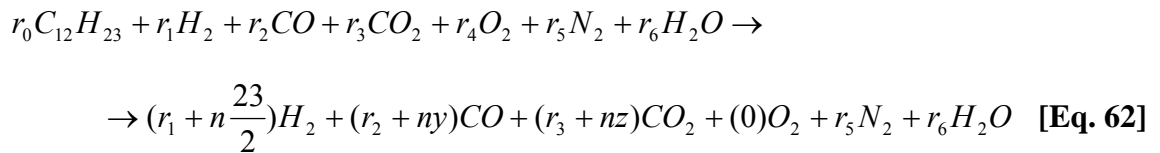


$$y = 24 - 2x$$

$$z = 2x - 12$$

$$\frac{O_2}{C} = \frac{x}{12} \quad \text{[Eq. 61]}$$

4. Bring the Rest of the LH Side of [Eq. 59] to the RH Side:



5. Find Chemical Equilibrium of Products at Inlet Mix Temperature

The CEA program⁽²⁷⁾ was not available within the iterations on the spreadsheet, so a simplified approach was used. Only the water gas shift (WGS) was considered – N₂ and O₂ did not take part in the equilibrium process.



The equilibrium constant is defined as:

$$K = \frac{N_c^{\nu_c} * N_d^{\nu_d}}{N_a^{\nu_a} * N_b^{\nu_b}} \left(\frac{P}{N_{total}} \right)^{\nu_c + \nu_d - \nu_a - \nu_b} \quad \text{[Eq. 64]}$$

Where: N is the number of moles.

For the WGS equation:

$$\nu_a = \nu_b = \nu_c = \nu_d = 1 \quad \text{[Eq. 65]}$$

So the equilibrium constant reduces to:

$$K = \frac{N_c * N_d}{N_a * N_b} = \frac{N_{H_2} * N_{CO_2}}{N_{CO} * N_{H_2O}} \quad \text{[Eq. 66]}$$

Several examples were run using the NASA Chemical Equilibrium Analysis (CEA) software. K was calculated for each example, and the results were plotted and curve fitted. The resulting curve fits are:

For $400 \text{ K} < T < 800 \text{ K}$, $R^2 = 0.9872$:

$$K = 1.36785 * 10^{25} * T^{-8.48422} \quad [\text{Eq. 67}]$$

For $800 \text{ K} < T < 1200 \text{ K}$, and $R^2 = 0.999967$:

$$K = 1.80893e-10 * T^4 - 7.96136e-7 * T^3 + 1.32170e-3 * T^2 - 9.84362e-1 * T + 2.79341e2 \quad [\text{Eq. 68}]$$

For $1200 \text{ K} < T < 2000 \text{ K}$, and $R^2 = 0.999973$:

$$K = 1.46062e-12 * T^4 - 1.05280e-8 * T^3 + 2.87406e-5 * T^2 - 3.54923e-2 * T + 1.70952e1 \quad [\text{Eq. 69}]$$

Calculate K for the temperature of the gas and set up the equation:

$$K = \frac{(N_{H_2} + x_{react}) * (N_{CO_2} + x_{react})}{(N_{CO} - x_{react}) * (N_{H_2O} - x_{react})} \quad [\text{Eq. 70}]$$

Then solve for x_{react} . x_{react} is the number of moles of H_2 and CO_2 added, and CO and H_2O removed to achieve equilibrium.

The heat released by the water gas shift (WGS) is:

$$\begin{aligned} \Delta H_{rxn,WGS} &= \Delta H_{f,H_2} + \Delta H_{f,CO_2} - (\Delta H_{f,CO} + \Delta H_{f,H_2O}) \quad [\text{Eq. 71}] \\ &= 0 + (-393.681) - (-110.028 - 244.047) \\ &= -39.606 \frac{\text{kJ}}{\text{mole of } H_2 \text{ produced}} \end{aligned}$$

So, add $x_{react} * 39.606 \text{ kJ}$ of enthalpy to the total enthalpy of the reformat gas and recalculate the temperature.

6. Calculate Delta Heat of Reaction:

$$\Delta H_{rxn} = \sum H_f(\text{products}) - \sum H_f(\text{reactants}) \quad [\text{Eq. 72}]$$

7. Calculate the Sum of Enthalpies (H) of Reactants:

$$H_{total} = \sum_i^{i=1,6} H_i \quad [\text{Eq. 73}]$$

8a. Calculate the Sum of H of Reactants:

First, calculate the energy required to vaporize the Jet-A fuel:

$$H_{vap,Jet-A} = m_{Jet-A}^* \Delta H_{vap,Jet-A} \quad [\text{Eq. 74}]$$

Similarly, for water (if liquid water is added):

$$H_{vap,water} = m_{Jwater}^* \Delta H_{vap,water} \quad [\text{Eq. 75}]$$

A heat loss is applied ($frac_{loss}$) as a fraction of the heat of reaction, and finally:

$$H_{prod} = \sum_i^{i=1,6} H_i + H_{Jet-A} - (1. - frac_{loss}) \Delta H_{rxn} - \Delta H_{vap,water} - \Delta H_{vap,Jet-A} - \Delta H_{rxn,WGS} \quad [\text{Eq. 76}]$$

8b. Calculate Temperature of Products:

Iterate on T to find:

$$H_{prod} = \sum_i^{i=1,6} H_i(T_{exit}) \quad [\text{Eq. 77}]$$

9. Find Chemical Equilibrium of Products at Exit Temperature:

Chemical equilibrium is found for the exit temperature using the same method described in Step 5, above, for the Exit Temperature.

10. Adjust Temperature for Delta Heat of Reaction of Equilibrium Shift:

The energy released by the water gas shift (WGS) is added to the enthalpy of the products and the adjusted T_{exit} is found by iteration:

$$H_{prod} + \Delta H_{rxn,WGS} = \sum_i^{i=1,6} H_i(T_{exit}) \quad [\text{Eq. 78}]$$

2.2.5.4 Combustion

Adding a catalytic combustor to the FCAPU system has the following potential benefits:

- Recovery of energy from the unused hydrogen by feeding the combustor exit gas to the turbine and/or using the exit gas to heat the fuel processing system
- Generation of system heat
- Reduction of CO emissions by converting unused CO to CO₂.

The fuel cell exit gas can be combusted catalytically or non-catalytically, according to the following equations [Eq. 79 and 80]:



One of the main advantages of a SOFC APU is the potential to produce fewer emissions; therefore, it is important to avoid the formation of nitrogen oxides (NO_x) in the combustor. Catalytic combustors can be operated at a lower temperatures than non-catalytic combustors, and therefore have less potential to produce NO_x. Over noble metal catalysts (such as Pt, Pd, or Rh), H₂ and CO have light-off temperatures of ~30°C and ~220°C, respectively.⁽²⁸⁾ However, if the turbine is placed directly after the combustor, the combustor exit temperatures needs to be kept below 1,000°C to avoid damaging the turbine. Combustor temperatures can be decreased by diluting the gas stream with air or by supporting the combustion catalyst on a heat exchanger. Combustor technology will be further investigated to determine a lightweight option for hydrogen and carbon monoxide combustion.

The reformer combines Jet-A fuel with air and stack anode recycle air to generate hydrogen through a partial oxidation reaction. A portion of the anode exhaust is recycled (~30 to 40 percent), which is sufficient to bring the reformer steam-to-carbon (W/C) ratio up to 0.4. An option to add liquid water is also available, but not necessary for this W/C value. The reformer has a loss of 5 percent of the heat generated by the reaction, and a 0.8 percent pressure loss. Six chemical constituents (H₂, CO, CO₂, O₂, N₂, and H₂O) from each inlet stream are tracked throughout the reformer process. Heat balance and the water-gas-shift (WGS) equilibrium reaction are taken into account during modeling.

The study operating temperature range was 750 to 890°C, using the estimated values in Table 6.

Table 6. Catalytic Combustor Characteristics.

Parameter	Value
H ₂ Conversion	~100 %
CO Conversion	~99.5 %
NO _x Produced by Combustor	<1 ppm
Maximum Operating Temperature	950°C

Combustor component sizing was based on estimates from commercial sources and mass and volume models developed at NASA-Glenn Research Center.⁽²⁶⁾

2.3 Additional Fuel Cell APU Components – Descriptions

2.3.1 DC/DC Converter

A DC/DC converter will be necessary to regulate the bus voltage (± 270 Vdc) given the modulation of the fuel cell voltage output during normal operation. The DC/DC converter was modeled very simply using a power conversion efficiency of 90 percent.

2.3.2 Turbine

The turbine expands the discharge gas from the combustor, and shares the same shaft as the combustor, providing power for its operation. A scaled turbine map was used to determine the turbine efficiency values at various pressure and flow conditions. Preliminary values used in this study were 82 to 88 percent efficiency, at a Pressure Ratio (PR) = 1.9 to 3.7. Final matching between the compressor and turbine will need to be undertaken during final development.

2.3.3 Generator/Rectifier/Bearings

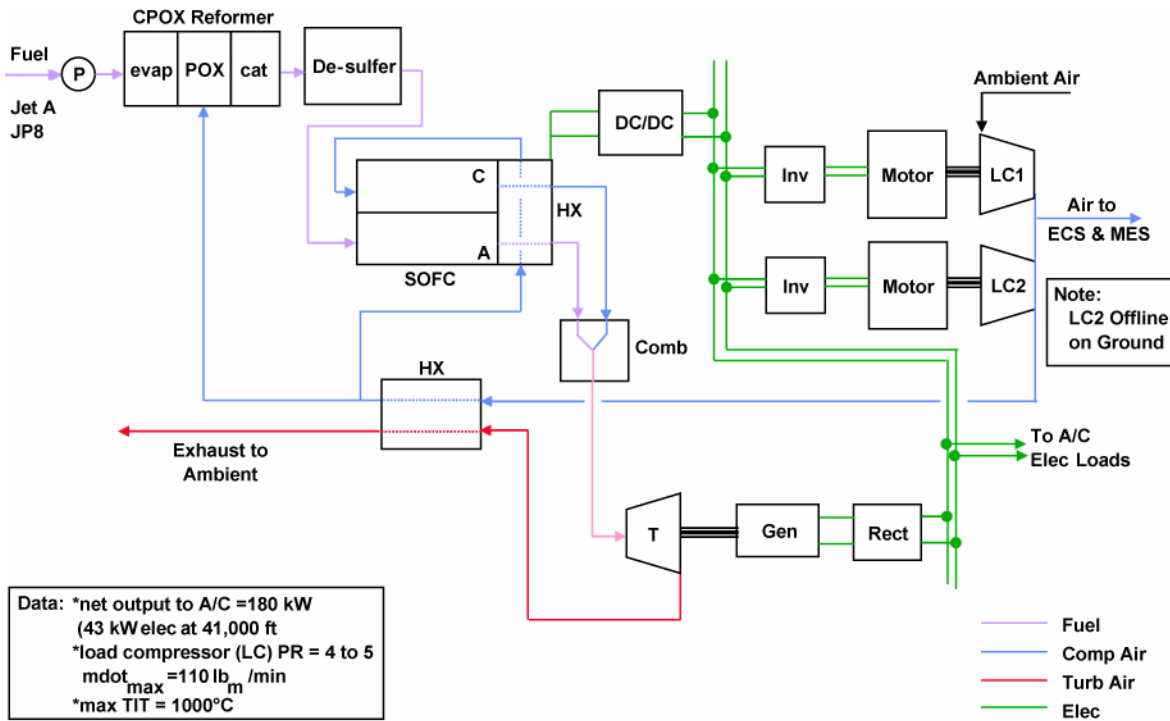
The generator converts excess power from the turbine/compressor shaft into power on the aircraft electrical DC bus. Three efficiency values were used in this study to represent the losses associated with the bearings and shafting (92 percent), the generator (95 percent) and the rectifier (95 percent).

2.4 Task 2.3 – Fuel Cell Power System Architecture Concepts

The SOFC APU system architecture was developed and modeled for a range of power output in-flight and on the ground, based on the mission load requirements established in Part I/Task 1.1. The component and system weight, volume, power density, and energy density were also established for the aircraft mission analysis.

2.4.1 SOFC APU System Architecture

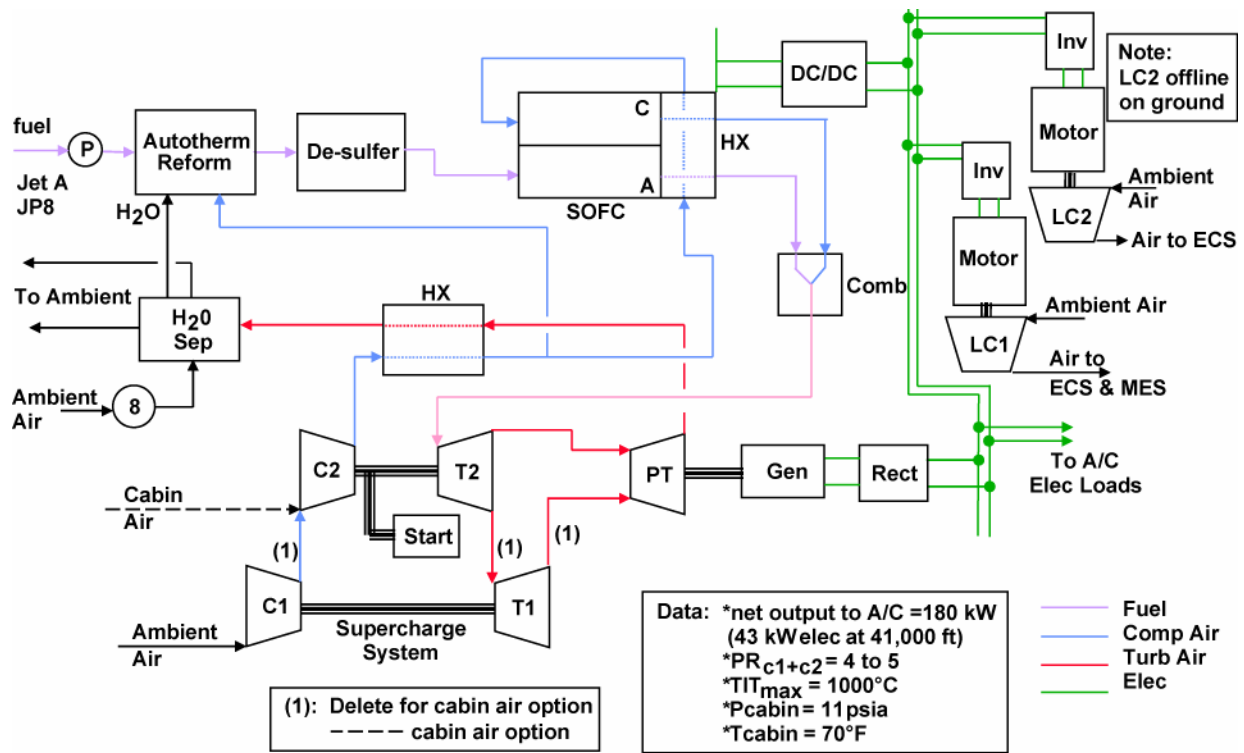
Three SOFC APU system architecture concepts were generated (see Figures 5 through 7) and then consolidated into one system architecture (Figure 8) for analysis with both ambient air and cabin air supply. Differences in the original architectures lies essentially in the use of a Environmental Control System (ECS) load compressor, or a super-charged compressor, or a single-spool compressor. Use of a water separator to recoup the turbine exhaust water-vapor for recycling into the reformer was replaced with recycling from the SOFC stack anode.



G05-377-22A

System 1. Combustion Air Supplied by Load Compressor

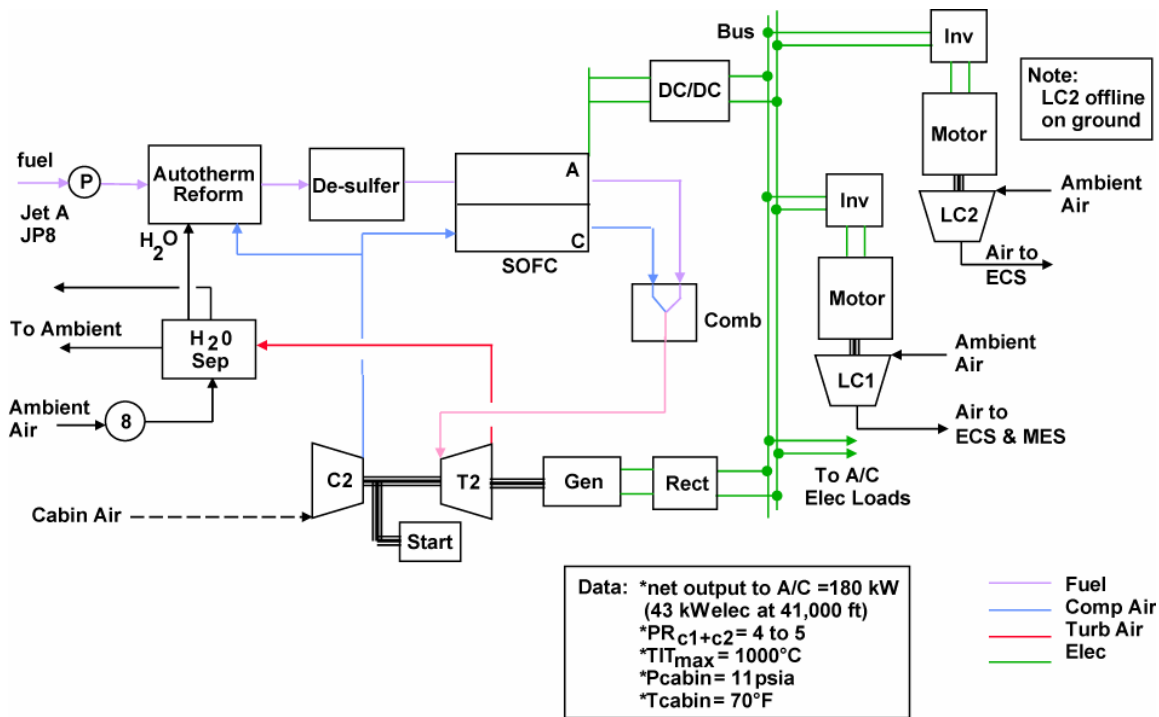
Figure 5. SOFC APU System Architecture – Option 1.



System 2a & 2b.
 (a) Combustion air compression system with supercharge
 (b) Combustion air from cabin

G05-377-23A

Figure 6. SOFC APU System Architecture – Option 2.



System 3.

Figure 7. SOFC APU System Architecture – Option 3.

G05-377-24A

Figure 8 shows the consolidated SOFC APU architecture derived and evolved from the original three concepts.

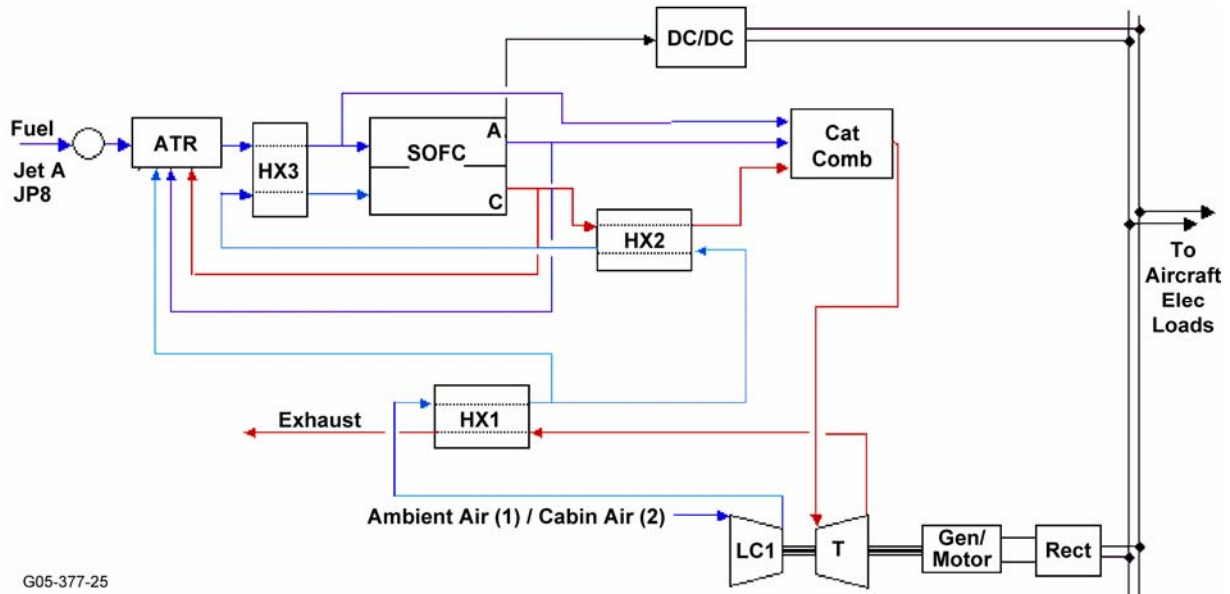


Figure 8. Consolidated SOFC APU System Architecture.

The consolidated SOFC APU system architecture incorporates the following characteristics:

- SOFC stack operating at $850 \pm 75^\circ\text{C}$
- Anode and Cathode maintained at same temperature
- Temperature difference between stack inlet and exit $< 150^\circ\text{C}$
- Auto-thermal jet fuel reformer with anode recirculation
- Ground-based desulfurization
- Catalytic combustor to burn excess H_2 and CO
- Turbine inlet temperature limited to $1,000^\circ\text{C}$
- Single-spool turbogenerator
- Generator capable of operating in Motoring mode
- Three heat exchangers for energy recovery and temperature control
- DC/DC converter(s) and rectifier for regulated DC voltage ($\pm 270 \text{ Vdc}$) on system bus
- Turbogenerator exhaust provides thrust contribution to aircraft
- Two air supply options: ambient air and cabin air.

2.4.2 SOFC APU System Modeling

The SOFC APU system model was created in an Excel spreadsheet with the following features:

- Use of Excel spreadsheet for zero-dimensional (0-D) steady-state model
- Spreadsheets used as “front end” or graphic user interface (GUI) for various modules
 - Solid oxide fuel cell (SOFC)
 - Reformer
 - Combustor
 - Heat exchangers (3 each)
 - Turbomachinery (compressor/turbine spool)
 - Mass and volume calculations
 - Main cycle sheet
 - Input parameters
 - Summary sheets (stack polarization, results, etc.)
- Use of Visual Basic scripting for actual calculations
- Equilibrium iterations performed at system level
- Heat loss function
 - Based on SOFC geometry (cells and active area)
 - Function of ambient (altitude adjusted) and SOFC temperature
 - Insulation sized to adjust heat loss via natural convection to ~3 to 5% of heat generated
- Polarization function
 - Based on SOFC operating temperature, pressure and current density
 - Use of partial pressures for incoming H₂ and O₂ and outgoing H₂O
 - Both current state-of-the-art (2005) and 2015 estimates available for study – with improvements made in the cell resistance (ohmic losses) and exchange current (activation losses)
- SOFC bulk temperature
 - Use of inlet and exit stream enthalpies (given SOFC efficiency and heat loss)
 - Constrain system such that anode/cathode exit stream temperatures are equal
 - Iteration of outlet stream temperature (and corresponding gas mixture properties) through split of available enthalpy
 - Bulk temperature set as average between inlet/exit streams

Model includes:

- SOFC electrical, heat, and mass transport information
- Flow, pressure, and temperature of both oxidant and fuel streams
- Chemical composition of fuel via mole/mass fractions; six constituents – H₂, CO, CO₂, O₂, N₂, and H₂O
- Gas mixture properties, etc. tracked from reformer through stack and combustor
- Electrical power transfer to/from components to/from the ± 270 Vdc bus

- Losses in the system:
 - Pressure drop, heat loss, and inefficiencies regarding electrical, fluid, and thermal calculations
 - Bulk representation at component level (no separate piping losses)
- Mass and volume estimates for components and system
- Power and energy density calculations given regional jet mission
- Aircraft thrust calculations, including ECS and FCAPU air inlet/exit
- Overall system efficiency calculation: ratio of total Jet-A fuel power (LHV) and net power output on the DC bus

Model does not include:

- Small pumps (fuel, anode recycle) – estimates show that this may account for up to 1.5 kW (or less than 1% of power), depending on conditions
- Valves for bypass flow and throttling
- Flow restrictions for pressure regulation
- System packaging configuration
- Controls simulation, etc.
- SOFC stack packaging to achieve ± 270 Vdc (dependent on series/parallel arrangement and DC/DC-converter design)

Tables 7 through 12 summarize the SOFC stack and balance-of-plant component characteristics, constraints, and losses, based on current year 2005 and projected year 2015 technologies.

The SOFC stack anode fuel utilization used in the study was 0.70, based on H₂ and CO input into the stack. An increase in fuel utilization to 0.85 is presented in Appendix A for a single case study (System 1, Case 2b), which showed an advantage of +2 to +3 percent in SOFC APU system efficiency, but with additional stack weight resulting in +3 to +4 percent SOFC APU system weight.

Table 7. SOFC Stack Characteristics.

Parameter	2005	2015
Polarization Curve = f(T, p, Geometry)	i_o, r_{eff}	$i_o' = 6*i_o, r_{eff}' = 0.5*r_{eff}$
Anode Fuel Utilization	0.70	(same)
No. of Cells/Stack (Mass Estimate)	30.0	50.0
Interconnect Material	Metallic	Ceramic
Pressure Drop Through Stack	5% of Input Pressure	(same)
Thermal Losses From Stack	Via Natural Convection (-3%)	(same)
Operating Temperature Range	850°C \pm 75°C	(same)
Delta T Stack Cathode Exit – Inlet Limit	150°C	(same)

Table 8. Reformer Characteristics.

Parameter	2005	2015
Pressure Drop	2.5% of input pressure	(same)
Mass, Volume	0.0343 kg/kW, 0.1029 L/kW (As a function of SOFC power output)	(same)
Thermal Losses	5% of heat generated	(same)
Liquid Water Added to Prevent Coking	0.0 (Anode recycle only, such that H ₂ O/C >0.4	(same)
Operating Temperature Limit	950°C	(same)

Table 9. Catalytic Combustor Characteristics.

Parameter	2005	2015
H ₂ Conversion Efficiency	100% of H ₂ oxidized to H ₂ O	(same)
CO Conversion Efficiency	99.5% of CO oxidized to CO ₂	(same)
Mass, Volume	0.0467 kg/kW, 0.0156 L/kW (As a function of SOFC power output)	(same)
Pressure Drop Through Catalytic Combustor	1.5% of input pressure	(same)
Thermal Losses In Catalytic Combustor	5% of heat generated	
Temperature Limit for Combustor Exit	950°C	(same)

Table 10. Heat Exchanger Characteristics.

Parameter	2005	2015
Pressure Drop (Per Pass)	5% of input pressure	(same)
Mass, Volume	(Est. per work by Honeywell)	(same)
Thermal Loss	5% of total heat transferred	(same)
Effectiveness	HX1 = 0.75; HX2 = 0.30; HX3 = 1.0	(same)

Table 11. Turbomachinery Characteristics.

Parameter	2005	2015
Inlet Recovery Factor	0.90	(same)
Compressor/Turbine Efficiency	Per scaled mapping/0.85	(same)
Turbomachinery Mass and Volume	Based on small APU scaling	(same)
System Exit Pressure Margin to Ambient	5% above ambient	(same)
Temperature Limit for Turbine Inlet	1850°F (1010°C) Maximum for uncooled turbine	(same)

Table 12. Electrical Components and Other Characteristics.

Parameter	2005	2015
DC/DC Converter Efficiency for Stack Electric Output	0.90	(same)
Bearings/Motor/Inverter Efficiencies for LC2 (ECS) Drive	0.92 / 0.95 / 0.95	(same)
Bearings/Motor/Rectifier Efficiencies for Motor-Generator	0.92 / 0.95 / 0.95	(same)
Rectifier Mass, Volume	0.20 kg/kW, 0.067 L/kW (As a function of turbine power output)	(same)
Motor-Generator Mass, Volume	0.10 kg/kW, 0.020 L/kW (As a function of turbine power output)	(same)

Tables 13 and 14 list the SOFC APU model input and output parameters, respectively.

Table 13. SOFC APU Model Input Parameters.

Parameter	Units	Description	Model Value/Range
N	---	Stack geometry, Number of cells	550 to 950
A	cm ²	Stack geometry, Active area, expressed as L x W	400
St_c	---	Oxidant flowrate, Cathode stoichiometric ratio	4 to 5
St_a	---	Fuel flowrate, Anode stoichiometric ratio	1.0
U	---	Flow flowrate, anode Utilization	0.70
i	A	SOFC current demand	75 to 275
q_{loss}	kW	SOFC heat loss – from loss function	2 to 3
V_{fc}	V/cell	SOFC polarization Voltage – from polarization function	0.77 to 0.89
η_{fc}	---	SOFC Efficiency – from polarization function	0.68 to 0.77

Table 14. SOFC APU Model Output Parameters.

Parameter	Units	Description
P_{fc}	kW	SOFC output electrical power
T_{fc}	°C	SOFC bulk operating temperature, constrained to average of inlet and exit stream temperatures
T_{co}	°C	Outlet temperature, cathode
T_{ao}	°C	Outlet temperature, anode
p_{co}	psia	Outlet pressure, cathode
p_{ao}	psia	Outlet pressure, anode
y_{ao}(1-6)	mole frac.	Anode constituents
y_{co}(1-6)	mole frac.	Cathode constituents
ΔT_{o-i}	°C	Inlet to exit temperature difference across SOFC

The SOFC APU model output parameters include:

- Outlet gas mixture composition – based on electrochemical processing of hydrogen only (CO processed via a water gas shift [WGS] reaction)
- Anode/Cathode Stream flowrates, temperatures, and pressures
- SOFC operating temperature
- SOFC electrical power output.

The SOFC APU Model execution includes:

- One sheet of the model is dedicated to input parameter sets (i.e., cases)
- Input parameter set includes:
 - SOFC geometry
 - SOFC stoichiometry, utilization, and current draw
 - Altitude information (i.e., inlet conditions in case of ambient air source)
 - Heat exchanger effectiveness values
 - Turbomachinery pressure ratio and efficiency (from mapping)
 - Settings for mass/volume calculations
- Main cycle sheet used for initiating and tracking model runs
- Numerical stability and equilibrium tracked via graphical output (plotting of net output power and catalytic combustor temperature per iteration)
- Temperature and pressure limit feedback via color-coded cells on cycle sheet.

Figure 9 shows a sample main cycle sheet.

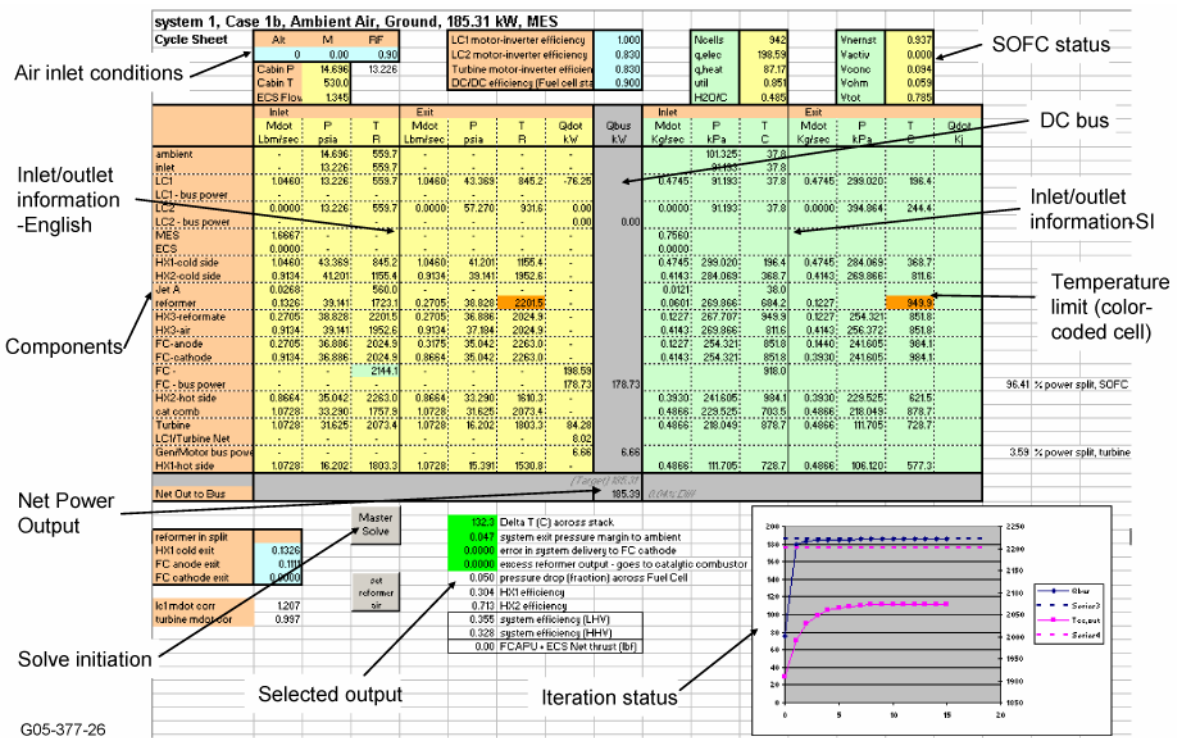


Figure 9. SOFC APU Model Sample Main Cycle Sheet.

The model output data are presented in various forms:

- Summary for each component on individual module status sheets
- Final cycle sheet (pressure, temperature, and massflow for each component, power on DC bus, etc.)
- Graphical representation of SOFC polarization
- Mass/volume roll-up for overall system; power/energy density calculations
- Summary of thrust calculations
- Graphical representation of reformer/stack sub-system with massflow, temperature and anode/cathode constituent breakdown
- Graphical representation of thermodynamic inlet/exit conditions for each component superimposed on system schematic
- Tabular summary of pertinent model results.

The system schematic is presented with cycle data labeled at each component, as shown in the sample schematic (Figure 10).

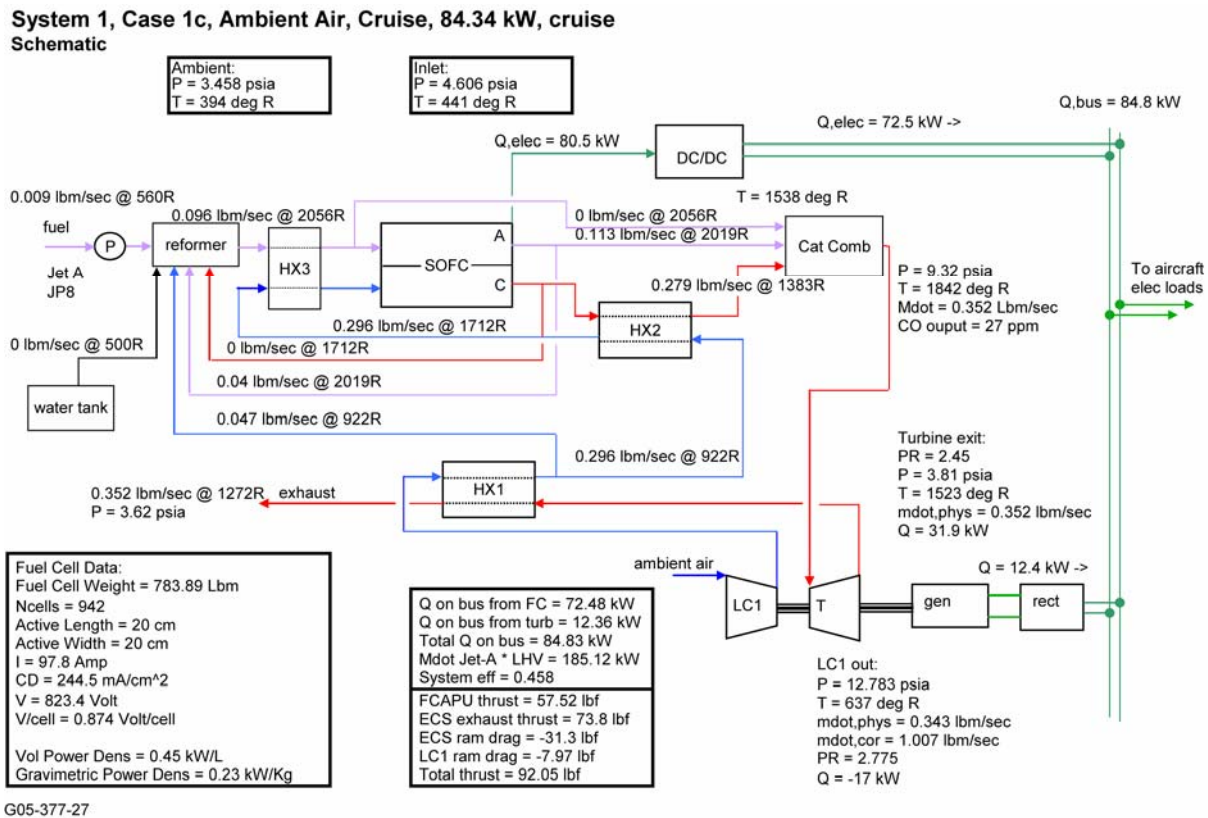


Figure 10. Sample SOFC APU System Schematic with Component Output Data. (System 1, Case 1C, Ambient Air, Cruise, 84.34 kW)

Cycle data for each component is also tabulated as shown in Table 15.

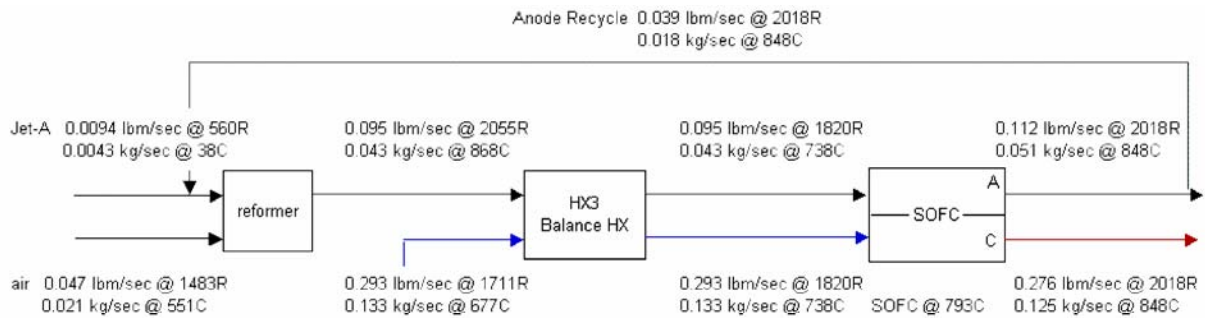
Table 15. Sample SOFC APU Component Output Data Tabulation.

	Inlet			Exit		
	Mdot Lbm/sec	P psia	T R	Mdot Lbm/sec	P psia	T R
ambient inlet	-	14.696	559.7	-	-	-
LC1	0.6392	13.226	559.7	0.6392	29.416	750.8
LC1 - bus power	-	-	-	-	-	-
LC2	0.0000	13.226	559.7	0.0000	57.270	931.6
LC2 - bus power	-	-	-	-	-	-
MES	1.6667	-	-	-	-	-
ECS	0.0000	-	-	-	-	-
HX1-cold side	0.6392	29.416	750.8	0.6392	27.945	1107.9
HX2-cold side	0.5587	27.945	1107.9	0.5587	26.548	1841.4
Jet A reformer	0.0163	0.0805	26.548	0.1643	26.335	2142.0
HX3-reformate	0.1643	26.335	2142.0	0.1643	25.018	1929.2
HX3-air	0.5587	26.548	1841.4	0.5587	25.220	1929.2
FC-anode	0.1643	25.018	1929.2	0.1931	23.767	2127.9
FC-cathode	0.5587	25.018	1929.2	0.5300	23.767	2127.9
FC - bus power	-	-	2028.7	-	-	-
HX2-hot side	0.5300	23.767	2127.9	0.5300	22.579	1525.3
cat comb	0.6555	22.579	1660.4	0.6555	21.450	1964.4
Turbine	0.6555	21.450	1964.4	0.6555	16.213	1851.8
LC1/Turbine Net	-	-	-	-	-	-
Gen/Motor bus power	-	-	-	-	-	-
HX1-hot side	0.6555	16.213	1851.8	0.6555	15.403	1541.0

G05-377-28

(Note: Cells highlighted in Brown or Blue indicate components reaching temperature limits.)

Subsystem schematics of the SOFC stack and reformer, showing anode/cathode data are also available from the model, as shown in Figure 11.



	Anode mol/frac	Cathode mol/frac		Anode mol/frac	Cathode mol/frac		Anode mol/frac	Cathode mol/frac
H ₂	0.178	0.000		0.174	0.000		0.048	0.000
CO	0.186	0.000		0.190	0.000		0.052	0.000
CO ₂	0.074	0.003		0.071	0.003		0.209	0.003
O ₂	0.000	0.208		0.000	0.208		0.000	0.165
N ₂	0.480	0.772		0.480	0.772		0.480	0.814
H ₂ O	0.081	0.017		0.084	0.017		0.211	0.018

G05-377-29

Figure 11. Sample SOFC Stack and Reformer Schematic.
(System 1, Case 1C, Ambient Air, Cruise, 84.34 kW)

Table 16 shows sample performance results from the model in tabulated format.

Table 16. Sample SOFC APU System Performance Output Data Tabulation.

Parameter Description	Gate (107.5 kW)	MES (185.3 kW)	Cruise (84.3 kW)	Cruise, EO (124.1 kW)
SOFC number of cells	942	942	942	942
SOFC active area size (cm ²)	20 x 20	20 x 20	20 x 20	20 x 20
SOFC current demand (A)	164.3	268.6	97.8	139.3
SOFC volt/cell (V)	0.86	0.78	0.87	0.85
SOFC efficiency	0.75	0.69	0.76	0.75
SOFC power output on bus (kW)	119.1	178.7	72.5	100.9
SOFC operating temperature (°C)	853.9	918.0	793.7	821.2
SOFC inlet/exit dT (°C)	110.4	132.3	110.1	119.2
Reformer operating temperature (°C)	916.9	949.9	868.8	883.4
Anode recycle amount	0.35	0.35	0.35	0.35
Compressor PR	2.22	3.28	2.78	3.75
Compressor corrected flow (lbm/s)	0.74	1.21	1.01	1.44
Compressor efficiency	0.75	0.79	0.76	0.78
Turbine power output on bus (kW)	-11.67	6.66	12.36	23.30
Turbine PR	1.32	1.95	2.45	3.30
Turbine corrected flow (lbm/s)	0.87	1.00	1.05	1.12
Turbine efficiency	0.85	0.85	0.85	0.85
Total power on bus (kW)	107.5	185.4	84.8	124.2
Combustor operating temperature (°C)	818.2	878.7	750.1	777.5
Combustor CO output (ppm exhaust)	34	40	27	30
Combustor CO output (g/kg fuel)	1.31	1.55	0.96	1.07
Additional fuel to combustor	0.0	0.0	0.0	0.0
System efficiency	0.34	0.35	0.46	0.47
Net Thrust, aircraft basis (lbf)	0.0	0.0	92.0	111.5

2.5 SOFC APU System Performance

Case studies over a large range of the SOFC APU system power output have been performed, based on the Regional Jet mission load profile established in Part I/Task 1.1. A summary of Case Studies 1 through 7 is tabulated in Table 17, for situations with the SOFC APU supplying total power at the terminal gate and for Main Engine Start (MES), as well as splitting power supply with the main engine generator and/or providing full power during Cruise operation at altitude. Cases 1 and 2 are larger systems, allowing full electric power to stay on during MES. Cases 3 and 4 are the same as Cases 1 and 2, except for the use of the cabin air supply instead of an ambient air supply for the SOFC APU. Case 5 assumes the use of ground equipment for MES, and a split power supply with the main engine generator during Cruise. Cases 6 and 7 are minimum-sized APU cases, with the original (prior to use of SOFC) bleed power kept the same as in Cases 1 and 2, but with electrical power reduced similar to a 50-passenger Regional Jet. These two cases (6 and 7) were considered with additional input from the aircraft OEM, in that other than bleed load, the electrical load of a 90-passenger Regional Jet may be somewhat similar to that of a 50-passenger Regional Jet. Cases 6 and 7 also assume most electric power to be turned off during MES, and use of only minimum electric load during Cruise.

Table 17. Summary of SOFC APU System Case Studies.

		SOFC APU Power, kw						
		Air			Cruise		SOFC	
		Supply	Gate	MES	Normal	1-Engine Out	Full Power	Size
System 1	Case 1	Ambient	107.5	185.4	84.8	124.2		Maximum
	Case 2	Ambient	107.5	185.4			164	
System 2	Case 3	Cabin	107.5	185.4	84.5	125.4		
	Case 4	Cabin	107.5	185.4			164	
System 1	Case 5	Ambient	113	Ground	84.3			
	Case 6	Ambient	86.35	116	84.1	100		
	Case 7	Ambient	86.35	116			116.2	Minimum

Normal – SOFC powers ECS & de-ice in flight, main engine powers electric Full Power – SOFC powers all ECS, de-ice and electric load

Case 1	Maximum SOFC size with all electrical on at MES and main engine power split at Cruise
Case 2	Same as Case 1 except SOFC provides all power at Cruise
Case 3	Same as Case 1 except using cabin air (minimum impact)
Case 4	Same as Case 2 except using cabin air (minimum impact)
Case 5	Ground equipment used for MES to reduce SOFC size
Case 6	Reduced electrical load mostly off at MES. Main engine power split at Cruise
Case 7	Minimum SOFC size same as Case 6 except SOFC provides all power at Cruise

Ground and Cruise performance estimates were iterated based on the following criteria:

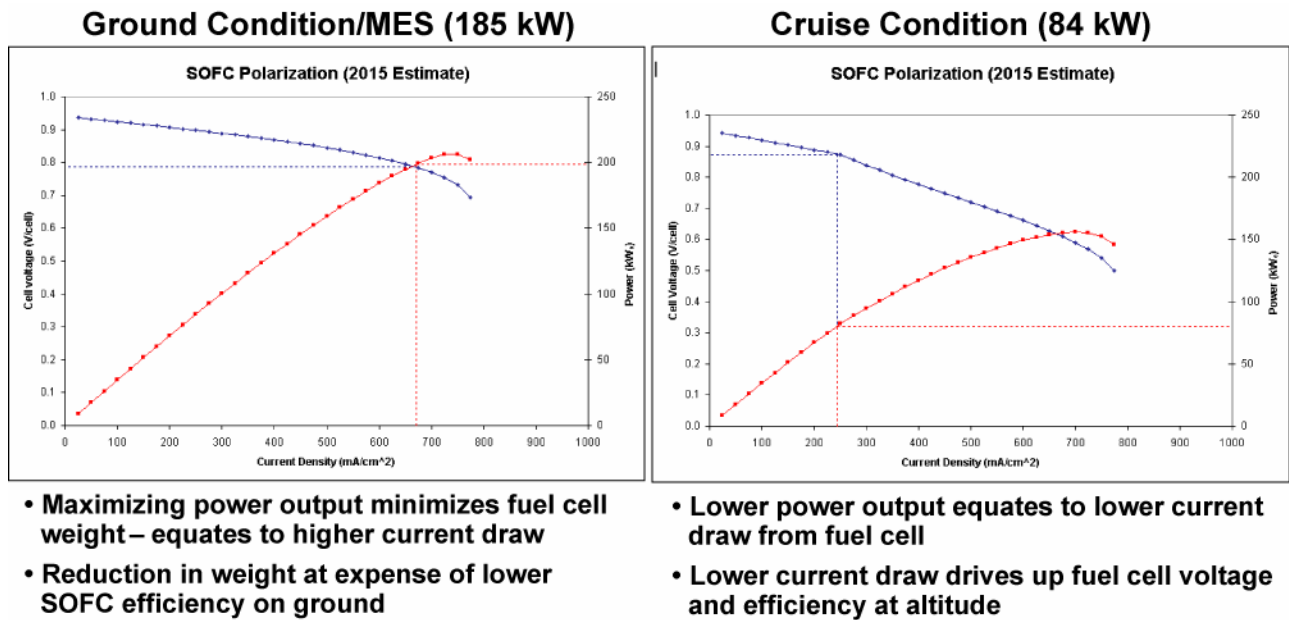
Ground Conditions:

- SOFC power output maximized to reduce weight
- Reduction in weight at expense of lower SOFC efficiency on ground
- Added waste heat drives up overall temperature in system components
- Component temperature limits constrain system such that power split on ground is ~95 percent due to fuel cell
- Lower overall system efficiency seen due to fuel cell sizing and power split ratio.

Cruise Conditions:

- Larger corrected flows drive up performance of turbomachinery, changing power split to ~70 percent due to fuel cell
- Lower power levels cause “throttling” of stack in flight, reducing current demand
- Lower current demand drives SOFC efficiency higher, reducing waste heat output relative to ground condition
- Less waste heat output reduces overall temperature levels in system components
 - No temperature limits reached in flight
- Larger power split and higher SOFC efficiency drives up overall system efficiency at altitude.

Figure 12 illustrates a visual method for better understanding of the effects of fuel cell sizing and performance for On Ground vs. In-Flight Cruise conditions.



G05-377-32

Figure 12. SOFC Stack Performance On Ground Versus In-Flight Cruise.

SOFC APU Model results for the various Cases are given in the Tables and Figures listed in Table 18.

Table 18. Summary of SOFC APU Performance Model Cases and Output Data.

System No.	Case No.	Conditions	Table No.	Fig. No.
1	1(all)	System 1, Case 1 Summary	19	---
1	1(a)	Ambient Air, Ground, 107.45 kW, Gate	---	13
1	1(b)	MES, 185.3 kW	---	14
1	1(c)	Cruise, 84.3 kW	---	15
1	1(d)	Cruise, EO, 124.1 kW	---	16
1	2(all)	System 1, Case 2 Summary	20	---
1	2(a)	Ambient Air, 5:1 Compressor, Ground, 107.5 kW, Gate	---	17
1	2(b)	Ambient Air, 5:1 Compressor, 185.31 kW, MES	---	18
1	2(c)	Ambient Air, 5:1 Compressor, Cruise, 164. kW, Full Power	---	19
2	3(all)	System 2, Case 3 Summary	21	---
2	3(a)	Cabin Air, Ground, 107.45 kW, Gate	---	20
2	3(b)	Cabin Air, Ground, 185.31 kW, MES	---	21
2	3(c)	Cabin Air, Cruise, 84.34 kW	---	22
2	3(d)	Cabin Air, Cruise, 124.15 kW, Engine Out	---	23
2	4(all)	System 2, Case 4 Summary	22	---
2	4(a)	Cabin Air, Ground, 107.45 kW, Gate	---	24
2	4(b)	Cabin Air, Ground, 185.31 kW, MES	---	25
2	4(c)	Cabin Air, Cruise, 164.00 kW, Full Power	---	26
1	5(all)	System 1, Case 1 Summary	23	---
1	5(a)	Ambient Air, Ground, 112.82 kW, Gate/MES	---	27
1	5(b)	Ambient Air, Cruise, 84.34 kW, Cruise Power	---	28
1	6(all)	System 1, Case 6 Summary)	24	---
1	6(a)	Ambient Air, Ground, 86.26 kW, Gate	---	29
1	6(b)	Ambient Air, Ground, 116 kW, MES	---	30
1	6(c)	Ambient Air, Cruise, 84.34 kW, Cruise Power	---	31
1	6(d)	Ambient Air, Cruise, 100 kW, Engine Out	---	32
1	7(all)	System 1, Case 7 Summary	25	---
1	7(a)	Ambient Air, Ground, 86.26 kW, Gate	---	33
1	7(b)	Ambient Air, Ground, 116 kW, MES	---	34
1	7(c)	Ambient Air, Cruise, 116 kW, Full Power	---	35

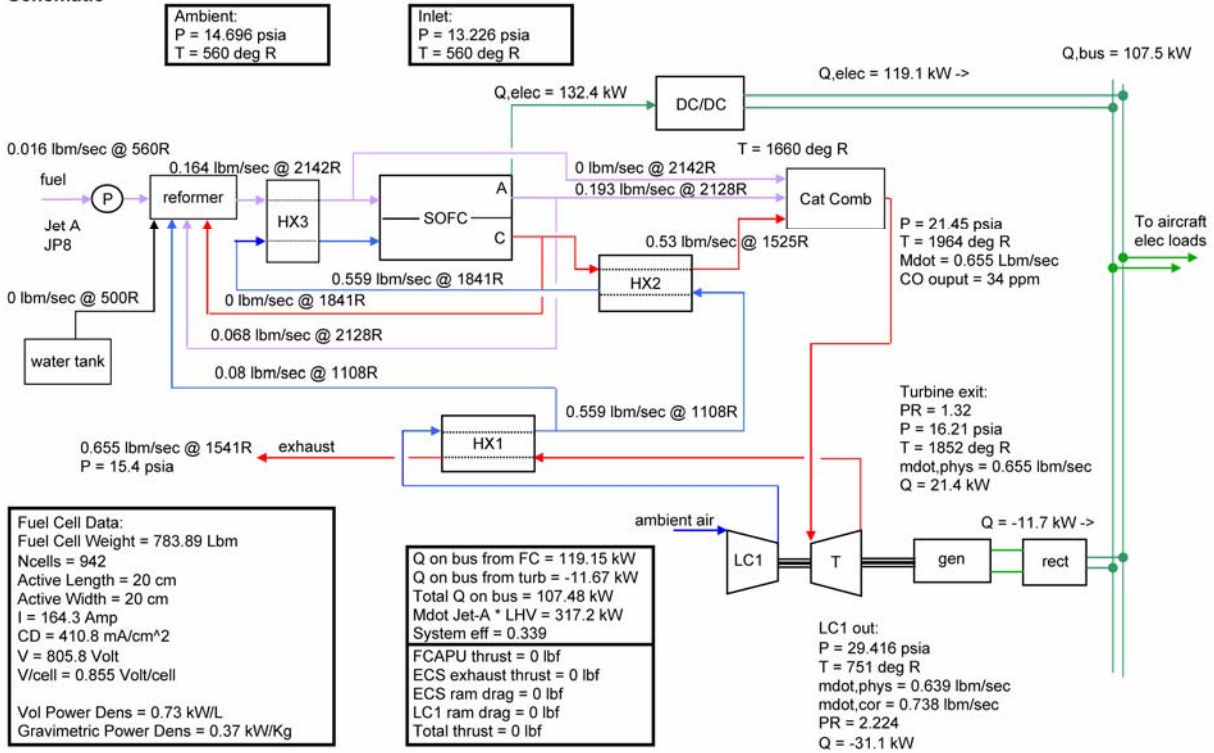
Table 19. SOFC APU System 1, Case 1 Performance Results Summary.

	a	b	c	d
Parameter Description	Gate (107.5 kW)	MES (185.3 kW)	Cruise (84.3 kW)	Cruise, EO (124.1 kW)
SOFC number of cells	942	942	942	942
SOFC active area size (cm ²)	20 x 20	20 x 20	20 x 20	20 x 20
SOFC current demand (A)	164.3	268.6	97.8	139.3
SOFC volt/cell (V)	0.86	0.78	0.87	0.85
SOFC efficiency	0.75	0.69	0.76	0.75
SOFC power output on bus (kW)	119.1	178.7	72.5	100.9
SOFC operating temperature (°C)	853.9	918.0	793.7	821.2
SOFC inlet/exit dT (°C)	110.4	132.3	110.1	119.2
Reformer operating temperature (°C)	916.9	949.9	868.8	883.4
Anode recycle amount	0.35	0.35	0.35	0.35
Compressor PR	2.22	3.28	2.78	3.75
Compressor corrected flow (lbm/s)	0.74	1.21	1.01	1.44
Compressor efficiency	0.75	0.79	0.76	0.78
Turbine power output on bus (kW)	-11.67	6.66	12.36	23.30
Turbine PR	1.32	1.95	2.45	3.30
Turbine corrected flow (lbm/s)	0.87	1.00	1.05	1.12
Turbine efficiency	0.85	0.85	0.85	0.85
Total power on bus (kW)	107.5	185.4	84.8	124.2
Combustor operating temperature (°C)	818.2	878.7	750.1	777.5
Combustor CO output (ppm exhaust)	34	40	27	30
Combustor CO output (g/kg fuel)	1.31	1.55	0.96	1.07
Additional fuel to combustor	0.0	0.0	0.0	0.0
System efficiency	0.34	0.35	0.46	0.47
Net Thrust, aircraft basis (lbf)	0.0	0.0	92.0	111.5

G05-377-33

Figure 13. SOFC APU System 1, Case 1(a) Performance Results.

System 1, Case 1a, Ambient Air, Ground, 107.45 kW, Gate Schematic



G05-377-34

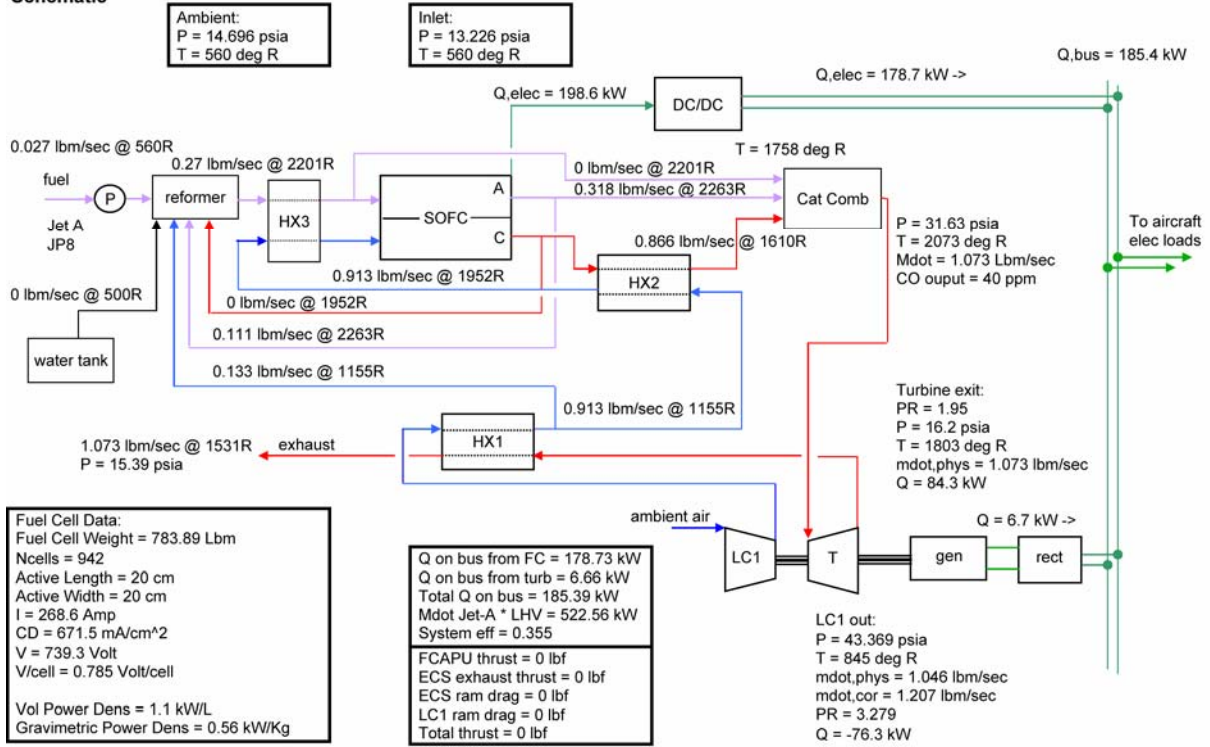
	Inlet			Exit		
	Mdot Lbm/sec	P psia	T R	Mdot Lbm/sec	P psia	T R
ambient	-	14.696	559.7	-	-	-
inlet	-	13.226	559.7	-	-	-
LC1	0.6392	13.226	559.7	0.6392	29.416	750.8
LC1 - bus power	-	-	-	-	-	-
LC2	0.0000	13.226	559.7	0.0000	57.270	931.6
LC2 - bus power	-	-	-	-	-	-
MES	1.6667	-	-	-	-	-
ECS	0.0000	-	-	-	-	-
HX1-cold side	0.6392	29.416	750.8	0.6392	27.945	1107.9
HX2-cold side	0.5587	27.945	1107.9	0.5587	26.548	1841.4
Jet A	0.0163	-	560.0	-	-	-
reformer	0.0805	26.548	1629.4	0.1643	26.335	2142.0
HX3-reformate	0.1643	26.335	2142.0	0.1643	25.018	1929.2
HX3-air	0.5587	26.548	1841.4	0.5587	25.220	1929.2
FC-anode	0.1643	25.018	1929.2	0.1931	23.767	2127.9
FC-cathode	0.5587	25.018	1929.2	0.5300	23.767	2127.9
FC -	-	-	2028.7	-	-	-
FC - bus power	-	-	-	-	-	-
HX2-hot side	0.5300	23.767	2127.9	0.5300	22.579	1525.3
cat comb	0.6555	22.579	1660.4	0.6555	21.450	1964.4
Turbine	0.6555	21.450	1964.4	0.6555	16.213	1851.8
LC1/Turbine Net	-	-	-	-	-	-
Gen/Motor bus power	-	-	-	-	-	-
HX1-hot side	0.6555	16.213	1851.8	0.6555	15.403	1541.0

G05-377-35

Note: Cells highlighted in Brown or Blue indicate components reaching temperature limits.

Figure 14. SOFC APU System 1, Case 1(b) Performance Results.

System 1, Case 1b, Ambient Air, Ground, 185.31 kW, MES
Schematic



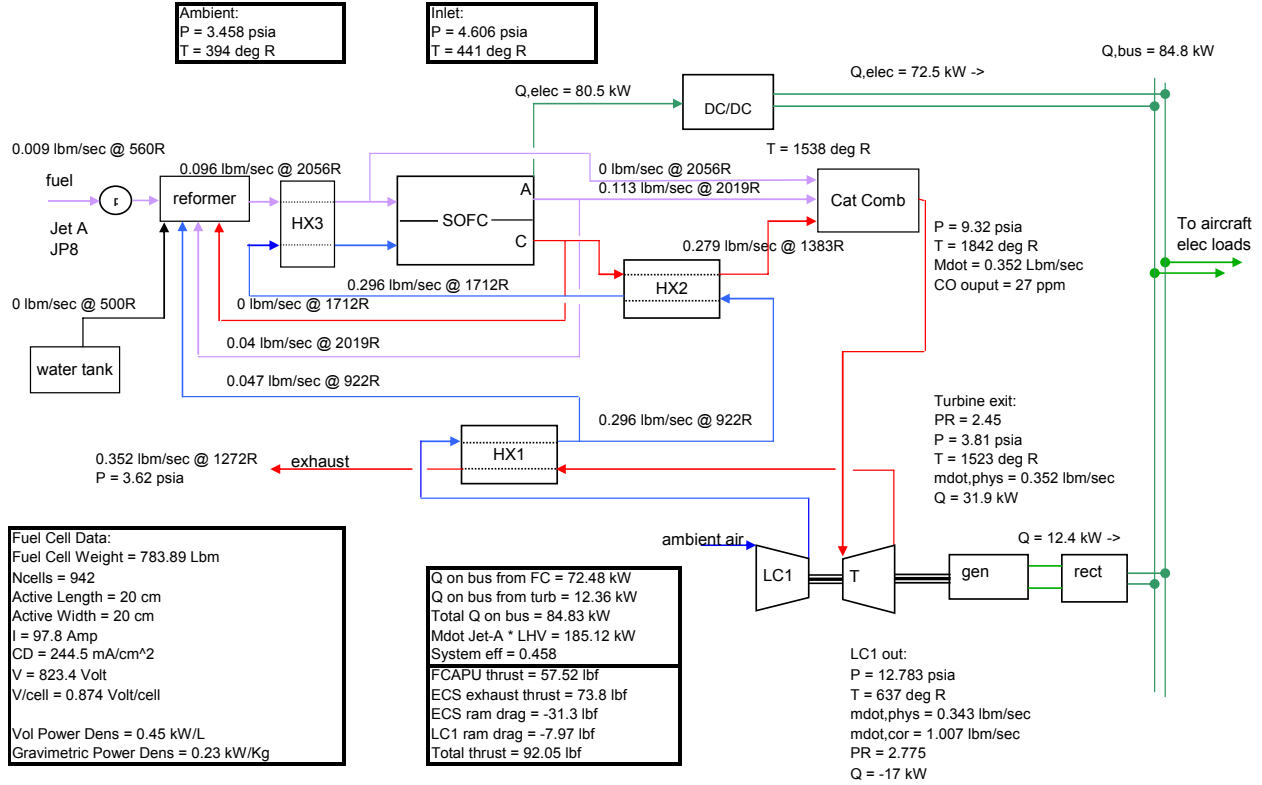
G05-377-36

	Inlet			Exit		
	Mdot Lbm/sec	P psia	T R	Mdot Lbm/sec	P psia	T R
ambient	-	14.696	559.7	-	-	-
inlet	-	13.226	559.7	-	-	-
LC1	1.0460	13.226	559.7	1.0460	43.369	845.2
LC1 - bus power	-	-	-	-	-	-
LC2	0.0000	13.226	559.7	0.0000	57.270	931.6
LC2 - bus power	-	-	-	-	-	-
MES	1.6667	-	-	-	-	-
ECS	0.0000	-	-	-	-	-
HX1-cold side	1.0460	43.369	845.2	1.0460	41.201	1155.4
HX2-cold side	0.9134	41.201	1155.4	0.9134	39.141	1952.6
Jet A	0.0268	-	560.0	-	-	-
reformer	0.1326	39.141	1723.1	0.2705	38.828	2201.5
HX3-reformate	0.2705	38.828	2201.5	0.2705	36.886	2024.9
HX3-air	0.9134	39.141	1952.6	0.9134	37.184	2024.9
FC-anode	0.2705	36.886	2024.9	0.3175	35.042	2263.0
FC-cathode	0.9134	36.886	2024.9	0.8664	35.042	2263.0
FC -	-	-	2144.1	-	-	-
FC - bus power	-	-	-	-	-	-
HX2-hot side	0.8664	35.042	2263.0	0.8664	33.290	1610.3
cat comb	1.0728	33.290	1757.9	1.0728	31.625	2073.4
Turbine	1.0728	31.625	2073.4	1.0728	16.202	1803.3
LC1/Turbine Net	-	-	-	-	-	-
Gen/Motor bus power	-	-	-	-	-	-
HX1-hot side	1.0728	16.202	1803.3	1.0728	15.391	1530.8

G05-377-37

Figure 15. SOFC APU System 1, Case 1(c) Performance Results.

System 1, Case 1c, Ambient Air, Cruise, 84.34 kW, cruise Schematic



G05-377-038

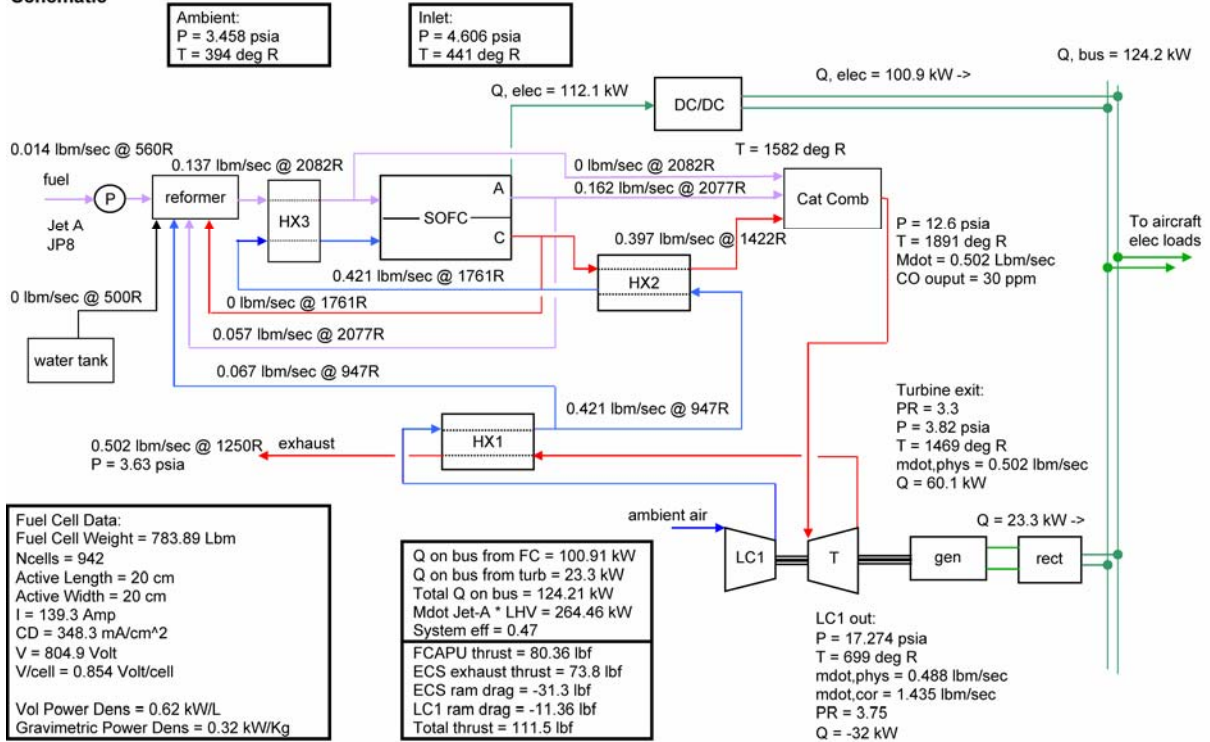
	Inlet			Exit		
	Mdot Lbm/sec	P psia	T R	Mdot Lbm/sec	P psia	T R
ambient	-	3.458	393.9	-	-	-
inlet	-	4.606	440.6	-	-	-
LC1	0.3426	4.606	440.6	0.3426	12.783	636.7
LC1 - bus power	-	-	-	-	-	-
LC2	0.0000	4.606	440.6	0.0000	19.945	733.8
LC2 - bus power	-	-	-	-	-	-
MES	0.0000	-	-	-	-	-
ECS	1.4167	-	-	-	-	-
HX1-cold side	0.3426	12.783	636.7	0.3426	12.143	922.4
HX2-cold side	0.2956	12.143	922.4	0.2956	11.536	1712.0
Jet A	0.0095	-	560.0	-	-	-
reformer	0.0470	11.536	1484.2	0.0961	11.444	2055.5
HX3-reformate	0.0961	11.444	2055.5	0.0961	10.872	1821.1
HX3-air	0.2956	11.536	1712.0	0.2956	10.959	1821.1
FC-anode	0.0961	10.872	1821.1	0.1132	10.328	2019.3
FC-cathode	0.2956	10.872	1821.1	0.2785	10.328	2019.3
FC -	-	-	1920.3	-	-	-
FC - bus power	-	-	-	-	-	-
HX2-hot side	0.2785	10.328	2019.3	0.2785	9.812	1382.9
cat comb	0.3521	9.812	1537.6	0.3521	9.321	1841.7
Turbine	0.3521	9.321	1841.7	0.3521	3.812	1522.9
LC1/Turbine Net	-	-	-	-	-	-
Gen/Motor bus power	-	-	-	-	-	-
HX1-hot side	0.3521	3.812	1522.9	0.3521	3.622	1272.4

G05-377-39

Note: Cells highlighted in Brown or Blue indicate components reaching temperature limits.

Figure 16. SOFC APU System 1, Case 1(d) Performance Results.

System 1, Case 1d, Ambient Air, Cruise, 124.15 kW, engine out Schematic



G05-377-40

	Inlet			Exit		
	Mdot Lbm/sec	P psia	T R	Mdot Lbm/sec	P psia	T R
ambient	-	3.458	393.9	-	-	-
inlet	-	4.606	440.6	-	-	-
LC1	0.4882	4.606	440.6	0.4882	17.274	699.4
LC1 - bus power	-	-	-	-	-	-
LC2	0.0000	4.606	440.6	0.0000	19.945	733.8
LC2 - bus power	-	-	-	-	-	-
MES	0.0000	-	-	-	-	-
ECS	1.4167	-	-	-	-	-
HX1-cold side	0.4882	17.274	699.4	0.4882	16.410	947.3
HX2-cold side	0.4211	16.410	947.3	0.4211	15.589	1760.8
Jet A	0.0135	-	560.0	-	-	-
reformer	0.0671	15.589	1526.5	0.1372	15.465	2081.6
HX3-reformate	0.1372	15.465	2081.6	0.1372	14.692	1862.3
HX3-air	0.4211	15.589	1760.8	0.4211	14.810	1862.3
FC-anode	0.1372	14.692	1862.3	0.1616	13.957	2077.0
FC-cathode	0.4211	14.692	1862.3	0.3967	13.957	2076.9
FC -	-	-	1969.8	-	-	-
FC - bus power	-	-	-	-	-	-
HX2-hot side	0.3967	13.957	2076.9	0.3967	13.259	1422.3
cat comb	0.5017	13.259	1582.0	0.5017	12.596	1891.1
Turbine	0.5017	12.596	1891.1	0.5017	3.817	1469.3
LC1/Turbine Net	-	-	-	-	-	-
Gen/Motor bus power	-	-	-	-	-	-
HX1-hot side	0.5017	3.817	1469.3	0.5017	3.626	1250.3

G05-377-41

Note: Cells highlighted in Brown or Blue indicate components reaching temperature limits.

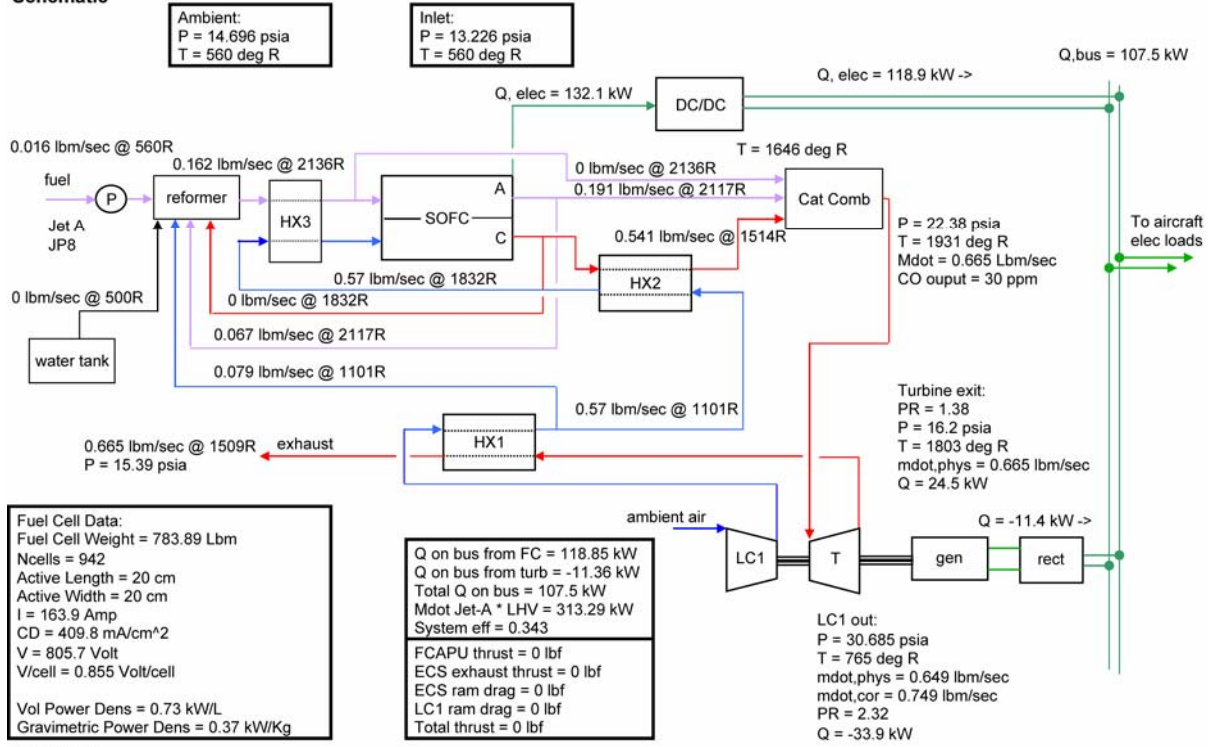
Table 20. SOFC APU System 1, Case 2 Performance Results Summary.

	a	b	c
Parameter Description	Gate (107.5 kW)	MES (185.3 kW)	Cruise, Full Power (164.0 kW)
SOFC number of cells	942	942	942
SOFC active area size (cm ²)	20 x 20	20 x 20	20 x 20
SOFC current demand (A)	163.9	268.6	180.8
SOFC volt/cell (V)	0.86	0.79	0.84
SOFC efficiency	0.75	0.69	0.73
SOFC power output on bus (kW)	118.9	179.0	128.2
SOFC operating temperature (°C)	847.9	915.4	847.9
SOFC inlet/exit dT (°C)	110.1	130.7	126.5
Reformer operating temperature (°C)	913.7	949.6	898.2
Anode recycle amount	0.35	0.35	0.35
Compressor PR	2.32	3.46	5.00
Compressor corrected flow (lbm/s)	0.75	1.23	1.86
Compressor efficiency	0.74	0.77	0.78
Turbine power output on bus (kW)	-11.36	6.34	35.81
Turbine PR	1.38	2.06	4.40
Turbine corrected flow (lbm/s)	0.84	0.96	1.10
Turbine efficiency	0.85	0.85	0.85
Total power on bus (kW)	107.5	185.4	164.0
Combustor operating temperature (°C)	799.4	872.4	806.1
Combustor CO output (ppm exhaust)	30	39	33
Combustor CO output (g/kg fuel)	1.22	1.54	1.19
Additional fuel to combustor	0.0	0.0	0.0
System efficiency	0.34	0.35	0.48
Net Thrust, aircraft basis (lbf)	0.0	0.0	131.5

G05-377-42

Figure 17. SOFC APU System 1, Case 2(a) Performance Results.

System 1, Case 2a, Ambient Air, 5:1 Compr, Ground, 107.45 kW, Gate Schematic



G05-377-43

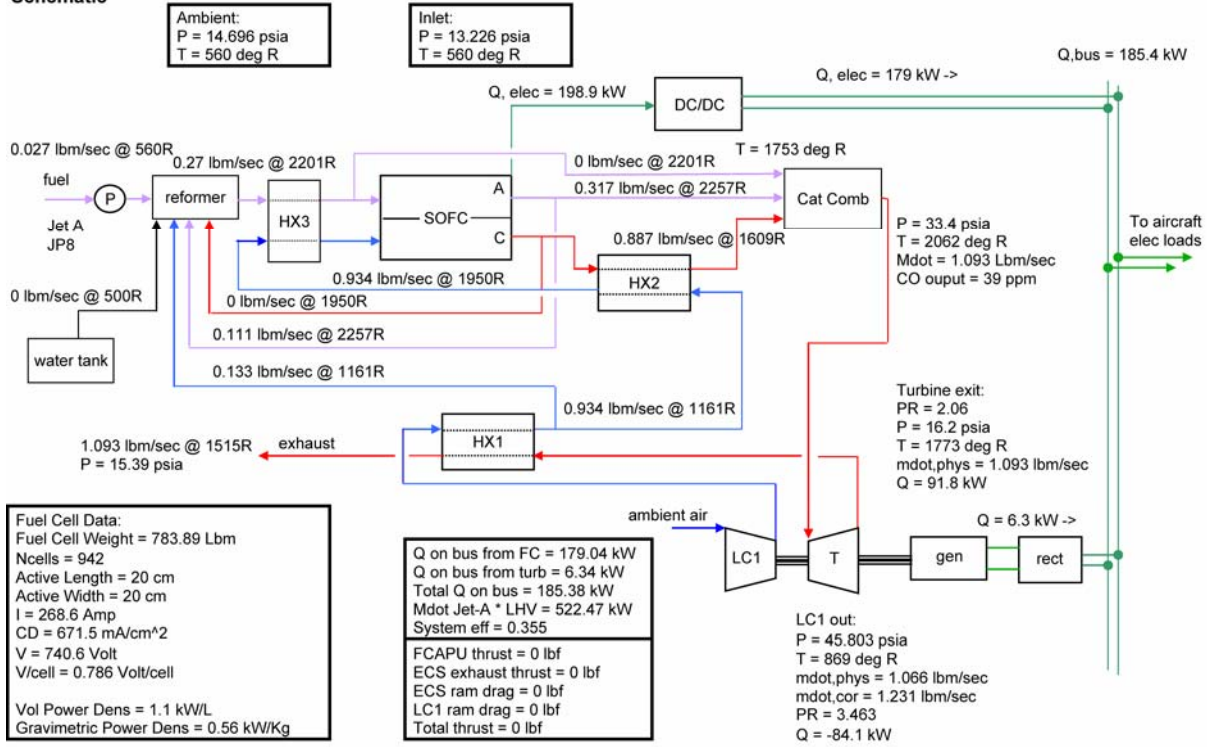
	Inlet			Exit		
	Mdot Lbm/sec	P psia	T R	Mdot Lbm/sec	P psia	T R
ambient	-	14.696	559.7	-	-	-
inlet	-	13.226	559.7	-	-	-
LC1	0.6492	13.226	559.7	0.6492	30.685	764.9
LC1 - bus power	-	-	-	-	-	-
LC2	0.0000	13.226	559.7	0.0000	57.270	931.6
LC2 - bus power	-	-	-	-	-	-
MES	1.6667	-	-	-	-	-
ECS	0.0000	-	-	-	-	-
HX1-cold side	0.6492	30.685	764.9	0.6492	29.151	1101.0
HX2-cold side	0.5698	29.151	1101.0	0.5698	27.693	1831.6
Jet A	0.0161	-	560.0	-	-	-
reformer	0.0795	27.693	1620.8	0.1624	27.472	2136.2
HX3-reformate	0.1624	27.472	2136.2	0.1624	26.098	1918.7
HX3-air	0.5698	27.693	1831.6	0.5698	26.309	1918.7
FC-anode	0.1624	26.098	1918.7	0.1911	24.793	2116.9
FC-cathode	0.5698	26.098	1918.7	0.5411	24.793	2116.9
FC -	-	-	2017.9	-	-	-
FC - bus power	-	-	-	-	-	-
HX2-hot side	0.5411	24.793	2116.9	0.5411	23.554	1513.7
cat comb	0.6653	23.554	1645.6	0.6653	22.376	1930.6
Turbine	0.6653	22.376	1930.6	0.6653	16.203	1803.3
LC1/Turbine Net	-	-	-	-	-	-
Gen/Motor bus power	-	-	-	-	-	-
HX1-hot side	0.6653	16.203	1803.3	0.6653	15.393	1509.1

G05-377-44

Note: Cells highlighted in Brown or Blue indicate components reaching temperature limits.

Figure 18. SOFC APU System 1, Case 2(b) Performance Results.

System 1, Case 2b, Ambient Air, 5:1 Compr, Ground, 185.31 kW, MES Schematic



G05-377-45

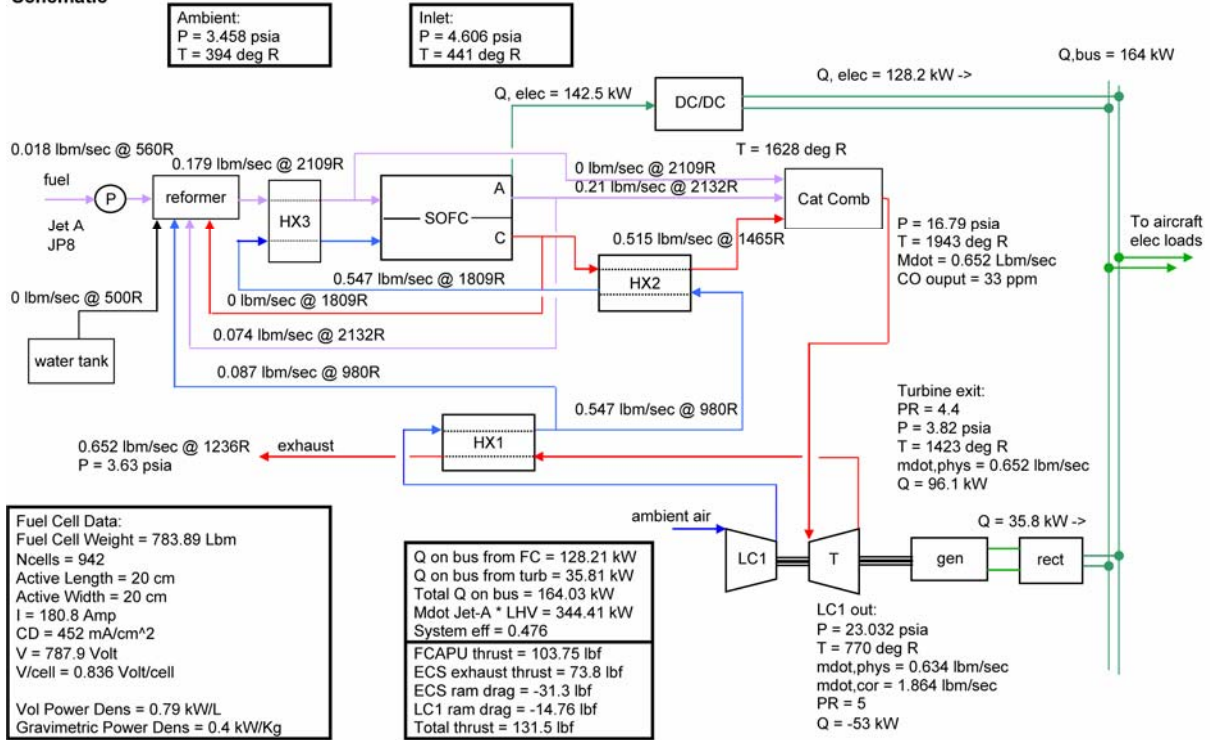
	Inlet			Exit		
	Mdot Lbm/sec	P psia	T R	Mdot Lbm/sec	P psia	T R
ambient	-	14.696	559.7	-	-	-
inlet	-	13.226	559.7	-	-	-
LC1	1.0663	13.226	559.7	1.0663	45.803	868.5
LC1 - bus power	-	-	-	-	-	-
LC2	0.0000	13.226	559.7	0.0000	57.270	931.6
LC2 - bus power	-	-	-	-	-	-
MES	1.6667	-	-	-	-	-
ECS	0.0000	-	-	-	-	-
HX1-cold side	1.0663	45.803	868.5	1.0663	43.513	1160.9
HX2-cold side	0.9337	43.513	1160.9	0.9337	41.337	1949.7
Jet A	0.0268	-	560.0	-	-	-
reformer	0.1325	41.337	1722.6	0.2704	41.007	2201.0
HX3-reformate	0.2704	41.007	2201.0	0.2704	38.956	2021.6
HX3-air	0.9337	41.337	1949.7	0.9337	39.270	2021.6
FC-anode	0.2704	38.956	2021.6	0.3175	37.008	2256.9
FC-cathode	0.9337	38.956	2021.6	0.8867	37.008	2256.9
FC -	-	-	2139.4	-	-	-
FC - bus power	-	-	-	-	-	-
HX2-hot side	0.8867	37.008	2256.9	0.8867	35.158	1608.7
cat comb	1.0930	35.158	1752.6	1.0930	33.400	2062.1
Turbine	1.0930	33.400	2062.1	1.0930	16.198	1772.9
LC1/Turbine Net	-	-	-	-	-	-
Gen/Motor bus power	-	-	-	-	-	-
HX1-hot side	1.0930	16.198	1772.9	1.0930	15.388	1514.8

G05-377-46

Note: Cells highlighted in Brown or Blue indicate components reaching temperature limits.

Figure 19. SOFC APU System 1, Case 2(c) Performance Results.

System 1, Case 2c, Ambient Air, 5:1 Compr, Cruise, 164.00 kW, Full Power Schematic



G05-377-47

	Inlet			Exit		
	Mdot Lbm/sec	P psia	T R	Mdot Lbm/sec	P psia	T R
ambient	-	3.458	393.9	-	-	-
inlet	-	4.606	440.6	-	-	-
LC1	0.6339	4.606	440.6	0.6339	23.032	769.7
LC1 - bus power	-	-	-	-	-	-
LC2	0.0000	4.606	440.6	0.0000	19.945	733.8
LC2 - bus power	-	-	-	-	-	-
MES	0.0000	-	-	-	-	-
ECS	1.4167	-	-	-	-	-
HX1-cold side	0.6339	23.032	769.7	0.6339	21.880	980.1
HX2-cold side	0.5465	21.880	980.1	0.5465	20.786	1809.4
Jet A	0.0176	-	560.0	-	-	-
reformer	0.0874	20.786	1570.8	0.1786	20.620	2108.5
HX3-reformate	0.1786	20.620	2108.5	0.1786	19.589	1903.9
HX3-air	0.5465	20.786	1809.4	0.5465	19.747	1903.9
FC-anode	0.1786	19.589	1903.9	0.2103	18.609	2131.5
FC-cathode	0.5465	19.589	1903.9	0.5149	18.609	2131.5
FC -	-	-	2017.8	-	-	-
FC - bus power	-	-	-	-	-	-
HX2-hot side	0.5149	18.609	2131.5	0.5149	17.679	1464.8
cat comb	0.6515	17.679	1628.0	0.6515	16.795	1942.6
Turbine	0.6515	16.795	1942.6	0.6515	3.817	1423.1
LC1/Turbine Net	-	-	-	-	-	-
Gen/Motor bus power	-	-	-	-	-	-
HX1-hot side	0.6515	3.817	1423.1	0.6515	3.626	1235.8

G05-377-48

Note: Cells highlighted in Brown or Blue indicate components reaching temperature limits.

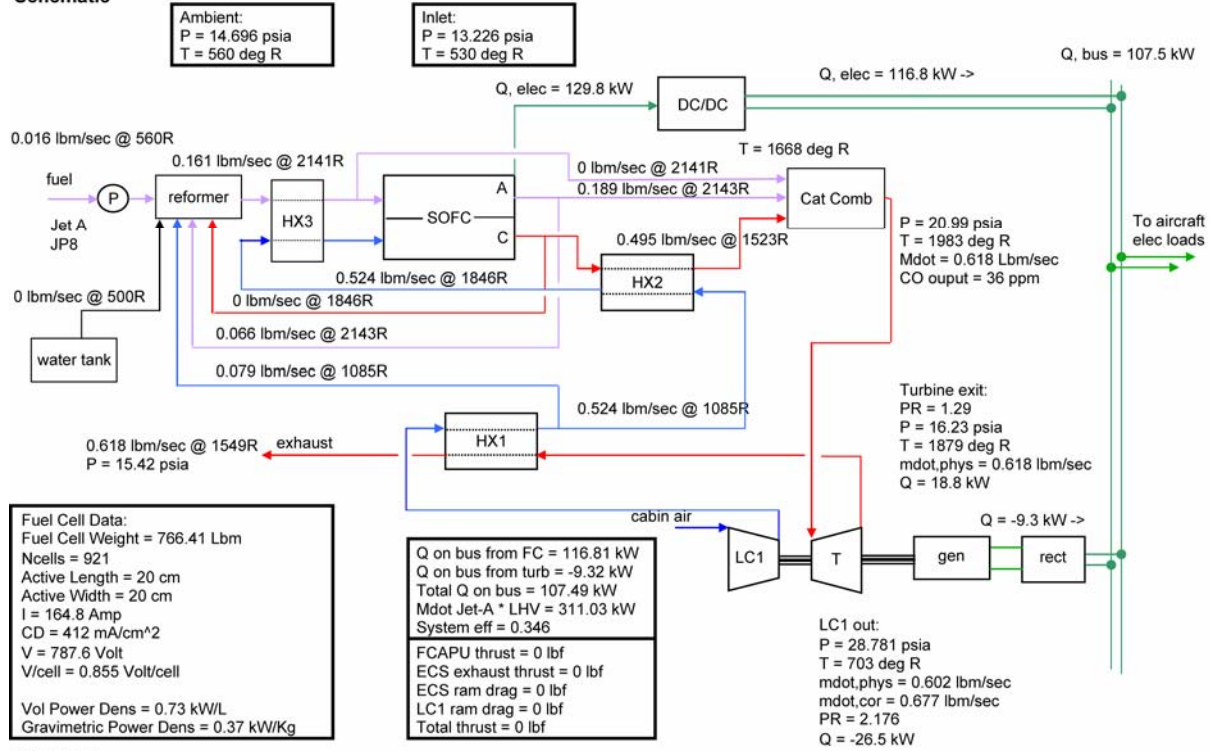
Table 21. SOFC APU System 2, Case 3 Performance Summary.

	a	b	c	d
Parameter Description	Gate (107.5 kW)	MES (185.3 kW)	Cruise (84.3 kW)	Cruise, EO (124.1 kW)
SOFC number of cells	921	921	921	921
SOFC active area size (cm ²)	20 x 20	20 x 20	20 x 20	20 x 20
SOFC current demand (A)	164.8	270.0	86.8	127.0
SOFC volt/cell (V)	0.855	0.783	0.888	0.868
SOFC efficiency	0.750	0.695	0.774	0.759
SOFC power output on bus (kW)	116.8	175.2	63.9	91.4
SOFC operating temperature (°C)	859.7	922.8	799.6	826.8
SOFC inlet/exit dT (°C)	115.6	138.2	113.8	121.7
Reformer operating temperature (°C)	916.2	948.3	869.0	883.8
Anode recycle amount	0.35	0.35	0.35	0.35
Compressor PR	2.18	3.23	1.64	2.05
Compressor corrected flow (lbm/s)	0.68	1.10	0.43	0.63
Compressor efficiency	0.76	0.8	0.73	0.75
Turbine power output on bus (kW)	-9.3	10.2	20.6	34.0
Turbine PR	1.29	1.92	3.08	3.85
Turbine corrected flow (lbm/s)	0.85	0.96	0.69	0.83
Turbine efficiency	0.85	0.85	0.85	0.85
Total power on bus (kW)	107.5	185.4	84.5	125.4
Combustor operating temperature (°C)	828.5	887.9	759.5	796.6
Combustor CO output (ppm exhaust)	36	42	28	33
Combustor CO output (g/kg fuel)	1.33	1.57	0.97	1.13
Additional fuel to combustor	0.0	0.0	0.0	0.0
System efficiency	0.35	0.36	0.53	0.53
Net Thrust, aircraft basis (lbf)	0.0	0.0	73.9	88.5

G05-377-49

Figure 20. SOFC APU System 2, Case 3(a) Performance Results.

System 2, Case 3a, Cabin Air, Ground, 107.45 kW, Gate Schematic



G05-377-50

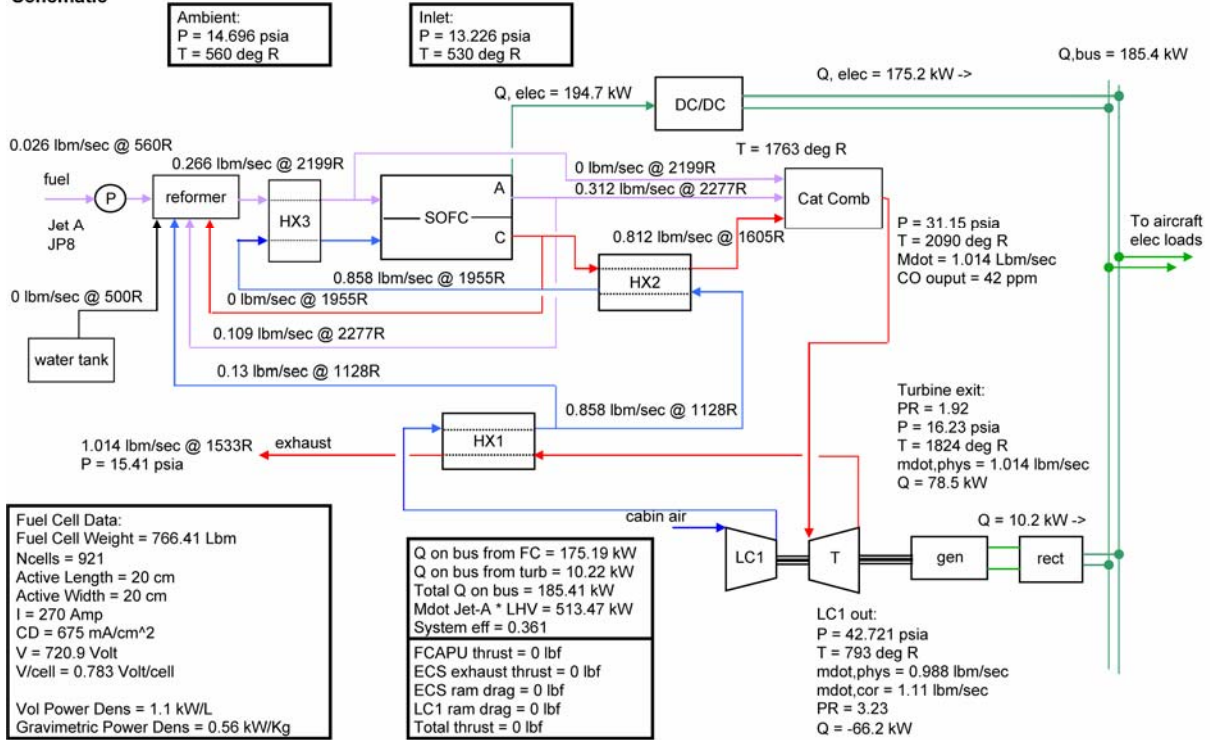
	Inlet			Exit		
	Mdot Lbm/sec	P psia	T R	Mdot Lbm/sec	P psia	T R
ambient	-	14.696	559.7	-	-	-
inlet	-	13.226	530.0	-	-	-
LC1	0.6025	13.226	530.0	0.6025	28.781	703.3
LC1 - bus power	-	-	-	-	-	-
LC2	0.0000	13.226	530.0	0.0000	57.270	882.3
LC2 - bus power	-	-	-	-	-	-
MES	1.6667	-	-	-	-	-
ECS	0.0000	-	-	-	-	-
HX1-cold side	0.6025	28.781	703.3	0.6025	27.342	1085.2
HX2-cold side	0.5236	27.342	1085.2	0.5236	25.975	1846.2
Jet A	0.0159	-	560.0	-	-	-
reformer	0.0789	25.975	1626.6	0.1611	25.767	2140.8
HX3-reformate	0.1611	25.767	2140.8	0.1611	24.478	1935.1
HX3-air	0.5236	25.975	1846.2	0.5236	24.676	1935.1
FC-anode	0.1611	24.478	1935.1	0.1893	23.254	2143.1
FC-cathode	0.5236	24.478	1935.1	0.4954	23.254	2143.1
FC -	-	-	2039.2	-	-	-
FC - bus power	-	-	-	-	-	-
HX2-hot side	0.4954	23.254	2143.1	0.4954	22.092	1523.2
cat comb	0.6184	22.092	1667.5	0.6184	20.987	1982.9
Turbine	0.6184	20.987	1982.9	0.6184	16.231	1878.5
LC1/Turbine Net	-	-	-	-	-	-
Generator bus power	-	-	-	-	-	-
HX1-hot side	0.6184	16.231	1878.5	0.6184	15.420	1548.5

G05-377-51

Note: Cells highlighted in Brown or Blue indicate components reaching temperature limits.

Figure 21. SOFC APU System 2, Case 3(b) Performance Results.

System 2, Case 3b, Cabin Air, Ground, 185.31 kW, MES
Schematic



G05-377-52

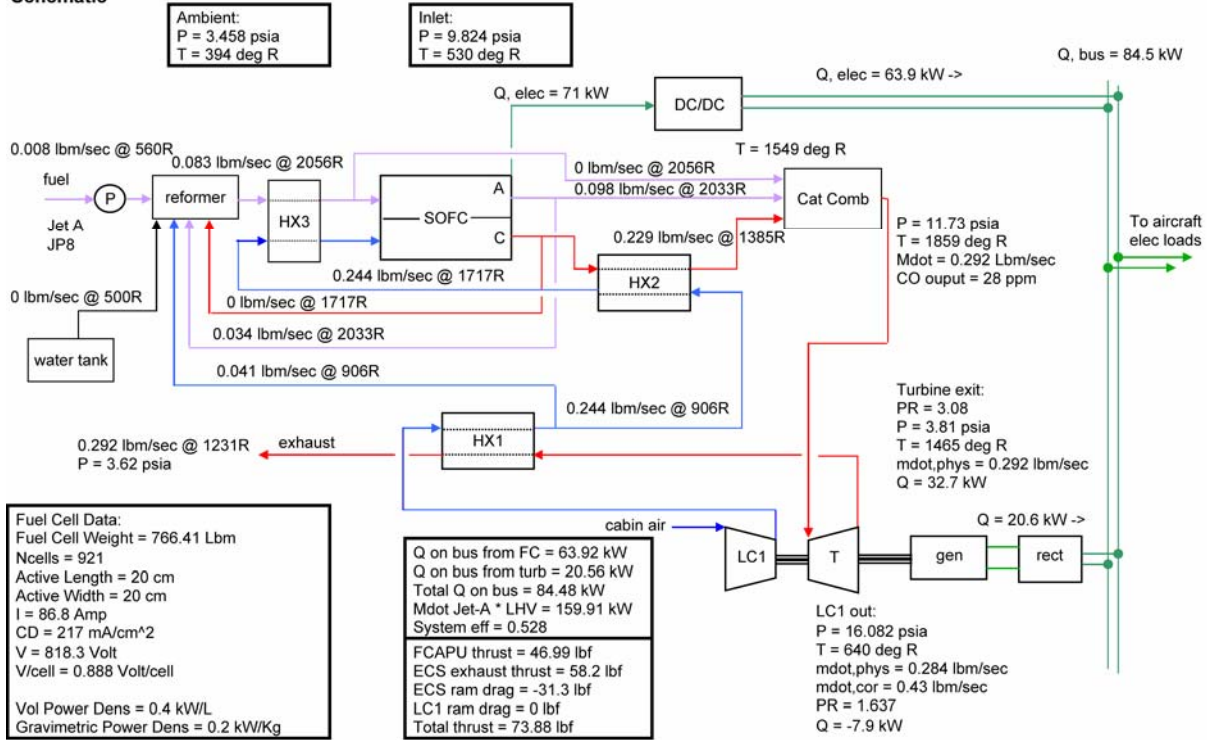
	Inlet			Exit		
	Mdot Lbm/sec	P psia	T R	Mdot Lbm/sec	P psia	T R
ambient	-	14.696	559.7	-	-	-
inlet	-	13.226	530.0	-	-	-
LC1	0.9881	13.226	530.0	0.9881	42.721	793.2
LC1 - bus power	-	-	-	-	-	-
LC2	0.0000	13.226	530.0	0.0000	57.270	882.3
LC2 - bus power	-	-	-	-	-	-
MES	1.6667	-	-	-	-	-
ECS	0.0000	-	-	-	-	-
HX1-cold side	0.9881	42.721	793.2	0.9881	40.585	1127.6
HX2-cold side	0.8578	40.585	1127.6	0.8578	38.556	1955.5
Jet A	0.0263	-	560.0	-	-	-
reformer	0.1302	38.556	1717.5	0.2657	38.248	2198.6
HX3-reformate	0.2657	38.248	2198.6	0.2657	36.335	2028.5
HX3-air	0.8578	38.556	1955.5	0.8578	36.628	2028.5
FC-anode	0.2657	36.335	2028.5	0.3120	34.518	2277.3
FC-cathode	0.8578	36.335	2028.5	0.8116	34.518	2277.3
FC -	-	-	2153.0	-	-	-
FC - bus power	-	-	-	-	-	-
HX2-hot side	0.8116	34.518	2277.3	0.8116	32.792	1605.4
cat comb	1.0144	32.792	1763.1	1.0144	31.153	2090.3
Turbine	1.0144	31.153	2090.3	1.0144	16.225	1824.6
LC1/Turbine Net	-	-	-	-	-	-
Generator bus power	-	-	-	-	-	-
HX1-hot side	1.0144	16.225	1824.6	1.0144	15.414	1532.9

G05-377-53

Note: Cells highlighted in Brown or Blue indicate components reaching temperature limits.

Figure 22. SOFC APU System 2, Case 3(c) Performance Results.

System 2, Case 3c, Cabin Air, Cruise, 84.34 kW, system1_rev_17a Schematic



G05-377-54

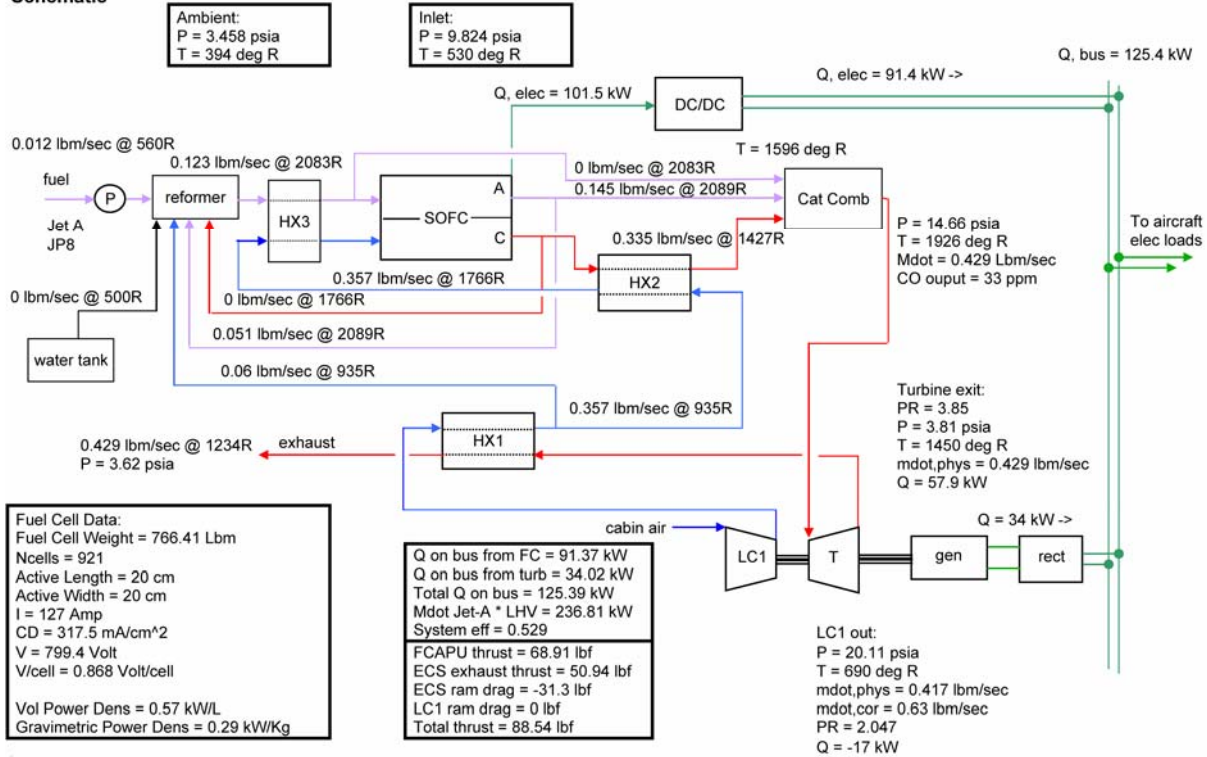
	Inlet			Exit		
	Mdot Lbm/sec	P psia	T R	Mdot Lbm/sec	P psia	T R
ambient	-	3.458	393.9	-	-	-
inlet	-	9.824	530.0	-	-	-
LC1	0.2843	9.824	530.0	0.2843	16.082	639.7
LC1 - bus power	-	-	-	-	-	-
LC2	0.0000	9.824	530.0	0.0000	42.538	882.3
LC2 - bus power	-	-	-	-	-	-
MES	0.0000	-	-	-	-	-
ECS	1.4167	-	-	-	-	-
HX1-cold side	0.2843	16.082	639.7	0.2843	15.278	905.5
HX2-cold side	0.2437	15.278	905.5	0.2437	14.514	1717.4
Jet A	0.0082	-	560.0	-	-	-
reformer	0.0406	14.514	1483.6	0.0830	14.398	2055.8
HX3-reformate	0.0830	14.398	2055.8	0.0830	13.678	1828.3
HX3-air	0.2437	14.514	1717.4	0.2437	13.788	1828.3
FC-anode	0.0830	13.678	1828.3	0.0979	12.994	2033.1
FC-cathode	0.2437	13.678	1828.3	0.2288	12.994	2033.0
FC -	-	-	1930.8	-	-	-
FC - bus power	-	-	-	-	-	-
HX2-hot side	0.2288	12.994	2033.0	0.2288	12.344	1384.8
cat comb	0.2925	12.344	1548.6	0.2925	11.727	1858.7
Turbine	0.2925	11.727	1858.7	0.2925	3.812	1464.5
LC1/Turbine Net	-	-	-	-	-	-
Generator bus power	-	-	-	-	-	-
HX1-hot side	0.2925	3.812	1464.5	0.2925	3.622	1231.3

G05-377-55

Note: Cells highlighted in Brown or Blue indicate components reaching temperature limits.

Figure 23. SOFC APU System 2, Case 3(d) Performance Results.

System 2, Case 3d, Cabin Air, Cruise, 124.15 kW, Engine Out Schematic



G05-377-56

	Inlet			Exit		
	Mdot Lbm/sec	P psia	T R	Mdot Lbm/sec	P psia	T R
ambient	-	3.458	393.9	-	-	-
inlet	-	9.824	530.0	-	-	-
LC1	0.4167	9.824	530.0	0.4167	20.110	690.3
LC1 - bus power	-	-	-	-	-	-
LC2	0.0000	9.824	530.0	0.0000	42.538	882.3
LC2 - bus power	-	-	-	-	-	-
MES	0.0000	-	-	-	-	-
ECS	1.4167	-	-	-	-	-
HX1-cold side	0.4167	20.110	690.3	0.4167	19.104	935.2
HX2-cold side	0.3566	19.104	935.2	0.3566	18.149	1766.4
Jet A	0.0121	-	560.0	-	-	-
reformer	0.0601	18.149	1527.0	0.1228	18.004	2082.6
HX3-reformate	0.1228	18.004	2082.6	0.1228	17.104	1870.3
HX3-air	0.3566	18.149	1766.4	0.3566	17.242	1870.3
FC-anode	0.1228	17.104	1870.3	0.1445	16.249	2089.3
FC-cathode	0.3566	17.104	1870.3	0.3348	16.249	2089.3
FC -	-	-	1979.9	-	-	-
FC - bus power	-	-	-	-	-	-
HX2-hot side	0.3348	16.249	2089.3	0.3348	15.436	1427.4
cat comb	0.4288	15.436	1596.2	0.4288	14.664	1925.6
Turbine	0.4288	14.664	1925.6	0.4288	3.813	1450.0
LC1/Turbine Net	-	-	-	-	-	-
Generator bus power	-	-	-	-	-	-
HX1-hot side	0.4288	3.813	1450.0	0.4288	3.622	1234.4

G05-377-57

Note: Cells highlighted in Brown or Blue indicate components reaching temperature limits.

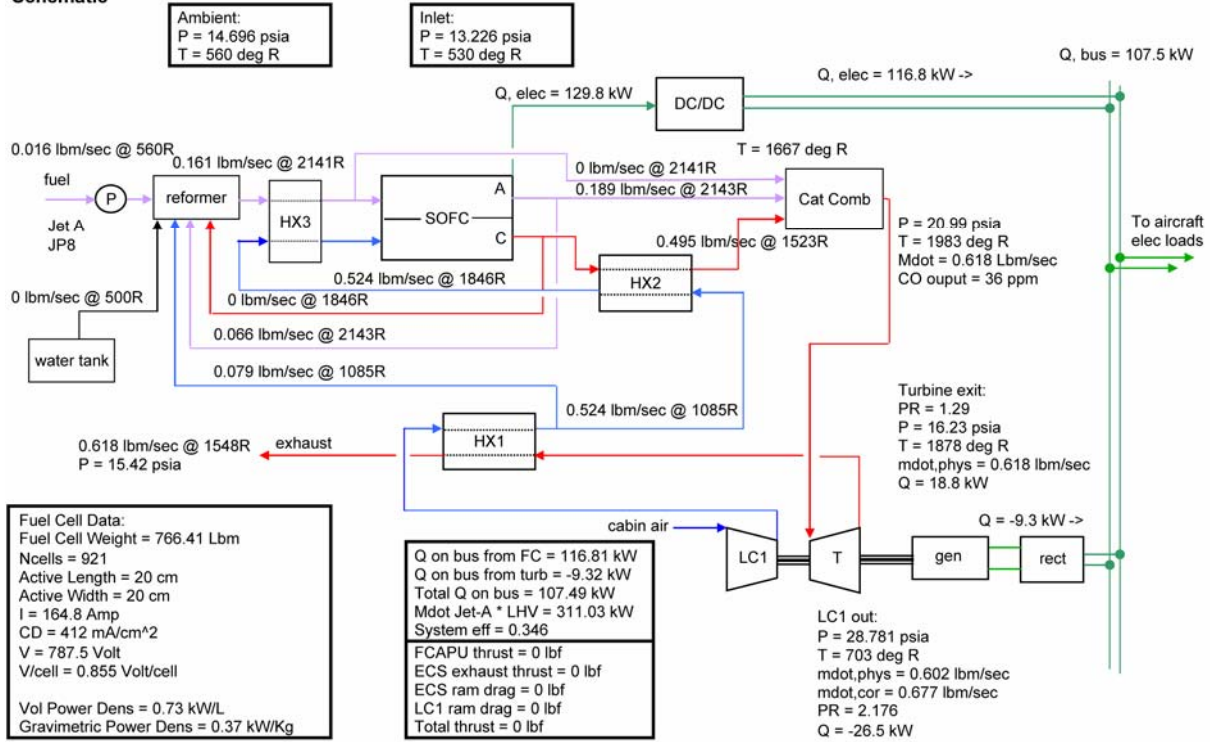
Table 22. SOFC APU System 2, Case 4 Performance Summary.

Parameter Description	a	b	c
	Gate (107.5 kW)	MES (185.3 kW)	Cruise, Full Power (164.0 kW)
SOFC number of cells	921	921	921
SOFC active area size (cm ²)	20 x 20	20 x 20	20 x 20
SOFC current demand (A)	164.8	270.0	164.6
SOFC volt/cell (V)	0.855	0.783	0.850
SOFC efficiency	0.750	0.695	0.745
SOFC power output on bus (kW)	116.8	175.2	115.9
SOFC operating temperature (°C)	859.6	922.8	848.1
SOFC inlet/exit dT (°C)	115.5	138.2	128.9
Reformer operating temperature (°C)	916.2	948.2	895.0
Anode recycle amount	0.35	0.35	0.35
Compressor PR	2.18	3.23	2.50
Compressor corrected flow (lbm/s)	0.68	1.10	0.82
Compressor efficiency	0.76	0.8	0.78
Turbine power output on bus (kW)	-9.3	10.2	48.2
Turbine PR	1.29	1.92	4.68
Turbine corrected flow (lbm/s)	0.85	0.96	0.89
Turbine efficiency	0.85	0.85	0.85
Total power on bus (kW)	107.5	185.4	164.1
Combustor operating temperature (°C)	828.4	887.9	817.7
Combustor CO output (ppm exhaust)	36	42	36
Combustor CO output (g/kg fuel)	1.33	1.57	1.21
Additional fuel to combustor	0.0	0.0	0.0
System efficiency	0.35	0.36	0.53
Net Thrust, aircraft basis (lbf)	0.0	0.0	102.0

G05-377-58

Figure 24. SOFC APU System 2, Case 4(a) Performance Results.

System 2, Case 4a, Cabin Air, Ground, 107.45 kW, Gate Schematic



G05-377-59

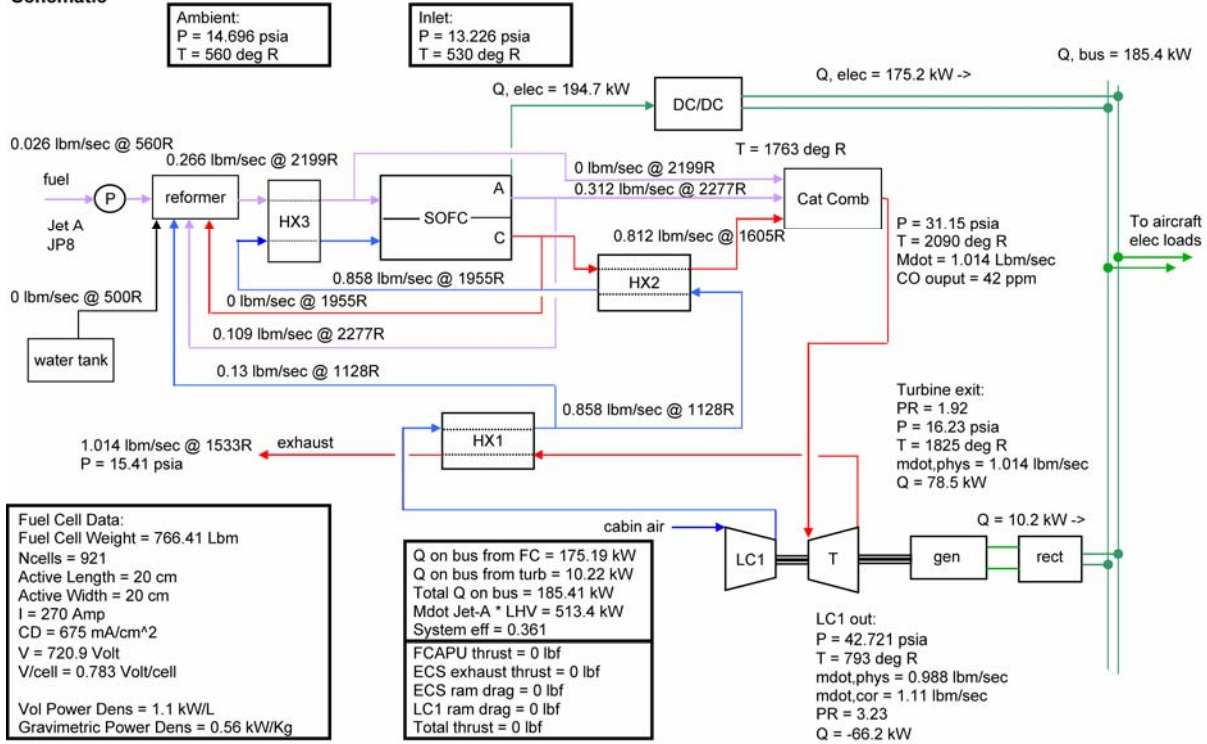
	Inlet			Exit		
	Mdot Lbm/sec	P psia	T R	Mdot Lbm/sec	P psia	T R
ambient	-	14.696	559.7	-	-	-
inlet	-	13.226	530.0	-	-	-
LC1	0.6025	13.226	530.0	0.6025	28.781	703.3
LC1 - bus power	-	-	-	-	-	-
LC2	0.0000	13.226	530.0	0.0000	57.270	882.3
LC2 - bus power	-	-	-	-	-	-
MES	1.6667	-	-	-	-	-
ECS	0.0000	-	-	-	-	-
HX1-cold side	0.6025	28.781	703.3	0.6025	27.342	1085.2
HX2-cold side	0.5236	27.342	1085.2	0.5236	25.975	1846.2
Jet A	0.0159	-	560.0	-	-	-
reformer	0.0789	25.975	1626.6	0.1611	25.767	2140.8
HX3-reformate	0.1611	25.767	2140.8	0.1611	24.478	1935.1
HX3-air	0.5236	25.975	1846.2	0.5236	24.676	1935.1
FC-anode	0.1611	24.478	1935.1	0.1893	23.254	2143.1
FC-cathode	0.5236	24.478	1935.1	0.4954	23.254	2143.1
FC -	-	-	2039.2	-	-	-
FC - bus power	-	-	-	-	-	-
HX2-hot side	0.4954	23.254	2143.1	0.4954	22.092	1523.2
cat comb	0.6184	22.092	1667.5	0.6184	20.987	1982.9
Turbine	0.6184	20.987	1982.9	0.6184	16.231	1878.5
LC1/Turbine Net	-	-	-	-	-	-
Generator bus power	-	-	-	-	-	-
HX1-hot side	0.6184	16.231	1878.5	0.6184	15.420	1548.5

G05-377-60

Note: Cells highlighted in Brown or Blue indicate components reaching temperature limits.

Figure 25. SOFC APU System 2, Case 4(b) Performance Results.

System 2, Case 4b, Cabin Air, Ground, 185.31 kW, MES
Schematic



G05-377-61

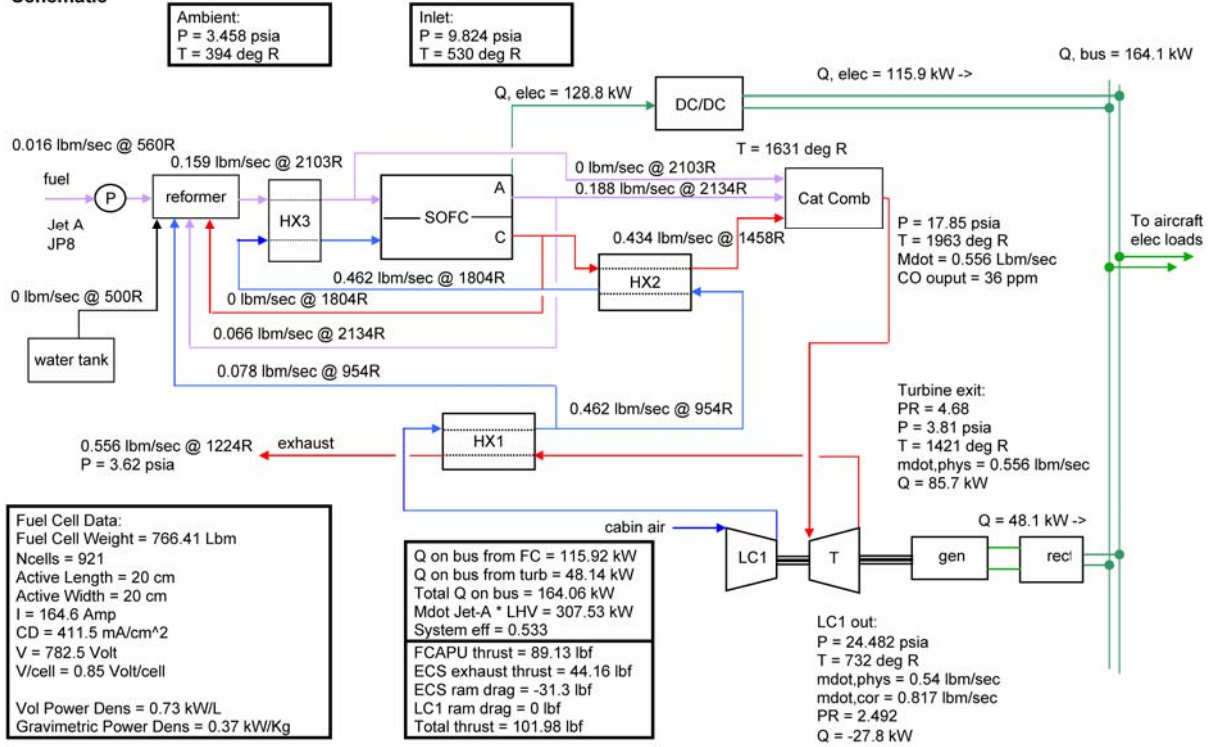
	Inlet			Exit		
	Mdot Lbm/sec	P psia	T R	Mdot Lbm/sec	P psia	T R
ambient	-	14.696	559.7	-	-	-
inlet	-	13.226	530.0	-	-	-
LC1	0.9881	13.226	530.0	0.9881	42.721	793.2
LC1 - bus power	-	-	-	-	-	-
LC2	0.0000	13.226	530.0	0.0000	57.270	882.3
LC2 - bus power	-	-	-	-	-	-
MES	1.6667	-	-	-	-	-
ECS	0.0000	-	-	-	-	-
HX1-cold side	0.9881	42.721	793.2	0.9881	40.585	1127.6
HX2-cold side	0.8578	40.585	1127.6	0.8578	38.556	1955.5
Jet A	0.0263	-	560.0	-	-	-
reformer	0.1302	38.556	1717.5	0.2657	38.248	2198.7
HX3-reformate	0.2657	38.248	2198.7	0.2657	36.335	2028.5
HX3-air	0.8578	38.556	1955.5	0.8578	36.628	2028.5
FC-anode	0.2657	36.335	2028.5	0.3120	34.518	2277.3
FC-cathode	0.8578	36.335	2028.5	0.8116	34.518	2277.3
FC -	-	-	2153.1	-	-	-
FC - bus power	-	-	-	-	-	-
HX2-hot side	0.8116	34.518	2277.3	0.8116	32.792	1605.4
cat comb	1.0144	32.792	1763.2	1.0144	31.153	2090.3
Turbine	1.0144	31.153	2090.3	1.0144	16.225	1824.6
LC1/Turbine Net	-	-	-	-	-	-
Generator bus power	-	-	-	-	-	-
HX1-hot side	1.0144	16.225	1824.6	1.0144	15.414	1532.9

G05-377-62

Note: Cells highlighted in Brown or Blue indicate components reaching temperature limits.

Figure 26. SOFC APU System 2, Case 4(c) Performance Results.

System 2, Case 4c, Cabin Air, Cruise, 164.00 kW, Full Power Schematic



G05-377-63

	Inlet			Exit		
	Mdot Lbm/sec	P psia	T R	Mdot Lbm/sec	P psia	T R
ambient	-	14.696	559.7	-	-	-
inlet	-	13.226	530.0	-	-	-
LC1	0.9881	13.226	530.0	0.9881	42.721	793.2
LC1 - bus power	-	-	-	-	-	-
LC2	0.0000	13.226	530.0	0.0000	57.270	882.3
LC2 - bus power	-	-	-	-	-	-
MES	1.6667	-	-	-	-	-
ECS	0.0000	-	-	-	-	-
HX1-cold side	0.9881	42.721	793.2	0.9881	40.585	1127.6
HX2-cold side	0.8578	40.585	1127.6	0.8578	38.556	1955.5
Jet A	0.0263	-	560.0	-	-	-
reformer	0.1302	38.556	1717.5	0.2657	38.248	2198.7
HX3-reformate	0.2657	38.248	2198.7	0.2657	36.335	2028.5
HX3-air	0.8578	38.556	1955.5	0.8578	36.628	2028.5
FC-anode	0.2657	36.335	2028.5	0.3120	34.518	2277.3
FC-cathode	0.8578	36.335	2028.5	0.8116	34.518	2277.3
FC -	-	-	2153.1	-	-	-
FC - bus power	-	-	-	-	-	-
HX2-hot side	0.8116	34.518	2277.3	0.8116	32.792	1605.4
cat comb	1.0144	32.792	1763.2	1.0144	31.153	2090.3
Turbine	1.0144	31.153	2090.3	1.0144	16.225	1824.6
LC1/Turbine Net	-	-	-	-	-	-
Generator bus power	-	-	-	-	-	-
HX1-hot side	1.0144	16.225	1824.6	1.0144	15.414	1532.9

G05-377-64

Note: Cells highlighted in Brown or Blue indicate components reaching temperature limits.

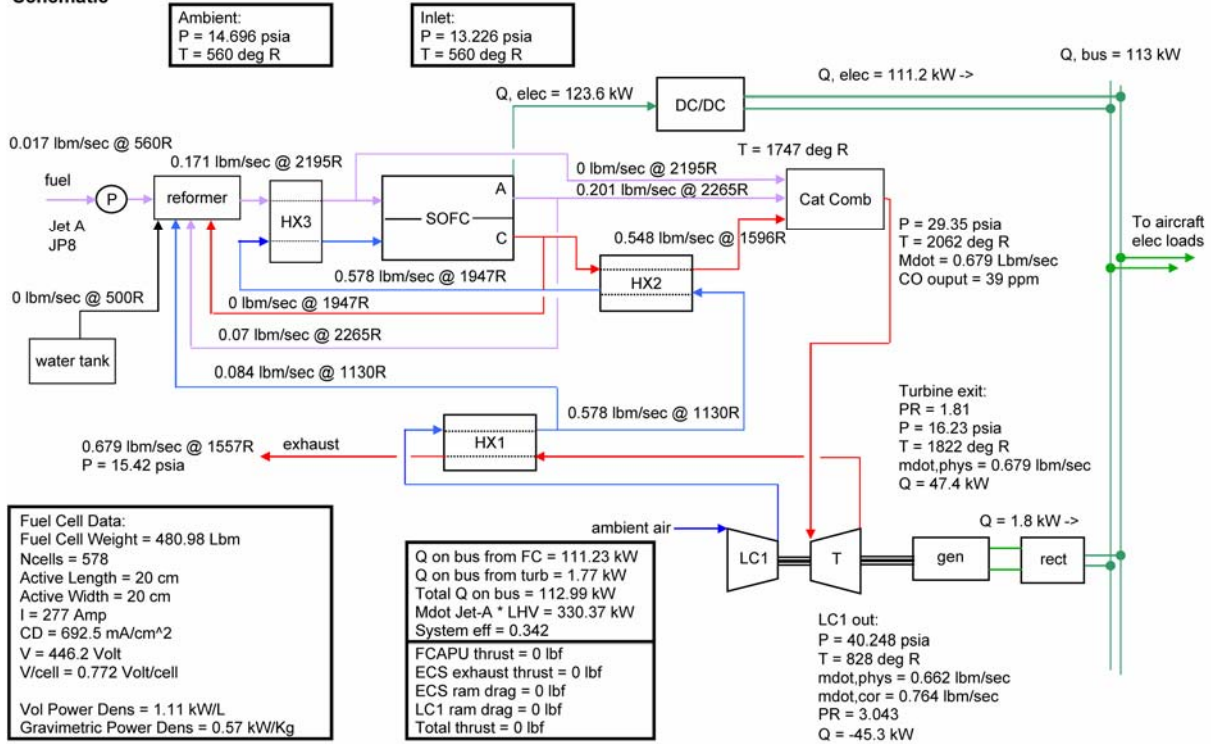
Table 23. SOFC APU System 1, Case 5 Performance Summary.

Parameter Description	a	b
	Gate/MES (112.8 kW)	Cruise (84.3 kW)
SOFC number of cells	578	578
SOFC active area size (cm ²)	20 x 20	20 x 20
SOFC current demand (A)	277	156
SOFC volt/cell (V)	0.77	0.84
SOFC efficiency	0.68	0.74
SOFC power output on bus (kW)	111.2	68.5
SOFC operating temperature (°C)	916.8	830.5
SOFC inlet/exit dT (°C)	136.5	122.2
Reformer operating temperature (°C)	946.2	888.4
Anode recycle amount	0.35	0.35
Compressor PR	3.04	3.75
Compressor corrected flow (lbm/s)	0.76	0.99
Compressor efficiency	0.78	0.76
Turbine power output on bus (kW)	1.77	15.84
Turbine PR	1.81	3.30
Turbine corrected flow (lbm/s)	0.68	0.77
Turbine efficiency	0.85	0.85
Total power on bus (kW)	113.0	84.3
Combustor operating temperature (°C)	872.1	786.8
Combustor CO output (ppm exhaust)	39	31
Combustor CO output (g/kg fuel)	1.52	1.11
Additional fuel to combustor	0.0	0.0
System efficiency	0.34	0.46
Net Thrust, aircraft basis (lbf)	0.0	90.2

G05-377-97

Figure 27. SOFC APU System 1, Case 5(a) Performance Results.

System 1, Case 5a, Ambient Air, Ground, 112.82 kW, Gate/MES Schematic



G05-377-65

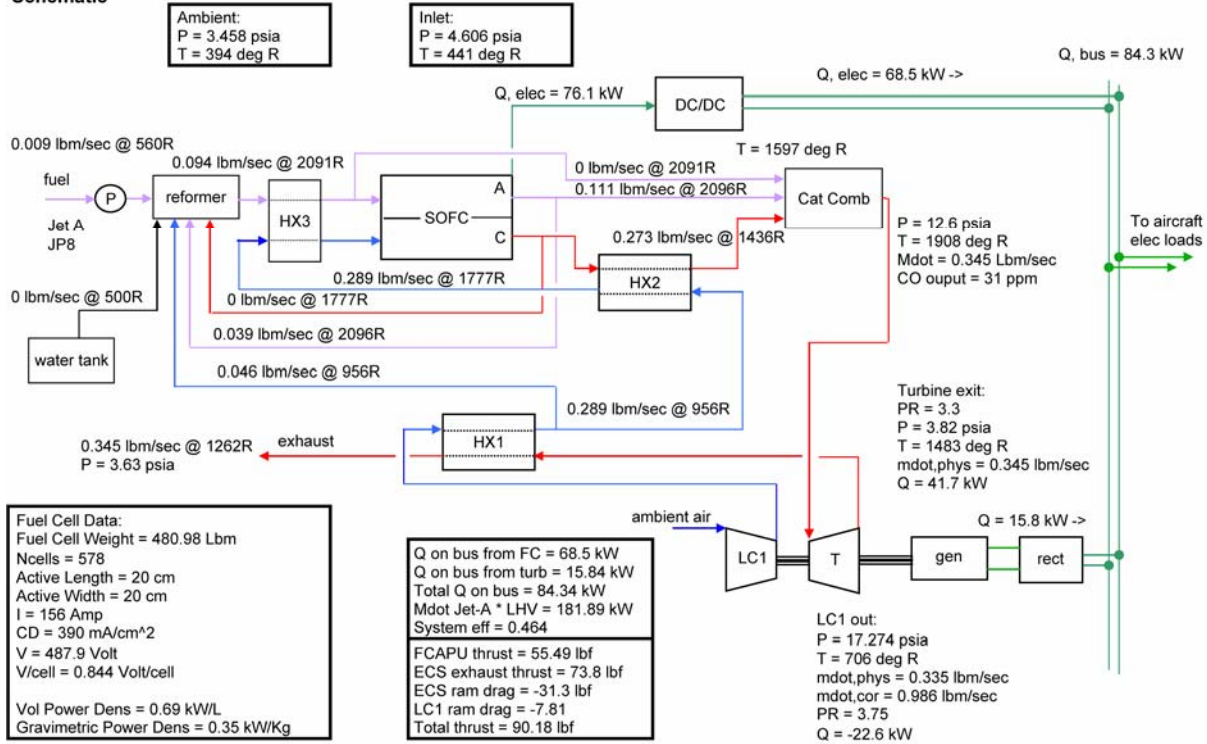
	Inlet			Exit		
	Mdot Lbm/sec	P psia	T R	Mdot Lbm/sec	P psia	T R
ambient	-	14.696	559.7	-	-	-
inlet	-	13.226	559.7	-	-	-
LC1	0.6618	13.226	559.7	0.6618	40.248	827.7
LC1 - bus power	-	-	-	-	-	-
LC2	0.0000	13.226	559.7	0.0000	57.270	931.6
LC2 - bus power	-	-	-	-	-	-
MES	1.6667	-	-	-	-	-
ECS	0.0000	-	-	-	-	-
HX1-cold side	0.6618	40.248	827.7	0.6618	38.236	1129.7
HX2-cold side	0.5780	38.236	1129.7	0.5780	36.324	1947.0
Jet A	0.0169	-	560.0	-	-	-
reformer	0.0838	36.324	1711.8	0.1710	36.033	2194.9
HX3-reformate	0.1710	36.033	2194.9	0.1710	34.232	2019.0
HX3-air	0.5780	36.324	1947.0	0.5780	34.508	2019.0
FC-anode	0.1710	34.232	2019.0	0.2008	32.520	2264.7
FC-cathode	0.5780	34.232	2019.0	0.5482	32.520	2264.7
FC -	-	-	2142.0	-	-	-
FC - bus power	-	-	-	-	-	-
HX2-hot side	0.5482	32.520	2264.7	0.5482	30.894	1596.1
cat comb	0.6787	30.894	1747.3	0.6787	29.349	2061.6
Turbine	0.6787	29.349	2061.6	0.6787	16.233	1821.7
LC1/Turbine Net	-	-	-	-	-	-
Gen/Motor bus power	-	-	-	-	-	-
HX1-hot side	0.6787	16.233	1821.7	0.6787	15.421	1557.4

G05-377-66

Note: Cells highlighted in Brown or Blue indicate components reaching temperature limits.

Figure 28. SOFC APU System 1, Case 5(b) Performance Results.

System 1, Case 5b, Ambient Air, Cruise, 84.34 kW, cruise Schematic



G05-377-67

	Inlet			Exit		
	Mdot Lbm/sec	P psia	T R	Mdot Lbm/sec	P psia	T R
ambient	-	3.458	393.9	-	-	-
inlet	-	4.606	440.6	-	-	-
LC1	0.3355	4.606	440.6	0.3355	17.274	706.2
LC1 - bus power	-	-	-	-	-	-
LC2	0.0000	4.606	440.6	0.0000	19.945	733.8
LC2 - bus power	-	-	-	-	-	-
MES	0.0000	-	-	-	-	-
ECS	1.4167	-	-	-	-	-
HX1-cold side	0.3355	17.274	706.2	0.3355	16.410	956.3
HX2-cold side	0.2893	16.410	956.3	0.2893	15.589	1777.4
Jet A	0.0093	-	560.0	-	-	-
reformer	0.0461	15.589	1541.0	0.0944	15.465	2090.7
HX3-reformate	0.0944	15.465	2090.7	0.0944	14.692	1876.4
HX3-air	0.2893	15.589	1777.4	0.2893	14.810	1876.4
FC-anode	0.0944	14.692	1876.4	0.1111	13.957	2096.3
FC-cathode	0.2893	14.692	1876.4	0.2726	13.957	2096.4
FC -	-	-	1986.5	-	-	-
FC - bus power	-	-	-	-	-	-
HX2-hot side	0.2726	13.957	2096.4	0.2726	13.259	1435.9
cat comb	0.3448	13.259	1597.2	0.3448	12.596	1907.9
Turbine	0.3448	12.596	1907.9	0.3448	3.817	1482.9
LC1/Turbine Net	-	-	-	-	-	-
Gen/Motor bus power	-	-	-	-	-	-
HX1-hot side	0.3448	3.817	1482.9	0.3448	3.626	1262.0

G05-377-68

Note: Cells highlighted in Brown or Blue indicate components reaching temperature limits.

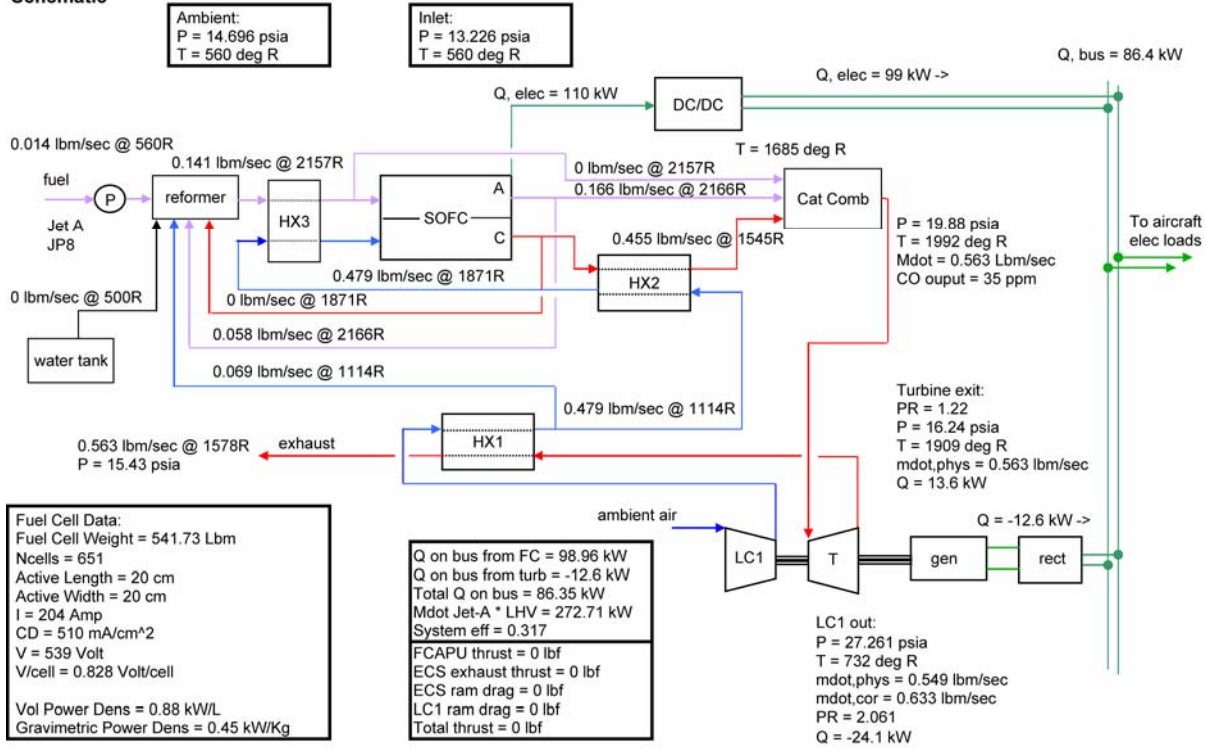
Table 24. SOFC APU System 1, Case 6 Performance Summary.

	a	b	c	d
Parameter Description	Gate (86.3 kW)	MES (116.0 kW)	Cruise (84.3 kW)	Cruise, EO (100.0 kW)
SOFC number of cells	651	651	651	651
SOFC active area size (cm ²)	20 x 20	20 x 20	20 x 20	20 x 20
SOFC current demand (A)	204	268.2	142.5	167.85
SOFC volt/cell (V)	0.83	0.78	0.84	0.83
SOFC efficiency	0.73	0.69	0.74	0.73
SOFC power output on bus (kW)	99.0	122.2	70.2	81.7
SOFC operating temperature (°C)	871.7	912.3	820.7	833.6
SOFC inlet/exit dT (°C)	117.8	132.5	121.7	125.9
Reformer operating temperature (°C)	925.1	945.5	881.4	888.3
Anode recycle amount	0.35	0.35	0.35	0.35
Compressor PR	2.06	2.47	2.87	3.27
Compressor corrected flow (lbm/s)	0.63	0.83	1.01	1.20
Compressor efficiency	0.744	0.765	0.78	0.78
Turbine power output on bus (kW)	-12.60	-6.06	13.83	18.29
Turbine PR	1.22	1.47	2.53	2.88
Turbine corrected flow (lbm/s)	0.82	0.91	1.03	1.07
Turbine efficiency	0.85	0.85	0.85	0.85
Total power on bus (kW)	86.4	116.2	84.1	100.0
Combustor operating temperature (°C)	833.5	870.8	774.1	786.9
Combustor CO output (ppm exhaust)	35	39	30	31
Combustor CO output (g/kg fuel)	1.37	1.52	1.06	1.11
Additional fuel to combustor	0.0	0.0	0.0	0.0
System efficiency	0.32	0.32	0.45	0.45
Net Thrust, aircraft basis (lbf)	0.0	0.0	92.8	100.3

G05-377-69

Figure 29. SOFC APU System 1, Case 6(a) Performance Results.

System 1, Case 6a/7a, Ambient Air, 86.26 kW, Ground/Gate Schematic



G05-377-70

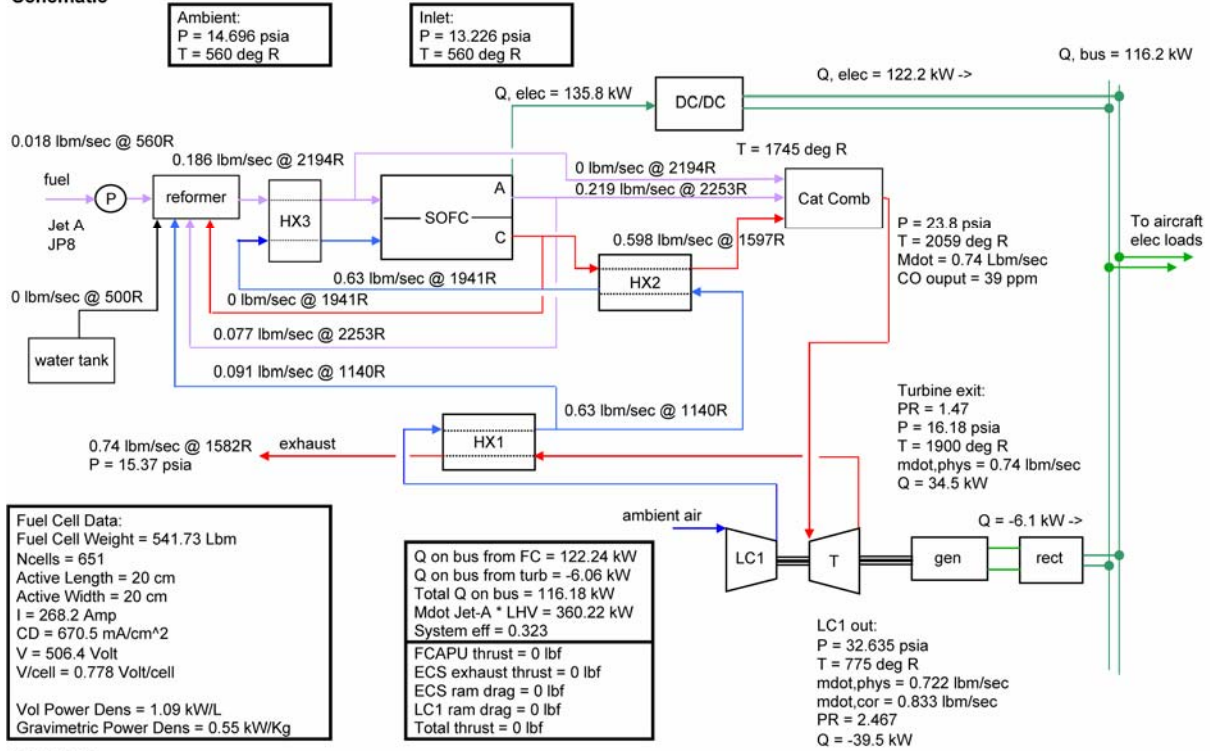
	Inlet			Exit		
	Mdot Lbm/sec	P psia	T R	Mdot Lbm/sec	P psia	T R
ambient	-	14.696	559.7	-	-	-
inlet	-	13.226	559.7	-	-	-
LC1	0.5486	13.226	559.7	0.5486	27.261	732.1
LC1 - bus power	-	-	-	-	-	-
LC2	0.0000	13.226	559.7	0.0000	57.270	931.6
LC2 - bus power	-	-	-	-	-	-
MES	1.6667	-	-	-	-	-
ECS	0.0000	-	-	-	-	-
HX1-cold side	0.5486	27.261	732.1	0.5486	25.898	1114.3
HX2-cold side	0.4794	25.898	1114.3	0.4794	24.603	1871.1
Jet A	0.0140	-	560.0	-	-	-
reformer	0.0692	24.603	1652.7	0.1412	24.406	2156.6
HX3-reformate	0.1412	24.406	2156.6	0.1412	23.186	1954.4
HX3-air	0.4794	24.603	1871.1	0.4794	23.373	1954.4
FC-anode	0.1412	23.186	1954.4	0.1659	22.027	2166.3
FC-cathode	0.4794	23.186	1954.4	0.4547	22.027	2166.3
FC -	-	-	2060.5	-	-	-
FC - bus power	-	-	-	-	-	-
HX2-hot side	0.4547	22.027	2166.3	0.4547	20.925	1545.3
cat comb	0.5626	20.925	1684.9	0.5626	19.879	1991.7
Turbine	0.5626	19.879	1991.7	0.5626	16.238	1908.8
LC1/Turbine Net	-	-	-	-	-	-
Gen/Motor bus power	-	-	-	-	-	-
HX1-hot side	0.5626	16.238	1908.8	0.5626	15.426	1577.6

G05-377-71

Note: Cells highlighted in Brown or Blue indicate components reaching temperature limits.

Figure 30. SOFC APU System 1, Case 6(b) Performance Results.

System 1, Case 6b/7b, Ambient Air, Ground, 116 kW, MES Schematic



G05-377-72

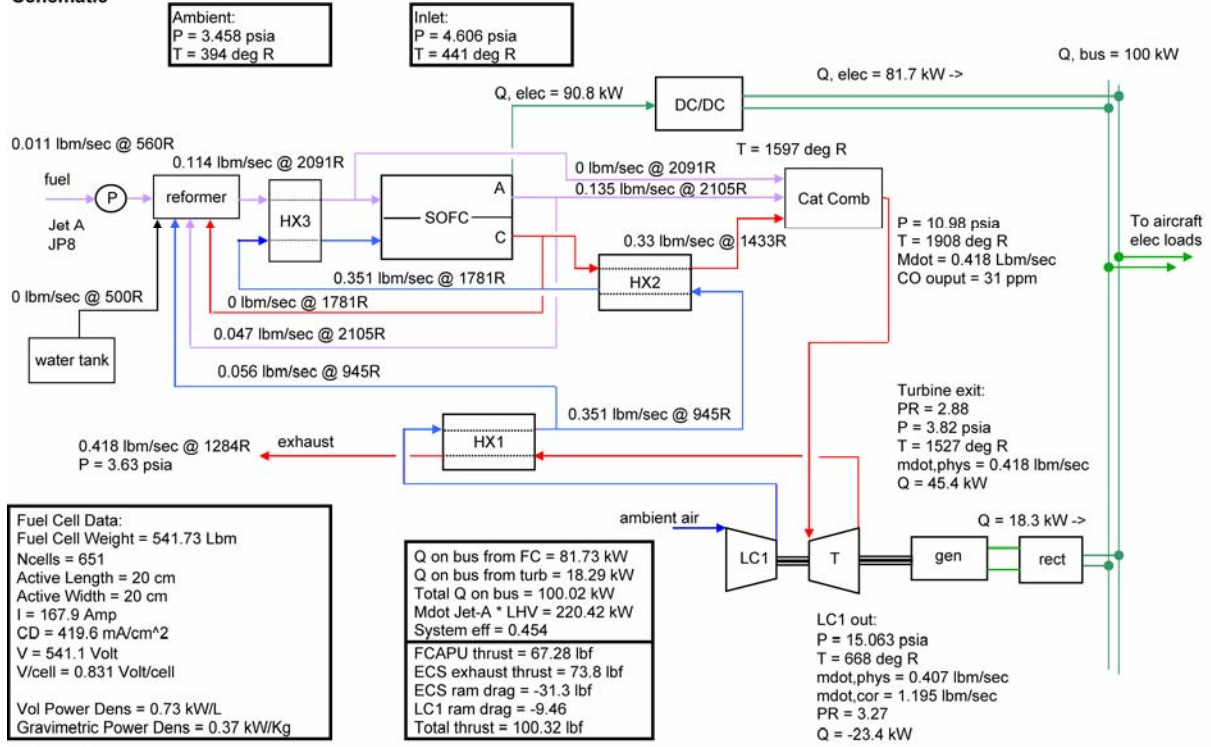
	Inlet			Exit		
	Mdot Lbm/sec	P psia	T R	Mdot Lbm/sec	P psia	T R
ambient	-	14.696	559.7	-	-	-
inlet	-	13.226	559.7	-	-	-
LC1	0.7217	13.226	559.7	0.7217	32.635	774.7
LC1 - bus power	-	-	-	-	-	-
LC2	0.0000	13.226	559.7	0.0000	57.270	931.6
LC2 - bus power	-	-	-	-	-	-
MES	1.6667	-	-	-	-	-
ECS	0.0000	-	-	-	-	-
HX1-cold side	0.7217	32.635	774.7	0.7217	31.003	1139.8
HX2-cold side	0.6303	31.003	1139.8	0.6303	29.453	1941.2
Jet A	0.0185	-	560.0	-	-	-
reformer	0.0914	29.453	1710.5	0.1865	29.217	2193.7
HX3-reformate	0.1865	29.217	2193.7	0.1865	27.756	2014.6
HX3-air	0.6303	29.453	1941.2	0.6303	27.980	2014.6
FC-anode	0.1865	27.756	2014.6	0.2189	26.369	2253.1
FC-cathode	0.6303	27.756	2014.6	0.5978	26.369	2253.1
FC -	-	-	2134.0	-	-	-
FC - bus power	-	-	-	-	-	-
HX2-hot side	0.5978	26.369	2253.1	0.5978	25.050	1597.1
cat comb	0.7401	25.050	1745.3	0.7401	23.798	2059.3
Turbine	0.7401	23.798	2059.3	0.7401	16.179	1899.7
LC1/Turbine Net	-	-	-	-	-	-
Gen/Motor bus power	-	-	-	-	-	-
HX1-hot side	0.7401	16.179	1899.7	0.7401	15.370	1582.3

G05-377-73

Note: Cells highlighted in Brown or Blue indicate components reaching temperature limits.

Figure 32. SOFC APU System 1, Case 6(d) Performance Results.

System 1, Case 6d, Ambient Air, Cruise, 100 kW, engine out Schematic



G05-377-76

	Inlet			Exit		
	Mdot Lbm/sec	P psia	T R	Mdot Lbm/sec	P psia	T R
ambient	-	3.458	393.9	-	-	-
inlet	-	4.606	440.6	-	-	-
LC1	0.4066	4.606	440.6	0.4066	15.063	667.9
LC1 - bus power	-	-	-	-	-	-
LC2	0.0000	4.606	440.6	0.0000	19.945	733.8
LC2 - bus power	-	-	-	-	-	-
MES	0.0000	-	-	-	-	-
ECS	1.4167	-	-	-	-	-
HX1-cold side	0.4066	15.063	667.9	0.4066	14.310	944.7
HX2-cold side	0.3506	14.310	944.7	0.3506	13.594	1780.8
Jet A	0.0113	-	560.0	-	-	-
reformer	0.0559	13.594	1540.2	0.1143	13.485	2090.5
HX3-reformate	0.1143	13.485	2090.5	0.1143	12.811	1878.7
HX3-air	0.3506	13.594	1780.8	0.3506	12.914	1878.7
FC-anode	0.1143	12.811	1878.7	0.1347	12.170	2105.3
FC-cathode	0.3506	12.811	1878.7	0.3303	12.170	2105.3
FC -	-	-	1992.1	-	-	-
FC - bus power	-	-	-	-	-	-
HX2-hot side	0.3303	12.170	2105.3	0.3303	11.562	1433.1
cat comb	0.4179	11.562	1597.4	0.4179	10.984	1908.2
Turbine	0.4179	10.984	1908.2	0.4179	3.820	1526.7
LC1/Turbine Net	-	-	-	-	-	-
Gen/Motor bus power	-	-	-	-	-	-
HX1-hot side	0.4179	3.820	1526.7	0.4179	3.629	1283.5

G05-377-77

Note: Cells highlighted in Brown or Blue indicate components reaching temperature limits.

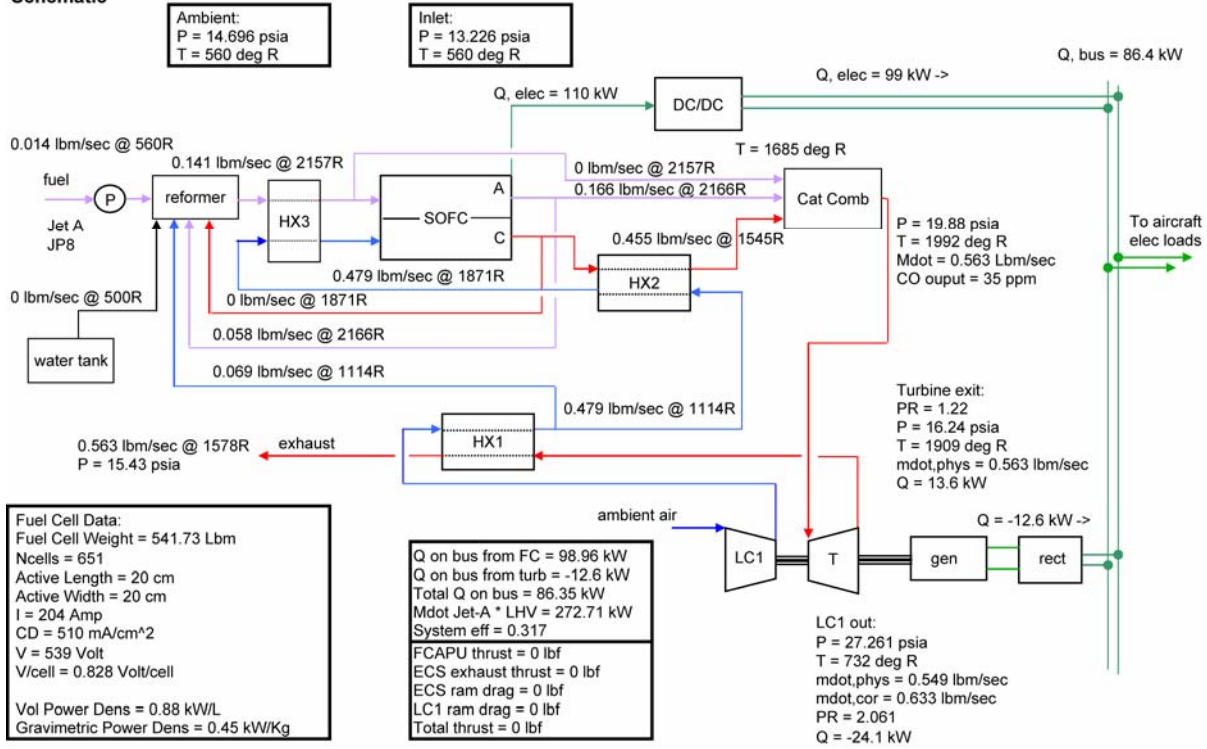
Table 25. SOFC APU System 1, Case 7 Performance Summary.

	a	b	c
Parameter Description	Gate (86.3 kW)	MES (116.0 kW)	Cruise, Full Power (116.0 kW)
SOFC number of cells	651	651	651
SOFC active area size (cm ²)	20 x 20	20 x 20	20 x 20
SOFC current demand (A)	204	268.2	193
SOFC volt/cell (V)	0.83	0.78	0.82
SOFC efficiency	0.73	0.69	0.73
SOFC power output on bus (kW)	99.0	122.2	92.8
SOFC operating temperature (°C)	871.7	912.3	847.2
SOFC inlet/exist dT (°C)	117.8	132.5	130.1
Reformer operating temperature (°C)	925.1	945.5	895.5
Anode recycle amount	0.35	0.35	0.35
Compressor PR	2.06	2.47	3.75
Compressor corrected flow (lbm/s)	0.63	0.83	1.37
Compressor efficiency	0.744	0.765	0.78
Turbine power output on bus (kW)	-12.60	-6.06	23.42
Turbine PR	1.22	1.47	3.30
Turbine corrected flow (lbm/s)	0.82	0.91	1.08
Turbine efficiency	0.85	0.85	0.85
Total power on bus (kW)	86.4	116.2	116.2
Combustor operating temperature (°C)	833.5	870.8	801.1
Combustor CO output (ppm exhaust)	35	39	33
Combustor CO output (g/kg fuel)	1.37	1.52	1.17
Additional fuel to combustor	0.0	0.0	0.0
System efficiency	0.32	0.32	0.46
Net Thrust, aircraft basis (lbf)	0.0	0.0	109.4

G05-377-78

Figure 33. SOFC APU System 1, Case 7(a) Performance Results.

System 1, Case 6a/7a, Ambient Air, 86.26 kW, Ground/Gate Schematic



G05-377-70

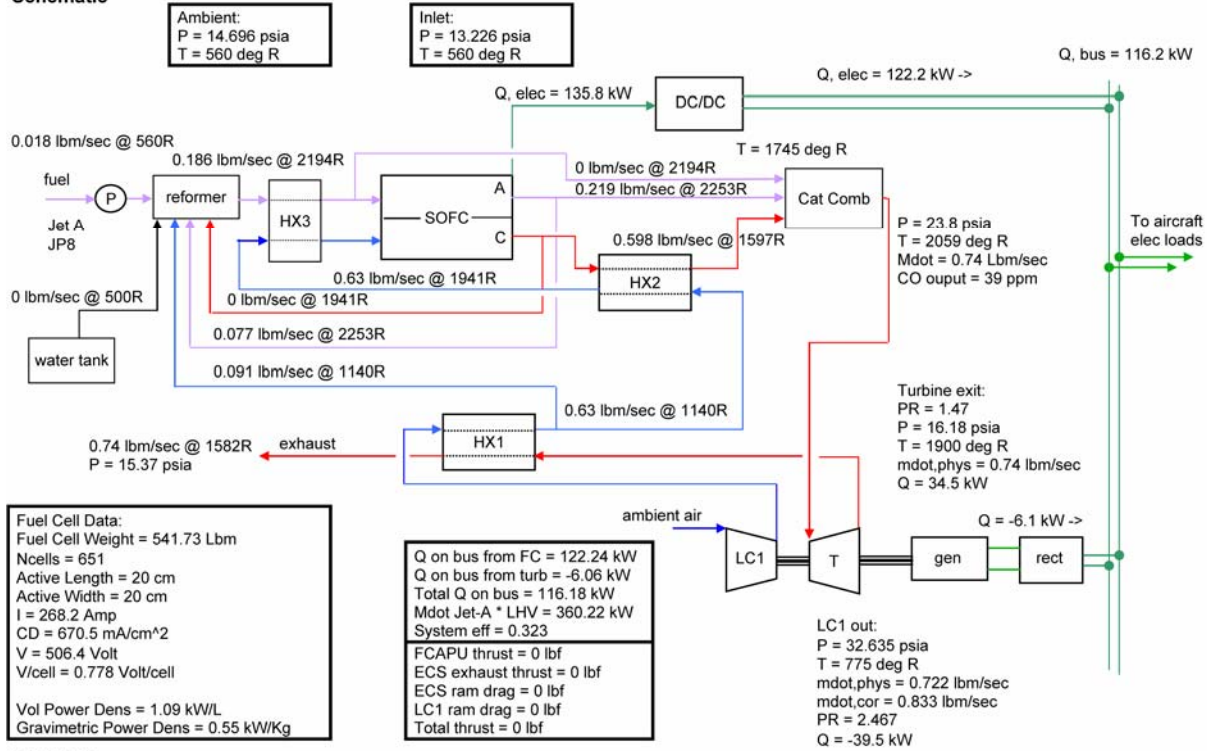
	Inlet			Exit		
	Mdot Lbm/sec	P psia	T R	Mdot Lbm/sec	P psia	T R
ambient	-	14.696	559.7	-	-	-
inlet	-	13.226	559.7	-	-	-
LC1	0.5486	13.226	559.7	0.5486	27.261	732.1
LC1 - bus power	-	-	-	-	-	-
LC2	0.0000	13.226	559.7	0.0000	57.270	931.6
LC2 - bus power	-	-	-	-	-	-
MES	1.6667	-	-	-	-	-
ECS	0.0000	-	-	-	-	-
HX1-cold side	0.5486	27.261	732.1	0.5486	25.898	1114.3
HX2-cold side	0.4794	25.898	1114.3	0.4794	24.603	1871.1
Jet A	0.0140	-	560.0	-	-	-
reformer	0.0692	24.603	1652.7	0.1412	24.406	2156.6
HX3-reformate	0.1412	24.406	2156.6	0.1412	23.186	1954.4
HX3-air	0.4794	24.603	1871.1	0.4794	23.373	1954.4
FC-anode	0.1412	23.186	1954.4	0.1659	22.027	2166.3
FC-cathode	0.4794	23.186	1954.4	0.4547	22.027	2166.3
FC -	-	-	2060.5	-	-	-
FC - bus power	-	-	-	-	-	-
HX2-hot side	0.4547	22.027	2166.3	0.4547	20.925	1545.3
cat comb	0.5626	20.925	1684.9	0.5626	19.879	1991.7
Turbine	0.5626	19.879	1991.7	0.5626	16.238	1908.8
LC1/Turbine Net	-	-	-	-	-	-
Gen/Motor bus power	-	-	-	-	-	-
HX1-hot side	0.5626	16.238	1908.8	0.5626	15.426	1577.6

G05-377-80

Note: Cells highlighted in Brown or Blue indicate components reaching temperature limits.

Figure 34. SOFC APU System 1, Case 7(b) Performance Results.

System 1, Case 6b/7b, Ambient Air, Ground, 116 kW, MES Schematic



G05-377-72

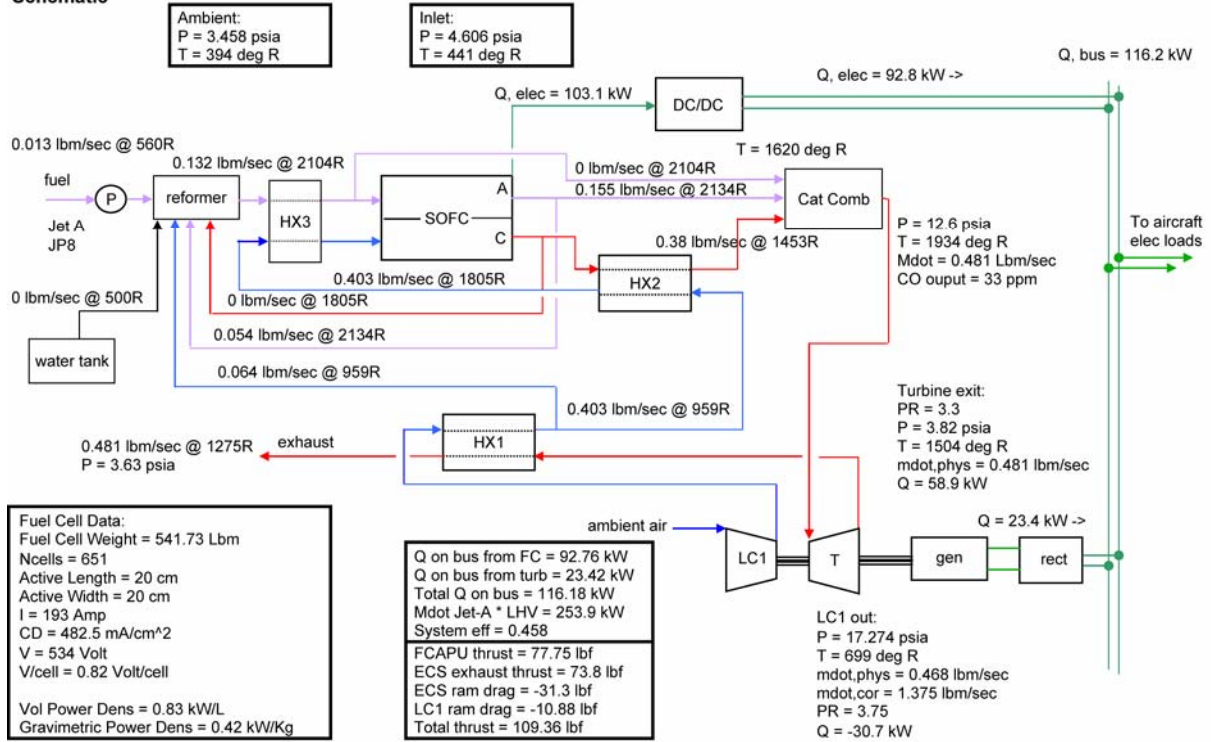
	Inlet			Exit		
	Mdot Lbm/sec	P psia	T R	Mdot Lbm/sec	P psia	T R
ambient	-	14.696	559.7	-	-	-
inlet	-	13.226	559.7	-	-	-
LC1	0.7217	13.226	559.7	0.7217	32.635	774.7
LC1 - bus power	-	-	-	-	-	-
LC2	0.0000	13.226	559.7	0.0000	57.270	931.6
LC2 - bus power	-	-	-	-	-	-
MES	1.6667	-	-	-	-	-
ECS	0.0000	-	-	-	-	-
HX1-cold side	0.7217	32.635	774.7	0.7217	31.003	1139.8
HX2-cold side	0.6303	31.003	1139.8	0.6303	29.453	1941.2
Jet A	0.0185	-	560.0	-	-	-
reformer	0.0914	29.453	1710.5	0.1865	29.217	2193.7
HX3-reformate	0.1865	29.217	2193.7	0.1865	27.756	2014.6
HX3-air	0.6303	29.453	1941.2	0.6303	27.980	2014.6
FC-anode	0.1865	27.756	2014.6	0.2189	26.369	2253.1
FC-cathode	0.6303	27.756	2014.6	0.5978	26.369	2253.1
FC -	-	-	2134.0	-	-	-
FC - bus power	-	-	-	-	-	-
HX2-hot side	0.5978	26.369	2253.1	0.5978	25.050	1597.1
cat comb	0.7401	25.050	1745.3	0.7401	23.798	2059.3
Turbine	0.7401	23.798	2059.3	0.7401	16.179	1899.7
LC1/Turbine Net	-	-	-	-	-	-
Gen/Motor bus power	-	-	-	-	-	-
HX1-hot side	0.7401	16.179	1899.7	0.7401	15.370	1582.3

G05-377-82

Note: Cells highlighted in Brown or Blue indicate components reaching temperature limits.

Figure 35. SOFC APU System 1, Case 7(c) Performance Results.

System 1, Case 7c, Ambient Air, Cruise, 116 kW, full power Schematic



G05-377-83

	Inlet			Exit		
	Mdot Lbm/sec	P psia	T R	Mdot Lbm/sec	P psia	T R
ambient	-	3.458	393.9	-	-	-
inlet	-	4.606	440.6	-	-	-
LC1	0.4676	4.606	440.6	0.4676	17.274	699.4
LC1 - bus power	-	-	-	-	-	-
LC2	0.0000	4.606	440.6	0.0000	19.945	733.8
LC2 - bus power	-	-	-	-	-	-
MES	0.0000	-	-	-	-	-
ECS	1.4167	-	-	-	-	-
HX1-cold side	0.4676	17.274	699.4	0.4676	16.410	958.6
HX2-cold side	0.4032	16.410	958.6	0.4032	15.589	1805.2
Jet A	0.0130	-	560.0	-	-	-
reformer	0.0644	15.589	1561.7	0.1317	15.465	2103.6
HX3-reformate	0.1317	15.465	2103.6	0.1317	14.692	1899.5
HX3-air	0.4032	15.589	1805.2	0.4032	14.810	1899.5
FC-anode	0.1317	14.692	1899.5	0.1550	13.957	2133.6
FC-cathode	0.4032	14.692	1899.5	0.3798	13.957	2133.6
FC -	-	-	2016.7	-	-	-
FC - bus power	-	-	-	-	-	-
HX2-hot side	0.3798	13.957	2133.6	0.3798	13.259	1453.4
cat comb	0.4806	13.259	1619.9	0.4806	12.596	1933.6
Turbine	0.4806	12.596	1933.6	0.4806	3.817	1503.7
LC1/Turbine Net	-	-	-	-	-	-
Gen/Motor bus power	-	-	-	-	-	-
HX1-hot side	0.4806	3.817	1503.7	0.4806	3.626	1275.3

G05-377-84

Note: Cells highlighted in Brown or Blue indicate components reaching temperature limits.

2.5.1 SOFC APU System Power, Efficiency, Mass, Power, and Energy Density

The mass and volume of the SOFC APU components were established, based on the following:

- SOFC stack established based on the following:
 - Based on SOFC geometry (cells and active area)
 - 50 (30) cells/sub-stack packaging estimate for 2015 (2005) technology
 - Investigation of two different interconnect options
 - Standard metallic
 - Bi-electrode supported cell (BSC) technology from NASA-Glenn
 - Includes cell tri-layer, endplates, interconnect, manifold, and insulation per each stack
 - Single SOFC used for thermodynamic/electrical modeling, but appropriate number of stacks modeled for mass/volume calculations
- Turbomachinery – based on conventional gas-turbine APUs (with similar flow size)
- Heat exchangers (3 each) – sized from work by Honeywell
- Fuel pump (Jet-A) – sizing of off-the-shelf unit with similar performance requirements
- Reformer – specific power number averaged
- Catalytic combustor – use of specific power numbers averaged
- DC/DC converter – sized for maximum power output of 200 kW (~ 0.08 kg/kW, ~ 0.1 L/kW)
- Motor-generator and rectifier – sized using specific power values using off-the-shelf information
- Piping – sized using inconel, ~10 cm diameter pipe, 275 cm total length

Estimated SOFC APU component weights/volumes were incorporated into the system model for power/energy density evaluation, as shown in Figure 36.

Table 26 shows SOFC APU system and component weights for Case 2 (185 kW MES/164 kW Cruise). The estimate of stack power density uses the current (year 2005) technology value of 0.56 kW/kg and projected (year 2015) technology values of 1.0 kW/kg and 1.4 kW/kg, based on NASA research utilizing a Bi-Electrode Supported Cell (BSC). The study results show estimated stack weights ranging between 46 to 68 percent of the total system weight, depending on the assumed stack power density. For comparison, the current baseline conventional gas turbine APU weight equals 240 lbs including accessories.

System 1, Case 1c, Ambient Air, Cruise, 84.34 kW, cruise
Weight, Energy Summary

Standard SOFC

Component	Volume (L)	Vol Fraction	Weight (Kg)	Wt Fraction
Compr./Turbine	47.19	0.162	26.31	0.057
HX1	3.40	0.012	11.97	0.026
HX2	10.56	0.036	19.41	0.042
Fuel pump	0.25	0.001	1.68	0.004
Reformer	20.58	0.071	6.86	0.015
HX3	3.18	0.011	6.49	0.014
Stack	180.66	0.620	355.50	0.772
DC/DC converter	20.48	0.070	15.36	0.033
Combustor	3.11	0.011	3.34	0.0020
Generator/rectifier	2.17	0.007	7.50	0.016
Piping	0.00	0.000	0.00	0.000
Total	291.59	1.000	460.43	1.000

Turbo toggle 0 (0=low PR/low, 1=high PR/low)
Comb/reform toggle 0 (0=200kW, 1=125kW, 2=135kW)

Total Output (kW)	84.83
Stack Output (kW)	80.53

HX toggle 0 (0=Std., 1=FP, 2=Gate, 3=MES-rev)
correction factor 1.000 square root of flow ratio

HeatX, standard - or low flow - sizes (per Honeywell)

	units	HX1	HX2	HX3
Hot Fluid	-	Turb Eth	Cathode Eth	Reformate
Cold Fluid	-	Air	Air	Air
Lhot	in.	2	4	2.9
Lcold	in.	8.31	13.2	8.8
Lno	in.	12.5	12.2	7.6
Core w/t.	lbm.	10.5	30.6	10.2
Unit w/t.	lbm.	26.4	42.8	14.3

G05-377-85A

Flight Condition	Power (kW)	Time (min)	Energy (kW-Hr)
Gate	107.45	60	107.5
Engine Start	185.31	1	3.1
Tail Flap Deploy	86.68	10	14.4
Lift-off - Climb	86.68	1	1.4
Hi-lift and Flap Stow	102.34	19	32.4
Cruise	84.34	175	246.0
Approach & Landing	102.34	20	34.1
Flap Deploy	86.68	3	4.3
Go-around	0.00	0	0.0
Taxi-in	63.86	10	10.6
Ground Maint.	0.00	0	0.0
Total		299	453.9

Power toggle 0 (0=Std., 1=FP, 2=Gate, 3=MES-rev)

System	Volumetric Energy-Density (kW-Hr/L)	Gravimetric Energy-Density (kW-Hr/Kg)
	1.56	0.99

	Volumetric Power-Density (kW/L)	Gravimetric Power-Density (kW/Kg)
SOFC Stack	0.45	0.23
Overall System	0.29	0.18

Fuel pump	
Volume (L)	0.25
den (g/cc)	6.72
Mass (kg)	1.68
Motor/Generator	(0=Std., 1=FP, 2=Gate)
Volume (L)	0.50
Motor/Gen toggle	0
Mass (kg)	2.50
Rectifier	
Volume (L)	1.87
Mass (kg)	5.00
DC/DC converter	
Volume (L)	20.48
Mass (kg)	15.36

Simple piping calculations (using Hastelloy)

	anode	cathode
Al. section	5	10
L. section (cm)	15.00	20.00
D. pipe (cm)	10.16	10.16
t. pipe (cm)	0.60	0.60
A. pipe (cm ²)	18.02	18.02
den (g/cc)	8.90	8.90
V. act (cc)	1351.51	3604.04
mass (g)	12028.47	32075.91
V. solid (cc)	6080.49	16214.64

Figure 36. Sample SOFC APU Model Incorporating Estimated Mass and Volume Values.

Table 26. Estimated SOFC APU System and Component Weight Distribution.

Component	STD Conventional Technology 0.56 kw/kg		BSC-2 NASA BSC Potential 1.0 kw/kg		BSC-1 NASA BSC Future 1.4 kw/kg	
	Weight (lb)	Wt Fraction	Weight (lb)	Wt Fraction	Weight (lb)	Wt Fraction
Compressor/Turbine	79.01	0.07	79.01	0.10	79.01	0.12
HX1	30.01	0.03	30.01	0.04	30.01	0.04
HX2	48.65	0.04	48.65	0.06	48.65	0.07
Fuel pump	3.70	0.00	3.70	0.00	3.70	0.01
Reformer	15.13	0.01	15.13	0.02	15.13	0.02
HX3	16.25	0.01	16.25	0.02	16.25	0.02
Stack	783.89	0.68	437.43	0.54	313.55	0.46
DC/DC converter	33.88	0.03	33.88	0.04	33.88	0.05
Combustor	20.59	0.02	20.59	0.03	20.59	0.03
Generator/Rectifier	23.15	0.02	23.15	0.03	23.15	0.03
Piping	97.25	0.08	97.25	0.12	97.25	0.14
Total	1151.52	1.00	805.06	1.00	681.18	1.00

Baseline Conventional APU Weighs 240 lb

G05-377-86A

Table 27 summarizes the estimated SOFC APU system weight for Cases 1, 2, 5, 6, and 7 (ambient air supply for SOFC APU). Table 30 also summarizes system weight, power output, and system efficiencies on the ground and during Cruise. These results show the estimated SOFC APU efficiency ranges from 32 to 36 percent on the ground, and from 45 to 48 percent during 35,000 ft altitude Cruise operation. The same SOFC APU has a higher system efficiency operating at higher power. The SOFC APU with higher power output (and size) appears to be reaching an asymptotic limit at around 50 percent system efficiency.

Table 27. Estimated SOFC APU System Mass, Power, and System Efficiency.

BSC-2 Technology 1.0kw/kg SOFC Stack

	SOFC		Ground				Cruise					
	System		Gate		MES		Normal		1-Engine Out Power		Full Power	
	Weight		Power	Efficiency	Power	Efficiency	Power	Efficiency	Power	Efficiency	Power	Efficiency
	lb		Kw		Kw		Kw		Kw		Kw	
Case 1	766.4		107.45	0.34	185	0.36	84.34	0.46	124	0.47		
Case 2	805.4		107.45	0.34	185	0.36					164	0.48
Case 5	562.8		112.82	0.34	Ground		84.34	0.46				
Case 6	617.6		86.26	0.32	116	0.323	84.34	0.45	100	0.45		
Case 7	617.6		86.26	0.32	116	0.323					116	0.46

* SOFC Weight is based on ground MES or max power requirement

In Table 28, the baseline conventional APU power density is compared against that of the SOFC APU on the ground and during altitude Cruise operation. The results show that the baseline APU power density should be compared to that of the SOFC APU at specific conditions, due to the altitude lapse rate characteristic of gas turbines, and the capability of the SOFC APU in retaining most of the power density at altitude. Table 28 shows that the available power for the baseline APU is 272 kW on the ground and 82 kW during altitude Cruise. The baseline APU power density is 2.5 kW/kg on the ground and 0.75 kW/kg at Cruise; that is, approximately ~5 to 6 times that of the SOFC APU on the ground, and approximately ~1.5 to 3 times the SOFC APU at altitude Cruise. The baseline APU is rated at 272 kW on the ground to meet the altitude power requirement and hot-day ECS load; it normally operates at <175 kW for part-load conditions on the ground. As a result, the baseline APU normal operating power density is ~1.6 kW/kg on the ground and 0.75 kW/g at altitude Cruise; that is, approximately ~3 to 4 times the SOFC APU on the ground, and approximately ~1.5 to 3 times the SOFC APU at altitude Cruise.

Table 28. Power Density Comparison of Baseline Gas Turbine APU Vs. SOFC APU.

BSC-2 Technology, 1.0 kW/kg SOFC Stack

	SOFC System Weight		Ground				Cruise	
			Gate		MES		35,000 ft	
	lbs	kg	Power, kW	Power Density, kW/kg	Power, kW	Power Density, kW/kg	Power, kW	Power Density, kW/kg
Conventional APU	240	109	272.0	2.50	272.0	2.50	82.0	0.75
Case 1	766	347	107.5	0.31	185.4	0.53	84.34	0.24
Case 2	805	365	107.5	0.29	185.4	0.51	164.0	0.45
Case 5	563	255	113.0	0.44	(GND)	(GND)	84.34	0.33
Case 6	618	280	86.35	0.31	116.0	0.41	84.34	0.30
Case 7	618	280	86.35	0.31	116.0	0.41	116.0	0.41

Table 29 summarizes the SOFC stack and APU mass, volume, gravimetric/volumetric power and energy density values for Cases 1, 2, 5, 6, and 7 (using ambient air). These results show that the estimated SOFC APU weight ranges between 486 lb (221 kg) to 1150 lb (522 kg); that is, 2 to 4.8 times the current weight of the baseline gas turbine APU, depending on the SOFC APU sizing and on the assumed stack power density.

Table 29. Estimated SOFC Stack/APU System Characteristics (Cases 1, 2, 5, 6, and 7 – Ambient Air).

	Case 1			Case 2			Case 5			Case 6/7		
Gate Power, kW	107.5			107.5			112.82			86.26		
Eff @ Gate Power	0.34			0.34			0.34			0.32		
MES Power, kW	185			185			Ground			116		
Eff @ MES Power	0.36			0.36			Ground			0.323		
Normal Cruise Power, kW	84.34						84.34			84.34		
Eff @ Normal Cruise Power	0.46						0.46			0.45		
Full Cruise Power, kW				164						116		
Eff @ Full Cruise Power				0.48						0.46		
Parameter Description	Std.	BSC-2	BSC-1	Std.	BSC-2	BSC-1	Std.	BSC-2	BSC-1	Std.	BSC-2	BSC-1
System total volume (L)	313.9	234.1	205.5	399.5	319.8	291.1	231.4	182.4	164.9	250	194.9	175.1
System total mass (kg)	504.5	347.6	291.2	522.2	365.3	308.9	351.6	255.3	220.7	388.6	280.2	241.2
SOFC volume (L)	180.7	100.9	72.3	180.7	100.9	72.3	110.9	61.9	44.3	124.9	69.7	49.9
SOFC mass (kg)	355.5	198.6	142.2	355.5	198.6	142.2	218.1	121.9	87.3	245.7	137.3	98.3
System volumetric energy density (kWh/L)	1.45	1.94	2.21	1.72	2.15	2.36	1.96	2.48	2.75	1.73	2.21	2.47
System gravimetric energy density (kWh/kg)	0.9	1.31	1.56	1.31	1.88	2.22	1.29	1.77	2.05	1.11	1.54	1.79
SOFC volumetric power density (kW/L)	1.1	1.97	2.75	1.1	1.97	2.75	1.11	2	2.79	1.09	1.95	2.72
SOFC gravimetric power density (kW/kg)	0.56	1	1.4	0.56	1	1.4	0.57	1.01	1.42	0.55	0.99	1.38
System volumetric power density (kW/L)	0.59	0.79	0.9	0.46	0.58	0.64	0.49	0.62	0.69	0.46	0.6	0.66
System gravimetric power density (kW/kg)	0.37	0.53	0.64	0.35	0.51	0.6	0.32	0.44	0.51	0.3	0.41	0.48

Table 30 shows a similar SOFC stack/APU system data summary for Cases 3 and 4 (using cabin air for the SOFC APU air supply). The results show similar power density values as in Cases 1 and 2, using ambient air.

Table 30. SOFC Stack/APU System Characteristics (Cases 3 and 4 – Cabin Air).

	Case 3			Case 4		
Parameter Description	Std.	BSC-2	BSC-1	Std.	BSC-2	BSC-1
System total volume (L)	308.6	230.6	202.6	392.3	314.3	286.3
System total mass (kg)	494.8	341.4	286.3	508.9	355.5	300.3
SOFC volume (L)	176.6	98.7	70.7	176.6	98.7	70.7
SOFC mass (kg)	347.6	194.2	139.0	347.6	194.2	139.0
System volumetric energy density (kWh/L)	1.47	1.97	2.24	1.75	2.18	2.40
System gravimetric energy density (kWh/kg)	0.92	1.33	1.59	1.35	1.93	2.28
SOFC volumetric power density (kW/L)	1.10	1.97	2.76	1.10	1.97	2.76
SOFC gravimetric power density (kW/kg)	0.56	1.00	1.40	0.56	1.00	1.40
System volumetric power density (kW/L)	0.60	0.80	0.92	0.47	0.59	0.65
System gravimetric power density (kW/kg)	0.37	0.54	0.65	0.36	0.52	0.62

Tables 31 through 36 provide summaries of all the SOFC APU system power, efficiency and component performance data, along with the estimated weight, volume, power, and energy density for each Case Study.

**Table 31. SOFC APU Performance Summary.
(System 1, Case 1 – Ambient Air).**

Parameter description	1(a)	1(b)	1(c)	1(d)
	Ground Operation, Gate: 107.45 kW	Ground Operation, MES: 185 kW	Cruise (Normal): 84.34 kW	Cruise (One Engine Out): 124
SOFC number of cells	942	942	942	942
SOFC active area size (cm)	20 x 20	20 x 20	20 x 20	20 x 20
SOFC current demand (A)	164.3	268.6	97.8	139.3
SOFC volt/cell (V)	0.855	0.785	0.874	0.854
SOFC efficiency	0.748	0.695	0.764	0.749
SOFC power output on bus (kW)	119.2	178.7	72.5	100.9
SOFC operating temperature (°C)	853.8	917.8	793.8	821.2
SOFC inlet/exit dT (°C)	110.4	132.2	110.2	119.2
Anode recycle amount	0.35	0.35	0.35	0.35
Compressor PR	2.22	3.28	2.78	3.75
Compressor corrected flow (lbm/s)	0.74	1.21	1.01	1.44
Compressor efficiency	0.75	0.79	0.76	0.78
Turbine power output on bus (kW)	-11.67	6.7	12.4	23.3
Turbine PR	1.32	1.95	2.45	3.3
Turbine corrected flow (lbm/s)	1.87	1	1.05	1.12
Turbine efficiency	0.85	0.85	0.85	0.85
Total power on bus (kW)	107.5	185.4	84.8	124.2
Combustor operating temperature (°C)	818.1	878.6	750.2	777.5
Combustor CO output (ppm)	34	40	27	30
Additional fuel to combustor	0	0	0	0
System efficiency	0.34	0.36	0.46	0.47
Net Thrust, aircraft basis (lbf)	0	0	92.1	111.5
Normal Tech:				
SOFC mass (lbm)	783.9	783.9	783.9	783.9
System total mass (lbm)	1112.3	1112.3	1112.3	1112.3
SOFC volumetric power density (kW/L)	0.73	1.1	0.45	0.62
SOFC gravimetric power density (kW/kg)	0.37	0.56	0.23	0.32
System volumetric power density (kW/L)	0.34	0.59	0.27	0.4
System gravimetric power density (kW/kg)	0.21	0.37	0.17	0.25
System volumetric energy density (kWh/L)	1.45	1.45	1.45	1.45
System gravimetric energy density (kWh/kg)	0.9	0.9	0.9	0.9
BSC-2 Tech (1.0 kW/kg):				
SOFC mass (lbm)	437.9	437.9	437.9	437.9
System total mass (lbm)	766.4	766.4	766.4	766.4
SOFC volumetric power density (kW/L)	1.31	1.97	0.8	1.11
SOFC gravimetric power density (kW/kg)	0.67	1	0.41	0.56
System volumetric power density (kW/L)	0.46	0.79	0.36	0.53
System gravimetric power density (kW/kg)	0.31	0.53	0.24	0.36
System volumetric energy density (kWh/L)	1.94	1.94	1.94	1.94
System gravimetric energy density (kWh/kg)	1.31	1.31	1.31	1.31
BSC-1 Tech (1.4 kW/kg):				
SOFC mass (lbm)	216.6	216.6	216.6	216.6
System total mass (lbm)	531.7	531.7	531.7	531.7
SOFC volumetric power density (kW/L)	2.2	2.75	1.11	1.55
SOFC gravimetric power density (kW/kg)	1.12	1.4	0.57	0.79
System volumetric power density (kW/L)	0.47	0.9	0.41	0.6
System gravimetric power density (kW/kg)	0.36	0.64	0.29	0.43
System volumetric energy density (kWh/L)	2.21	2.21	2.21	2.21
System gravimetric energy density (kWh/kg)	1.56	1.56	1.56	1.56

**Table 32. SOFC APU Performance Summary.
(System 1, Case 2 – Ambient Air).**

Parameter description	2(a)	2(b)	2(c)
	Ground Operation, Gate: 107.45 kW	Ground Operation, MES: 185 kW	Cruise (Full Power): 164 kW
SOFC number of cells	942	942	942
SOFC active area size (cm)	20 x 20	20 x 20	20 x 20
SOFC current demand (A)	163.9	268.6	180.8
SOFC volt/cell (V)	0.855	0.786	0.836
SOFC efficiency	0.746	0.694	0.735
SOFC power output on bus (kW)	118.9	179	128.2
SOFC operating temperature (°C)	847.9	915.2	848
SOFC inlet/exit dT (°C)	110.1	130.6	126.5
Anode recycle amount	0.35	0.35	0.35
Compressor PR	2.32	3.46	5
Compressor corrected flow (lbm/s)	0.749	1.23	1.86
Compressor efficiency	0.74	0.77	0.78
Turbine power output on bus (kW)	-11.4	6.3	35.8
Turbine PR	1.38	2.06	4.4
Turbine corrected flow (lbm/s)	0.843	1	1.1
Turbine efficiency	0.85	0.96	0.85
Total power on bus (kW)	107.5	185.4	164
Combustor operating temperature (°C)	799.3	872.3	806.2
Combustor CO output (ppm)	30	39	33
Additional fuel to combustor	0	0	0
System efficiency	0.34	0.36	0.48
Net Thrust, aircraft basis (lbf)	0	0	131.5
Normal Tech:			
SOFC mass (lbm)	783.9	783.9	783.9
System total mass (lbm)	1151.3	1151.3	1151.3
SOFC volumetric power density (kW/L)	0.73	1.1	0.79
SOFC gravimetric power density (kW/kg)	0.37	0.56	0.4
System volumetric power density (kW/L)	0.27	0.46	0.41
System gravimetric power density (kW/kg)	0.21	0.35	0.31
System volumetric energy density (kWh/L)	1.72	1.72	1.72
System gravimetric energy density (kWh/kg)	1.31	1.31	1.31
BSC-2 Tech (1.0 kW/kg):			
SOFC mass (lbm)	437.9	437.9	437.9
System total mass (lbm)	805.4	805.4	805.4
SOFC volumetric power density (kW/L)	1.58	1.95	1.12
SOFC gravimetric power density (kW/kg)	0.8	0.99	0.57
System volumetric power density (kW/L)	0.44	0.6	0.43
System gravimetric power density (kW/kg)	0.31	0.41	0.3
System volumetric energy density (kWh/L)	2.15	2.15	2.15
System gravimetric energy density (kWh/kg)	1.88	1.88	1.88
BSC-1 Tech (1.4 kW/kg):			
SOFC mass (lbm)	313.5	313.5	313.5
System total mass (lbm)	681.1	681.1	681.1
SOFC volumetric power density (kW/L)	2.2	2.72	1.56
SOFC gravimetric power density (kW/kg)	1.12	1.38	0.79
System volumetric power density (kW/L)	0.47	0.66	0.48
System gravimetric power density (kW/kg)	0.36	0.48	0.35
System volumetric energy density (kWh/L)	2.36	2.36	2.36
System gravimetric energy density (kWh/kg)	2.22	2.22	2.22

**Table 33. SOFC APU Performance Summary.
(System 2, Case 3 – Cabin Air).**

Parameter description	3(a) Ground Operation, Gate (2015/2020)	3(b) Ground Operation, MES (2015/2020)	3(c) Cruise Condition (2015/2020)	3(d) Cruise Emergency/Engine Out (2015/2020)
SOFC mass (lbm)	766.4	766.4	766.4	766.4
SOFC number of cells	921	921	921	921
SOFC active area size (cm)	20 x 20	20 x 20	20 x 20	20 x 20
SOFC current demand (A)	164.8	270.0	86.8	127.0
SOFC Volts/cell (V)	0.855	0.783	0.888	0.868
SOFC efficiency	0.750	0.695	0.774	0.759
SOFC volumetric power density (kW/L)	0.73	1.10	0.40	0.57
SOFC volumetric power density (kW/L))	0.37	0.56	0.20	0.29
SOFC power output on bus (kW)	116.8	175.2	63.9	91.4
SOFC operating temperature (°C)	859.7	922.8	799.6	826.8
SOFC inlet/exit dT (°C)	115.6	138.2	113.8	121.7
Anode recycle amount	0.35	0.35	0.35	0.35
Compressor Pressure Ratio (PR)	2.18	3.23	1.64	2.05
Compressor corrected flow (lbm/s)	0.68	1.10	0.43	0.63
Compressor efficiency	0.76	0.8	0.73	0.75
Turbine power output on bus (kW)	-9.32	10.2	20.6	34.0
Turbine Pressure Ratio (PR)	1.29	1.92	3.08	3.85
Turbine corrected flow (lbm/s)	0.85	0.96	0.69	0.83
Turbine efficiency	0.85	0.85	0.85	0.85
Total power on bus (kW)	107.5	185.4	84.5	125.4
Combustor operating temperature (°C)	828.5	887.9	759.5	796.6
Combustor CO output (ppm)	36	42	28	33
Additional fuel to combustor	0.0	0.0	0.0	0.0
System efficiency	0.35	0.36	0.53	0.53
Net Thrust, aircraft basis (lbf)	0.0	0.0	73.9	88.5
SOFC volumetric power density (kW/L)	0.31	0.53	0.24	0.36
SOFC volumetric power density (kW/L)	0.21	0.36	0.17	0.25

**Table 34. SOFC APU Performance Summary.
(System 2, Case 4 – Cabin Air).**

Parameter description	4(a)	4(b)	4(c)
	Ground Operation, Gate (2015/2020)	Ground Operation, MES (2015/2020)	Cruise Condition, Full Power (2015/2020)
SOFC mass (lbm)	766.4	766.4	766.4
SOFC number of cells	921	921	921
SOFC active area size (cm)	20 x 20	20 x 20	20 x 20
SOFC current demand (A)	164.8	270.0	164.6
SOFC Volts/cell (V)	0.855	0.783	0.850
SOFC efficiency	0.750	0.695	0.745
SOFC volumetric power density (kW/L)	0.73	1.10	0.73
SOFC volumetric power density (kW/L))	0.37	0.56	0.37
SOFC power output on bus (kW)	116.8	175.2	115.9
SOFC operating temperature (°C)	859.6	922.8	848.1
SOFC inlet/exit dT (°C)	115.5	138.2	128.9
Anode recycle amount	0.35	0.35	0.35
Compressor Pressure Ratio (PR)	2.18	3.23	2.50
Compressor corrected flow (lbm/s)	0.68	1.10	0.82
Compressor efficiency	0.76	0.8	0.78
Turbine power output on bus (kW)	-9.3	10.2	48.2
Turbine Pressure Ratio (PR)	1.29	1.92	4.68
Turbine corrected flow (lbm/s)	0.85	0.96	0.89
Turbine efficiency	0.85	0.85	0.85
Total power on bus (kW)	107.5	185.4	164.1
Combustor operating temperature (°C)	828.4	887.9	817.7
Combustor CO output (ppm)	36	42	36
Additional fuel to combustor	0.0	0.0	0.0
System efficiency	0.35	0.36	0.53
Net Thrust, aircraft basis (lbf)	0.0	0.0	102.0
SOFC volumetric power density (kW/L)	0.31	0.53	0.47
SOFC volumetric power density (kW/L)	0.21	0.36	0.32

**Table 35. SOFC APU Performance Summary.
(System 1, Case 5 – Ambient Air).**

Parameter description	5(a)	5(b)
	Ground Operation, Gate: 112.82 kW	Cruise (Normal): 84.34kW
SOFC number of cells	578	578
SOFC active area size (cm)	20 x 20	20 x 20
SOFC current demand (A)	277	156
SOFC volt/cell (V)	0.772	0.844
SOFC efficiency	0.685	0.742
SOFC power output on bus (kW)	111.2	68.5
SOFC operating temperature (°C)	916.5	830.6
SOFC inlet/exit dT (°C)	136.3	122.2
Anode recycle amount	0.35	0.35
Compressor PR	3.04	3.75
Compressor corrected flow (lbm/s)	0.76	0.99
Compressor efficiency	0.78	0.76
Turbine power output on bus (kW)	1.8	15.84
Turbine PR	1.81	3.3
Turbine corrected flow (lbm/s)	0.68	0.77
Turbine efficiency	0.85	0.85
Total power on bus (kW)	113	84.3
Combustor operating temperature (°C)	871.9	786.8
Combustor CO output (ppm)	39	31
Additional fuel to combustor	0	0
System efficiency	0.34	0.46
Net Thrust, aircraft basis (lbf)	0	90.2
Normal Tech:		
SOFC mass (lbm)	481	481
System total mass (lbm)	775	775
SOFC volumetric power density (kW/L)	1.11	0.69
SOFC gravimetric power density (kW/kg)	0.57	0.35
System volumetric power density (kW/L)	0.49	0.36
System gravimetric power density (kW/kg)	0.32	0.24
System volumetric energy density (kWh/L)	1.96	1.96
System gravimetric energy density (kWh/kg)	1.29	1.29
BSC-2 Tech (1.0 kW/kg):		
SOFC mass (lbm)	268.7	268.7
System total mass (lbm)	562.8	562.8
SOFC volumetric power density (kW/L)	2.00	1.23
SOFC gravimetric power density (kW/kg)	1.01	0.62
System volumetric power density (kW/L)	0.62	0.46
System gravimetric power density (kW/kg)	0.44	0.33
System volumetric energy density (kWh/L)	2.48	2.48
System gravimetric energy density (kWh/kg)	1.77	1.77
BSC-1 Tech (1.4 kW/kg):		
SOFC mass (lbm)	192.4	192.4
System total mass (lbm)	486.5	486.5
SOFC volumetric power density (kW/L)	2.79	1.72
SOFC gravimetric power density (kW/kg)	1.42	0.87
System volumetric power density (kW/L)	0.69	0.51
System gravimetric power density (kW/kg)	0.51	0.38
System volumetric energy density (kWh/L)	2.75	2.75
System gravimetric energy density (kWh/kg)	2.05	2.05

**Table 36. SOFC APU Performance Summary.
(System 1, Cases 6 and 7 – Ambient Air).**

Parameter description	(a)	(b)	(c)	(d)	(e)
	Ground Operation, Gate: 86.26 kW	Ground Operation, MES: 116 kW	Cruise (Normal): 84.34 kW	Cruise (Engine Out): 100 kW	Cruise (Full Power): 116 kW
SOFC number of cells	651	651	651	651	651
SOFC active area size (cm)	20 x 20	20 x 20	20 x 20	20 x 20	20 x 20
SOFC current demand (A)	204	268.2	142.5	167.9	193
SOFC volt/cell (V)	0.828	0.778	0.841	0.831	0.82
SOFC efficiency	0.73	0.693	0.742	0.734	0.726
SOFC power output on bus (kW)	99	122.2	70.2	81.7	92.8
SOFC operating temperature (°C)	871.6	912.4	820.7	833.6	847.2
SOFC inlet/exit dT (°C)	117.8	132.5	121.7	125.9	130.1
Anode recycle amount	0.35	0.35	0.35	0.35	0.35
Compressor PR	2.06	2.47	2.87	3.27	3.75
Compressor corrected flow (lbm/s)	0.63	0.833	1.02	1.19	1.375
Compressor efficiency	0.744	0.765	0.78	0.78	0.78
Turbine power output on bus (kW)	-12.6	-6.1	13.8	18.3	23.4
Turbine PR	1.224	1.47	2.53	2.88	3.3
Turbine corrected flow (lbm/s)	0.85	0.911	1.03	1.07	1.083
Turbine efficiency	0.85	0.85	0.85	0.85	0.85
Total power on bus (kW)	86.35	116.2	84.1	100.02	116.18
Combustor operating temperature (°C)	832.9	870.9	774.2	786.9	801.1
Combustor CO output (ppm)	35	39	30	31	33
Additional fuel to combustor	0	0	0	0	0
System efficiency	0.32	0.323	0.45	0.45	0.46
Net Thrust, aircraft basis (lbf)	0	0	92.82	100.32	109.36
Normal Tech:					
SOFC mass (lbm)	541.6	541.6	541.6	541.6	541.6
System total mass (lbm)	856.67	856.67	856.67	856.67	856.67
SOFC volumetric power density (kW/L)	0.88	1.09	0.62	0.73	0.83
SOFC gravimetric power density (kW/kg)	0.45	0.55	0.32	0.37	0.42
System volumetric power density (kW/L)	0.35	0.46	0.34	0.4	0.46
System gravimetric power density (kW/kg)	0.22	0.3	0.22	0.26	0.3
System volumetric energy density (kWh/L)	1.73	1.73	1.73	1.73	1.73
System gravimetric energy density (kWh/kg)	1.11	1.11	1.11	1.11	1.11
BSC-2 Tech (1.0 kW/kg):					
SOFC mass (lbm)	302.6	302.6	302.6	302.6	302.6
System total mass (lbm)	617.6	617.6	617.6	617.6	617.6
SOFC volumetric power density (kW/L)	1.58	1.95	1.12	1.3	1.48
SOFC gravimetric power density (kW/kg)	0.8	0.99	0.57	0.66	0.75
System volumetric power density (kW/L)	0.44	0.6	0.43	0.51	0.6
System gravimetric power density (kW/kg)	0.31	0.41	0.3	0.36	0.41
System volumetric energy density (kWh/L)	2.21	2.21	2.21	2.21	2.21
System gravimetric energy density (kWh/kg)	1.54	1.54	1.54	1.54	1.54
BSC-1 Tech (1.4 kW/kg):					
SOFC mass (lbm)	216.6	216.6	216.6	216.6	216.6
System total mass (lbm)	531.7	531.7	531.7	531.7	531.7
SOFC volumetric power density (kW/L)	2.2	2.72	1.56	1.82	2.06
SOFC gravimetric power density (kW/kg)	1.12	1.38	0.79	0.92	1.05
System volumetric power density (kW/L)	0.47	0.66	0.48	0.57	0.66
System gravimetric power density (kW/kg)	0.36	0.48	0.35	0.41	0.48
System volumetric energy density (kWh/L)	2.47	2.47	2.47	2.47	2.47
System gravimetric energy density (kWh/kg)	1.79	1.79	1.79	1.79	1.79

2.6 Task 2.4 – Evaluation of Fuel Cell Powered Architecture

This study results discussed in this section integrates the SOFC APU into the Regional Jet, and evaluates the impact of the SOFC APU weight and thermal efficiencies on the aircraft Take-Off Gross Weight (TOGW), mission fuel burn and emissions during Cruise, and the Landing and Take-Off (LTO) cycle, and in operation on ground at the terminal gate.

2.6.1 Aircraft Value Function/Index Evaluation

The Aircraft Value Function/Index based on the aircraft Take Off Gross Weight (TOGW) established in Part I/Task 1.1 was evaluated with the SOFC APU weight and efficiency results established in Part II/Task 2.3.

Weight Fractions (using the Breguet Equation) were generated by summing up all partial weights. The solution was iterated in an Excel spreadsheet (see Figure 37) generated for this purpose.

Value Index Calculator - Aircraft System Context									
Mission Parameter Inputs									
Mission Segment	SFC ₀	P ₂₀ (hp)	SFC _e	v ₂₀ (ft)	W/W	(L/D)	V	R	
Warmup/TO	0 - 1	0.611	422.9		0.1	0.97			
Climb	1 - 2	0.623	137.2		0.33	0.98			
Cruise 1	2 - 3	0.000	0.0	0.630	1.126		15.25	445	500
Loiter	3 - 4	0.000	0.0	0.000	0		19.06		
Cruise 2	4 - 5	0.000	0.0	0.630	1.126		15.25	445	500
Descent	5 - 6	0.499	137.2		0.3333	0.995			
Land	6 - e	0.474	116.2		0.05	1			
		lb/hp-hr		Use TSFC					
				lbm/lb-f-hr					
System Inputs									
W ₀	240.0	lb							
W _{UE}	16350	lb							
W _E	47260	lb							
k	1.1								
NUM	63929.65	lb							
DENOM	0.848179								
Value Index (TOGW)									
W ₀	75372.80	lb							
Solve for TOGW!									

Figure 37. Value Index Calculator (Excel Spreadsheet).

Since the common perception of value is “the bigger the better”, the TOGW-based Value Function Index (VI) should be:

$$VI = 1 / TOGW \quad [Eq. 81]$$

Or the Relative Value Index:

$$VI_R = TOGW_{ref} / TOGW \quad [Eq. 82]$$

The Value Index has been evaluated for a matrix of two independent variables:

- Aircraft mission length (in nmi)
- Power Specific Weight of the SOFC Stack (in kW/kg)

The results are shown in Table 37.

Table 37. Aircraft TOGW-Based Value Index.

Mission	Ref TOGW	TOGW, lb			VIR		
		Spec. Stack Weight			Spec. Stack Weight		
Nmi	lb	0.56	1.0	1.4	0.56	1.0	1.4
500	71,483	72,313	71,939	71,805	0.988	0.993	0.996
1000	75,799	76,606	76,218	76,079	0.989	0.994	0.996
1500	80,269	81,054	80,651	80,504	0.990	0.995	0.997

The results of this calculation with TOGW Relative Value Index (VI_R) = 0.988 to 0.997 suggests that the effects of the SOFC APU weight and system efficiency cancel each other, and hence have little impact on the aircraft TOGW. This is confirmed within 0.3 percent of the results obtained with an extensive Honeywell power plant system integration code used in the following Aircraft Fuel Burn analysis.

2.6.2 Aircraft Fuel Burn Analysis

The impact of the SOFC APU installation on estimated aircraft fuel burn was compared to data for the Regional Jet turbofan main engine bleed and extraction during Cruise, and compared against the baseline gas turbine APU during ground operation at the terminal gate.

2.6.2.1 Cruise Fuel Burn – SOFC APU Compared Against Main Engine Bleed and Extraction

The Regional Jet aircraft model and mission load requirements established in Part I/Task 1.1 were integrated with the SOFC APU performance and characteristics established in Part II/Task 2.3 for the total aircraft weight, fuel burn, and emissions analysis.

- The Regional Jet aircraft model was matched with published aircraft performance
- Missions with three different stage-lengths were chosen for comparisons: 500 nmi, 1,000 nmi, and 1,500 nmi.

Figure 38 illustrates the Regional Jet mission profile established for the aircraft fuel burn comparison. The mission plot shown is indicative of a standard Instrument Flight Rules (IFR) mission with reserve fuel calculation.

During a typical mission flight profile (see Figure 38), the majority of the fuel is consumed during Cruise operation. Therefore, the fuel burn benefit for the SOFC APU was quantified for this condition. During Cruise, the APU is normally turned off and is used for backup auxiliary power only. Regular auxiliary power (for accessories) is provided by the main engine bleed and extraction.

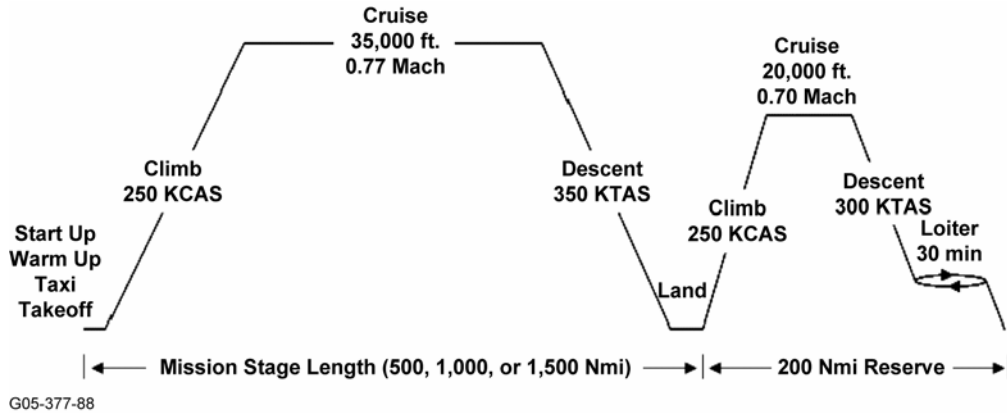


Figure 38. Regional Jet Mission Profile for Fuel Burn Evaluation.

The Baseline Cruise fuel burn per hour was established with auxiliary power provided through the aircraft main engine bleed and extraction (Table 38). This baseline is used for comparing the total aircraft fuel burn benefit from the use of the SOFC APU, with and without weight impact. The fuel burn benefits in optimizing the main engine bleed ports and in a More-Electric Aircraft (MEA) architecture with motorized pneumatic system is also shown (–0.4% and –0.3%, respectively). The analysis results shown in Table 38 also include the fuel burn benefit from use of the SOFC APU (with ambient air or cabin air supply) to generate auxiliary power, rather than deriving it from the main engines. This analysis includes utilizing the SOFC APU exhaust thrust energy, but does not include the impact of the SOFC APU weight. The results show that the difference in using ambient air vs. the cabin air supply for the SOFC APU is minimum (–1.2 percent vs. –1.0 percent), benefiting the use of ambient air when all exhaust thrust is accounted for.

A second factor in the analysis was the weight of the SOFC APU. The baseline gas turbine APU weighs 240 lbs (installed with accessories). The SOFC APU weight is summarized in Table 38.

Table 38. SOFC APU System Estimated Weight Summary.

System	Power Density, kW/kg	Weight, lbs				
		System 1, Case 1	System 1, Case 2	System 1, Case 5	System 1, Case 6	System 1, Case 7
Conventional	0.56	1112.30	1151.32	775.04	856.67	856.67
BSC	1.0	766.39	805.41	562.80	617.60	617.60
BSC	1.4	642.05	681.07	486.50	531.70	531.70
Conv. APU (Ref.)	---	240.00	---	---	---	---
		Weight, kg				
Conventional	0.56	504.53	522.23	351.55	388.58	388.58
BSC	1.0	347.63	365.33	255.28	280.14	280.14
BSC	1.4	291.23	308.93	220.67	241.18	241.18
Conv. APU (Ref.)	---	108.86	---	---	---	---

Only the use of ambient air supply for the SOFC APU was considered for the cruise fuel burn analysis including the SOFC APU weight impact, since the difference was minimal between the use of ambient versus use of cabin air, and benefiting the use of ambient air, as illustrated in Table 39.

**Table 39. SOFC APU Fuel Burn Comparison With Baseline Main Engine
(Without SOFC Weight Impact).**

**90 PAX COMMUTER 35K Mn .77 CRUISE
Power Extraction & Bleed Load Comparison Summary**

Assumes the Fuel Cell powers only the CAC in Cruise

Altitude 35000 ft
Mach No. 0.77
Cruise Thrust 2500 lbf
True Airspeed 749.3 ft/sec
Cabin Flow (Wb) 1.345 lb/sec

	Main-Engine Systems			Fuel Cell + Main Engines				
	Conventional			(ambient air)		(cabin air)		
	Existing IP Bleed (Baseline)	Optimum IP Bleed	MEA	Main Engines	Fuel Cell	Main Engines	Fuel Cell	
Flow/Extraction Inputs:								
Cabin Flow (Wb)	1.345	1.345	-	-	-	-	-	lb/sec
APU air flow	-	-	-	-	0.34	-	0.28	lb/sec
HPex CAC	-	-	84.3	-	84.3	-	84.3	kW
HPex A/C	79.6	79.6	79.6	79.6	0.0	79.6	0	kW
HP Provided to A/C	79.6	79.6	164.0	79.6	84.3	79.6	84.3	kW
Wb Per Engine	0.7	0.7	-	-	-	-	-	lb/sec
HPex Per Engine	39.8	39.8	82.0	39.8	-	39.8	-	kW
Other Model Parameters:								
Bleed Work Factor	0.979 (HPCA)	0.69 (HPCA)	-	-	-	-	-	
Inlet Recovery	0.998	0.998	0.998	0.998	0.900	0.998	0.900	
Aircraft Drag	5000	5000	5000	5000	-	5000	-	lbf
Ram Drag Increment	-	-	31.3	-	-	-	-	lbf
Aircraft Net Thrust ¹	73.8	73.8	73.8	-	92.1 ²	-	73.9 ³	lbf
Total Net Thrust / Engine	2463	2463	2479	2454	-	2463	-	lbf
T4.1	1929	1921	1924	1899	-	1902	-	°F
Fuel Burn Outputs:								
TSFC	0.63	0.63	0.62	0.62	-	0.62	-	lbm/lbf-hr
APU Efficiency	-	-	-	-	46%	-	53%	
Fuel Burn per Engine	1550	1543	1545	1515	-	1520	-	lbm/hr
Fuel Cell Fuel Burn	-	-	-	-	34.2	-	29.5	lbm/hr
System Fuel Burn	3100	3087	3089	3064		3069		lbm/hr
Δ(Fuel Burn)	0.0	-13.4	-10.6	-36.4		-30.6		lbm/hr
Δ(Fuel Burn) (%) from Baseline	0.0%	-0.4%	-0.3%	-1.2%		-1.0%		%

G05-377-89A

Footnotes:

¹ For conventional cases, this row is the outflow valve gross thrust.
For fuel cell cases, this row is the APU System **Net** Thrust including the effects below:

	2	3	
	(Ambient Air)	(Cabin Air)	
Fuel Cell Gross Thrust	57.5	47.0	lbf
Cabin Outflow Valve Gross Thrust	73.8	58.2	lbf
CAC Ram Drag	31.3	31.3	lbf
LC1 Ram Drag	8.0	0.0	lbf
APU System Net Thrust	92.1	73.9	lbf

APU System Net Thrust reduces main engine thrust requirement

Cabin Outflow for reference 1.345 1.073 Lbm/sec

Table 40 shows the results of the aircraft Cruise fuel burn analysis, including the SOFC APU weight impact. Aircraft and mission characteristic established in Part I/Task 1.1 were used, along with the SOFC APU characteristics established Part II/Task 2.3 and in the above section. The first line in Table 40, labeled “Δ Fuel Burn (%) from Baseline” shows the SOFC APU fuel burn benefit without the weight impact. This data was established from the analysis discussed above for each of Cases 1, 2, 5, 6, and 7 with the use of ambient air. The remaining analysis calculated the aircraft total fuel burn including the SOFC weight impact for three difference mission stage lengths: 500 nmi, 1,000 nmi, and 1,500 nmi. The Maximum Take-Off Gross Weight (MTOGW) was reached for the 1,500 nmi range. The aircraft total fuel burn for each Case and for each mission range is compared against the baseline main engine fuel burn with bleed and power extraction. The fuel burn benefit with the SOFC APU installation was shown to vary between -0.4% to -1.6% (-24 lbs to -235 lbs) depending on the SOFC APU design and mission range. These results show that heavier SOFC APU weight can be compensated by fuel burn reduction via the higher system efficiency of the heavier (larger) unit.

Table 40. SOFC APU Cruise Fuel Burn Summary (With SOFC Weight Impact).

	Baseline Conventional APU + Main Engine	Fuel Cell APU System 1														
		Case 1			Case 2			Case 5			Case 6			Case 7		
Δ Fuel Burn (%) from Baseline		-1.2%			-1.9%			-1.2%			-1.2%			-1.5%		
Fuel Cell Power Density		0.56 kW/kg	1.0 kW/kg	1.4 kW/kg	0.56 kW/kg	1.0 kW/kg	1.4 kW/kg	0.56 kW/kg	1.0 kW/kg	1.4 kW/kg	0.56 kW/kg	1.0 kW/kg	1.4 kW/kg	0.56 kW/kg	1.0 kW/kg	1.4 kW/kg
APU System Weight (lbs)	240	1112	766	642	1151	805	681	775	563	487	857	618	532	857	618	532
Δ Weight (lbs) from Baseline	0	872	526	402	911	565	441	535	323	247	617	378	292	617	378	292
OWE (lbs)	47500	48372	48026	47902	48411	48065	47941	48035	47823	47747	48117	47878	47792	48117	47878	47792
MTOGW (lbs)	80500	80500	80500	80500	80500	80500	80500	80500	80500	80500	80500	80500	80500	80500	80500	80500
Payload (86 pax) lbs	14620	14620	14620	14620	14620	14620	14620	14620	14620	14620	14620	14620	14620	14620	14620	14620
Max Useable Fuel (lbs)	19450	19450	19450	19450	19450	19450	19450	19450	19450	19450	19450	19450	19450	19450	19450	19450
500 Nmi Mission																
TOGW (lbs)	71483	72313	71939	71805	72288	71915	71781	71948	71719	71637	72037	71779	71686	72009	71750	71657
Block Fuel (lbs)	5594	5570	5553	5547	5533	5516	5510	5554	5543	5540	5558	5546	5542	5541	5529	5525
Δ Fuel (%) from Baseline	-	-0.4%	-0.7%	-0.8%	-1.1%	-1.4%	-1.5%	-0.7%	-0.9%	-1.0%	-0.6%	-0.9%	-0.9%	-0.9%	-1.2%	-1.2%
1,000 Nmi Mission																
TOGW (lbs)	75799	76606	76218	76079	76550	76163	76024	76229	75991	75906	76320	76053	75956	76278	76010	75914
Block Fuel (lbs)	9910	9864	9833	9822	9795	9764	9753	9834	9815	9808	9841	9820	9812	9810	9789	9781
Δ Fuel (%) from Baseline	-	-0.5%	-0.8%	-0.9%	-1.2%	-1.5%	-1.6%	-0.8%	-1.0%	-1.0%	-0.7%	-0.9%	-1.0%	-1.0%	-1.2%	-1.3%
1,500 Nmi Mission																
TOGW (lbs)	80269	81054	80651	80504	80964	80561	80417	80662	80415	80326	80757	80479	80379	80699	80421	80321
Block Fuel (lbs)	14381	14312	14266	14250	14209	14163	14146	14267	14239	14229	14278	14246	14235	14232	14200	14188
Δ Fuel (%) from Baseline	-	-0.5%	-0.8%	-0.9%	-1.2%	-1.5%	-1.6%	-0.8%	-1.0%	-1.1%	-0.7%	-0.9%	-1.0%	-1.0%	-1.3%	-1.3%

G05-377-98

Red text denotes cases that exceed 80,500 lb Maximum Takeoff Gross Weight Limit (MTOGW)

2.6.2.2 Ground/Gate Fuel Burn Analysis – SOFC APU Versus Baseline Conventional APU

When the aircraft is at the terminal gate, the main engine is turned off and the APU is turned on to provide pneumatic and electric power to the Environmental Control System (ECS), cockpit and cabin essential/non-essential (ESS/Non-ESS) electrical loads, and also for Main Engine Start (MES) when the aircraft is ready for the next flight. The On-Ground/Gate APU operating power and duration vary considerably, depending on operating site, weather, mission, and operator. Since the current baseline gas turbine APU can be turned on/off, while the SOFC APU may be limited by its thermal fatigue characteristic, a range of SOFC APU power and operating durations on the ground/gate were analyzed for a fuel burn comparison with the current baseline gas turbine APU installation.

Table 41 compares the estimated SOFC APU versus the baseline gas turbine APU fuel burn at different power and for various operating durations of 60, 30, and 10 minutes at the terminal/gate. The comparison results show that the SOFC APU, with 32 to 36 percent ground system efficiency, compared to the baseline gas turbine APU with 9 to 13 percent ground system efficiency, can have a considerable estimated fuel burn reduction of 66 to 78 percent over the baseline APU On-Ground/Gate operation; but the SOFC APU is limited by the SOFC stack thermal fatigue characteristics.

Table 41. SOFC APU Versus Baseline Gas Turbine APU Ground/Gate Fuel Burn Comparison.

Operating Time at Gate >		Fuel Burn, lbm					
		60 min		30 min		10 min	
System	Power, kW	Conv. APU	SOFC APU	Conv. APU	SOFC APU	Conv. APU	SOFC APU
Case 1	107.45	235.7	58	117.85	29.0	39.3	9.7
Case 2	107.45	235.7	58	117.85	29.0	39.3	9.7
Case 5	112.82	238.8	61	119.40	30.5	39.8	10.2
Case 6	86.26	224.1	50	112.05	25.0	37.4	8.3
Case 7	86.26	224.1	50	112.05	25.0	37.4	8.3
Case 1 and 2, Max.	185.0	278	94	139.0	47.0	46.3	15.7
Case 6 and 7, Max.	116.0	240	65	120.0	32.5	40.0	10.8

2.6.2.3 Fuel Burn Analysis Study Conclusions

The fuel burn study results showed that the SOFC APU would have a measurable, but not significant, in-flight fuel burn reduction benefit. Nevertheless, the SOFC APU could have a considerable fuel burn reduction benefit over the baseline gas turbine APU in operation on the ground, depending upon the ground operation duration.

2.6.3 Aircraft Emissions Analysis

Aircraft NOx and CO emissions with the SOFC APU installation were compared against the Regional Jet turbofan main engine bleed and extraction during Cruise; against the main engine bleed and extraction and the baseline gas turbine APU during the Landing and Take-Off (LTO) cycle; and against the baseline gas turbine APU during on-ground operation at the gate. Table 42 shows averaged estimated NOx and CO emissions for the corresponding systems.

Table 42. Estimated Emissions.

System	Units	Emissions	
		NOx	CO
Main Engine	g/kg (of jet fuel)	10* to 20	0.6
Baseline Gas Turbine APU	g/kg (of jet fuel)	6.75	5.8
SOFC APU	g/kg	(Negligible)	1.2 to 1.45**

* 10 g/kg used for advanced turbofan engine model. Older vintage engines can have higher emissions

** 0.6 g/kg is achievable at higher fuel utilization. 1.2 to 1.45 g/kg used for lower utilization.

2.6.3.1 Cruise Emissions Analysis

The impact of the SOFC APU installation on NOx and CO emissions was compared against the baseline aircraft emissions from the main engine. Table 43 shows the estimated baseline fuel burn and emissions for cruise ranges of 500, 1,000, and 1,500 nmi. Total aircraft emissions with the SOFC APU installation in each Case study are compared to the baseline aircraft emissions.

Table 43. Estimated SOFC APU Cruise Emissions.

SOFC APU CO emission, g/kg 1.2
 Main Engine CO emission, g/kg 0.6
 Main Engine NOx emission, g/kg 10

	Baseline Conventional APU + Main Engine	Fuel Cell APU System 1														
		Case 1			Case 2			Case 5			Case 6			Case 7		
Δ Fuel Burn (%) from Baseline		-1.2%			-1.9%			-1.2%			-1.2%			-1.5%		
Fuel Cell Power Density		0.56 kW/kg	1.0 kW/kg	1.4 kW/kg	0.56 kW/kg	1.0 kW/kg	1.4 kW/kg	0.56 kW/kg	1.0 kW/kg	1.4 kW/kg	0.56 kW/kg	1.0 kW/kg	1.4 kW/kg	0.56 kW/kg	1.0 kW/kg	1.4 kW/kg
APU System Weight (lbs)	240	1112	766	642	1151	805	681	775	563	487	857	618	532	857	618	532
SOFC APU Power (kw)		84.34	84.34	84.34	164	164	164	84.34	84.34	84.34	84.34	84.34	84.34	116	116	116
SOFC APU System Efficiency		0.46	0.46	0.46	0.48	0.48	0.48	0.46	0.46	0.46	0.45	0.45	0.45	0.46	0.46	0.46
Δ Weight (lbs) from Baseline	0	872	526	402	911	565	441	535	323	247	617	378	292	617	378	292
OWE (lbs)	47500	48372	48026	47902	48411	48065	47941	48035	47823	47747	48117	47878	47792	48117	47878	47792
MTOW (lbs)	80500	80500	80500	80500	80500	80500	80500	80500	80500	80500	80500	80500	80500	80500	80500	80500
Payload (86 pax) lbs	14620	14620	14620	14620	14620	14620	14620	14620	14620	14620	14620	14620	14620	14620	14620	14620
Max Useable Fuel (lbs)	19450	19450	19450	19450	19450	19450	19450	19450	19450	19450	19450	19450	19450	19450	19450	19450
500 Nmi Mission minute=	68															
TOGW (lbs)	71483	72313	71939	71805	72288	71915	71781	71948	71719	71637	72037	71779	71686	72009	71750	71657
Block Fuel (lbs)	5594	5570	5553	5547	5533	5516	5510	5554	5543	5540	5558	5546	5542	5541	5529	5525
Δ Fuel (%) from Baseline	-	-0.4%	-0.7%	-0.8%	-1.1%	-1.4%	-1.5%	-0.7%	-0.9%	-1.0%	-0.6%	-0.9%	-0.9%	-0.9%	-1.2%	-1.2%
SOFC APU fuel burn (lbs)	0	38	38	38	72	72	72	38	38	38	39	39	39	53	53	53
SOFC CO emission (kg)	0	0.021	0.021	0.021	0.039	0.039	0.039	0.021	0.021	0.021	0.021	0.021	0.021	0.029	0.029	0.029
Main engine CO emission (kg)	1.53	1.51	1.50	1.50	1.49	1.48	1.48	1.50	1.50	1.50	1.51	1.50	1.50	1.50	1.49	1.49
Total CO emission (kg)	1.526	1.530	1.525	1.523	1.529	1.524	1.522	1.525	1.522	1.521	1.527	1.523	1.522	1.526	1.522	1.521
Delta CO (%) from Baseline	0.3%	0.0%	-0.2%	-0.2%	0.2%	-0.1%	-0.2%	0.0%	-0.2%	-0.3%	0.1%	-0.2%	-0.2%	0.0%	-0.2%	-0.3%
Main engine NOx emission (kg)	25.43	25.32	25.24	25.21	25.15	25.07	25.05	25.25	25.20	25.18	25.26	25.21	25.19	25.19	25.13	25.11
Delta NOx (%) from Baseline	-	-0.4%	-0.7%	-0.8%	-1.1%	-1.4%	-1.5%	-0.7%	-0.9%	-1.0%	-0.6%	-0.9%	-0.9%	-0.9%	-1.2%	-1.2%
1,000 Nmi Mission minute=	136															
TOGW (lbs)	75799	76606	76218	76079	76550	76163	76024	76229	75991	75906	76320	76053	75956	76278	76010	75914
Block Fuel (lbs)	9910	9864	9833	9822	9795	9764	9753	9834	9815	9808	9841	9820	9812	9810	9789	9781
Δ Fuel (%) from Baseline	-	-0.5%	-0.8%	-0.9%	-1.2%	-1.5%	-1.6%	-0.8%	-1.0%	-1.0%	-0.7%	-0.9%	-1.0%	-1.0%	-1.2%	-1.3%
SOFC APU fuel burn (lbs)	0	77	77	77	143	143	143	77	77	77	79	79	79	106	106	106
SOFC CO emission (kg)	0	0.042	0.042	0.042	0.078	0.078	0.078	0.042	0.042	0.042	0.043	0.043	0.043	0.058	0.058	0.058
Main engine CO emission (kg)	2.70	2.67	2.66	2.66	2.63	2.62	2.62	2.66	2.66	2.65	2.66	2.66	2.65	2.65	2.64	2.64
Total CO emission (kg)	2.70	2.71	2.70	2.70	2.71	2.70	2.70	2.70	2.70	2.70	2.71	2.70	2.70	2.70	2.70	2.70
Delta CO (%) from Baseline	0.3%	0.0%	-0.1%	-0.1%	0.3%	0.0%	-0.1%	0.0%	-0.2%	-0.3%	0.1%	-0.1%	-0.2%	0.1%	-0.2%	-0.2%
Main engine NOx emission (kg)	45.05	44.84	44.70	44.65	44.52	44.38	44.33	44.70	44.61	44.58	44.73	44.64	44.60	44.59	44.50	44.46
Delta NOx (%) from Baseline	-	-0.5%	-0.8%	-0.9%	-1.2%	-1.5%	-1.6%	-0.8%	-1.0%	-1.0%	-0.7%	-0.9%	-1.0%	-1.0%	-1.2%	-1.3%
1,500 Nmi Mission minute=	204															
TOGW (lbs)	80269	81054	80651	80504	80964	80561	80417	80662	80415	80326	80757	80479	80379	80699	80421	80321
Block Fuel (lbs)	14381	14312	14266	14250	14209	14163	14146	14267	14239	14229	14278	14246	14235	14232	14200	14188
Δ Fuel (%) from Baseline	-	-0.5%	-0.8%	-0.9%	-1.2%	-1.5%	-1.6%	-0.8%	-1.0%	-1.1%	-0.7%	-0.9%	-1.0%	-1.0%	-1.3%	-1.3%
SOFC APU fuel burn (lbs)	0	115	115	115	215	215	215	115	115	115	118	118	118	159	159	159
SOFC CO emission (kg)	0	0.063	0.063	0.063	0.117	0.117	0.117	0.063	0.063	0.063	0.064	0.064	0.064	0.086	0.086	0.086
Main engine CO emission (kg)	3.92	3.87	3.86	3.85	3.82	3.80	3.80	3.86	3.85	3.85	3.86	3.85	3.85	3.84	3.83	3.83
Total CO emission (kg)	3.92	3.93	3.92	3.92	3.93	3.92	3.92	3.92	3.91	3.91	3.93	3.92	3.91	3.92	3.92	3.91
Delta CO (%) from Baseline	0.3%	0.0%	-0.1%	-0.1%	0.3%	0.0%	-0.1%	0.0%	-0.2%	-0.3%	0.1%	-0.1%	-0.2%	0.1%	-0.2%	-0.2%
Main engine NOx emission (kg)	65.37	65.05	64.85	64.77	64.59	64.38	64.30	64.85	64.72	64.68	64.90	64.75	64.70	64.69	64.55	64.49
Delta NOx (%) from Baseline	-	-0.5%	-0.8%	-0.9%	-1.2%	-1.5%	-1.6%	-0.8%	-1.0%	-1.1%	-0.7%	-0.9%	-1.0%	-1.0%	-1.3%	-1.3%

G05-377-99

The results of the Cruise emissions analysis showed that the estimated baseline NOx emission was ~25 to 65 kg, depending upon the range. Since NOx emissions from the SOFC APU are negligible, the estimated NOx emissions impact for the SOFC APU installation is the same as for the fuel burn, i.e., -0.4 to -1.6 percent (up to -1.0 kg out of 65 kg for 1,500 nmi range at Cruise). The baseline CO emissions were ~1.5 to 3.9 kg, depending upon the range. The estimated CO emissions impact was ±0.3 percent (<0.01 kg), depending upon the mission range and the SOFC APU design factors.

2.6.3.2 Landing and Takeoff (LTO) Cycle Emissions Analysis (Gate Operation Excluded)

Table 44 shows the Landing and Take Off (LTO) cycle parameters as specified by the Environmental Protection Agency (EPA) for aircraft emissions control, mainly from the main engine at ground level. Although the baseline gas turbine APU operation may vary with conditions and operators, the APU generally stays turned on to provide supplemental power.

Table 44. Landing and Takeoff (LTO) Cycle (EPA Definition).

LTO Cycle Phase	Takeoff	Climb	Approach	Taxi/Idle
Operating Time, min.	0.7	2.2	4.0	26.0
Percent Engine Thrust	100	85	30	7

Table 45 shows an operational data comparison of the baseline gas turbine APU and baseline turbofan main engines versus the SOFC APU during the LTO cycle as defined in Table 44. The impact of the SOFC APU installation was evaluated for each study Case and compared to the estimated baseline NOx and CO emissions. The analysis results showed that estimated baseline LTO cycle NOx emissions are ~4.92 kg (4.46 kg from the main engine, and 0.46 kg from the gas turbine APU). The estimated impact of the SOFC APU on LTO cycle NOx emissions can be ±3 percent (i.e., ±0.15 kg). The estimated baseline LTO cycle CO emissions are ~0.67 kg (0.27 kg from the main engine, and 0.4 kg from the gas turbine APU). The estimated impact of the SOFC APU on LTO cycle CO emissions can be -53 percent (-0.36 kg), mainly from diminished use of the gas turbine APU. These results do not include operation of the APU at the terminal gate.

Table 45. SOFC APU LTO Cycle Emissions Calculations (Gate Operation Excluded).

	Baseline Conventional APU + Main Engine	Fuel Cell APU System 1														
		Case 1			Case 2			Case 5			Case 6			Case 7		
Δ Fuel Burn (%) from Baseline		-1.2%			-1.9%			-1.2%			-1.2%			-1.5%		
Fuel Cell Power Density		0.56 kW/kg	1.0 kW/kg	1.4 kW/kg	0.56 kW/kg	1.0 kW/kg	1.4 kW/kg	0.56 kW/kg	1.0 kW/kg	1.4 kW/kg	0.56 kW/kg	1.0 kW/kg	1.4 kW/kg	0.56 kW/kg	1.0 kW/kg	1.4 kW/kg
APU System Weight (lbs)	240	1112	766	642	1151	805	681	775	563	487	857	618	532	857	618	532
SOFC APU Power (kw)		84.34	84.34	84.34	164	164	164	84.34	84.34	84.34	84.34	84.34	84.34	116	116	116
SOFC APU System Efficiency		0.32	0.32	0.32	0.35	0.35	0.35	0.32	0.32	0.32	0.32	0.32	0.32	0.323	0.323	0.323
Δ Weight (lbs) from Baseline	0	872	526	402	911	565	441	535	323	247	617	378	292	617	378	292
OWE (lbs)	47500	48372	48026	47902	48411	48065	47941	48035	47823	47747	48117	47878	47792	48117	47878	47792
MTOW (lbs)	80500	80500	80500	80500	80500	80500	80500	80500	80500	80500	80500	80500	80500	80500	80500	80500
Payload (86 pax) lbs	14620	14620	14620	14620	14620	14620	14620	14620	14620	14620	14620	14620	14620	14620	14620	14620
Max Useable Fuel (lbs)	19450	19450	19450	19450	19450	19450	19450	19450	19450	19450	19450	19450	19450	19450	19450	19450
LTO time, minute	32.9															
TOGW (lbs)	71483	72313	71939	71805	72288	71915	71781	71948	71719	71637	72037	71779	71686	72009	71750	71657
Main engine LTO fuel burn (lb)	981	1108	1091	1085	1071	1054	1048	1092	1081	1078	1096	1084	1080	1079	1067	1063
Main engine LTO CO emission (kg)	0.27	0.30	0.30	0.30	0.29	0.29	0.29	0.30	0.29	0.29	0.30	0.30	0.29	0.29	0.29	0.29
Main engine LTO NOx emission (kg)	4.46	5.04	4.96	4.93	4.87	4.79	4.76	4.96	4.91	4.90	4.98	4.93	4.91	4.90	4.85	4.83
RE220 LTO fuel burn (lb)	151															
RE220 LTO CO emission (kg)	0.40															
RE220 LTO NOx emission (kg)	0.46															
SOFC LTO fuel burn (lbs)	0	26.7	26.7	26.7	47.5	47.5	47.5	26.7	26.7	26.7	26.7	26.7	26.7	36.4	36.4	36.4
SOFC LTO CO emission (kg)	0	0.01	0.01	0.01	0.03	0.03	0.03	0.01	0.01	0.01	0.01	0.01	0.01	0.02	0.02	0.02
SOFC LTO NOx emission (kg)	0	1135	1118	1112	1119	1102	1096	1119	1108	1105	1123	1111	1107	1115	1103	1099
Total LTO Block Fuel (lbs)	1132															
Delta LTO Fuel (%) from Baseline		3	-14	-20	-13	-30	-36	-13	-24	-27	-9	-21	-25	-17	-29	-33
Delta LTO Fuel (%) from Baseline		0.2%	-1.3%	-1.8%	-1.2%	-2.7%	-3.2%	-1.2%	-2.1%	-2.4%	-0.8%	-1.9%	-2.2%	-1.5%	-2.5%	-2.9%
Total CO emission (kg)	0.67	0.32	0.31	0.31	0.32	0.31	0.31	0.31	0.31	0.31	0.31	0.31	0.31	0.31	0.31	0.31
Delta CO from Baseline (kg)		-0.35	-0.35	-0.36	-0.35	-0.35	-0.35	-0.35	-0.36	-0.36	-0.35	-0.36	-0.36	-0.35	-0.35	-0.36
Delta CO (%) from Baseline		-52.4%	-53.1%	-53.3%	-52.2%	-52.9%	-53.2%	-53.1%	-53.5%	-53.6%	-52.9%	-53.4%	-53.6%	-52.8%	-53.3%	-53.5%
Total NOx emission (kg)	4.92	5.04	4.96	4.93	4.87	4.79	4.76	4.96	4.91	4.90	4.98	4.93	4.91	4.90	4.85	4.83
Delta NOx emission (kg)		0.11	0.04	0.01	-0.05	-0.13	-0.16	0.04	-0.01	-0.02	0.06	0.01	-0.01	-0.02	-0.07	-0.09
Delta NOx (%) from Baseline		2.3%	0.8%	0.2%	-1.1%	-2.7%	-3.2%	0.8%	-0.2%	-0.5%	1.2%	0.1%	-0.3%	-0.4%	-1.5%	-1.8%

G05-377-100

2.6.3.3 On-Ground/Terminal Gate Emissions Analysis

Table 46 shows a comparison of SOFC APU versus baseline gas turbine APU fuel burn and NOx/CO emissions at different power settings and for different durations operating at the terminal/gate.

Table 46. SOFC APU On-Ground/Gate Emissions Calculations.

Operating Time at Gate >		Conventional APU				SOFC APU			
		60 min Operation							
Emissions, g/kg >				6.75	5.8			0	1.45
System	Power, kW	Fuel Flow		NOx	CO	Fuel Flow		NOx	CO
		lb	kg	kg	kg	lb	kg	kg	kg
Case 1	107.5	236	107	0.72	0.621	58	26	0	0.04
Case 2	107.5	236	107	0.72	0.621	58	26	0	0.04
Case 5	112.8	239	109	0.73	0.630	61	28	0	0.04
Case 6	86.3	24	102	0.69	0.591	50	23	0	0.03
Case 7	86.3	224	102	0.69	0.591	50	23	0	0.03
Case 1 and 2, Max.	185.0	278	126	0.85	0.733	94	43	0	0.06
Case 6 and 7, Max.	116.0	240	109	0.74	0.633	65	30	0	0.04
Operating Time at Gate >		30 min Operation							
Emissions, g/kg >				6.75	5.8			0	1.45
System	Power, kW	Fuel Flow		NOx	CO	Fuel Flow		NOx	CO
		lb	kg	kg	kg	lb	kg	kg	kg
Case 1	107.5	118	54	0.36	0.31	29	13	0	0.02
Case 2	107.5	118	54	0.36	0.31	29	13	0	0.02
Case 5	112.8	119	54	0.37	0.31	31	14	0	0.02
Case 6	86.3	112	54	0.34	0.31	25	11	0	0.02
Case 7	86.3	112	54	0.34	0.30	25	11	0	0.02
Case 1 and 2, Max.	185.0	139	63	0.43	0.30	47	21	0	0.02
Case 6 and 7, Max.	116.0	120	55	0.37	0.32	33	15	0	0.02
Operating Time at Gate >		10 min Operation							
Emissions, g/kg >				6.75	5.8			0	1.45
System	Power, kW	Fuel Flow		NOx	CO	Fuel Flow		NOx	CO
		lb	kg	kg	kg	lb	kg	kg	kg
Case 1	107.5	39	18	0.12	0.10	10	4	0	0.01
Case 2	107.5	39	18	0.12	0.10	10	4	0	0.01
Case 5	112.8	40	18	0.12	0.10	10	5	0	0.01
Case 6	86.3	37	17	0.11	0.10	8	4	0	0.01
Case 7	86.3	37	17	0.11	0.10	8	4	0	0.01
Case 1 and 2, Max.	185.0	46	21	0.14	0.12	16	7	0	0.01
Case 6 and 7, Max.	116.0	40	18	0.12	0.11	11	5	0	0.01

The estimated gas turbine NOx emissions values were based on an assumed value of 6.75 g/kg (of jet fuel), and CO emissions were based on 5.8 g/kg. The SOFC APU NOx emissions are negligible, and the CO emissions value is based on an assumed value of 1.45 g/kg. The analysis results show that the estimated baseline gas turbine APU NOx emission was ~0.7 to 0.9 kg operating for 1 hour on the ground, and ~0.11 to 0.14 kg operating for 10 minutes at the gate. The SOFC APU NOx emissions are practically negligible, and hence can achieve ~100 percent NOx reduction over the gas turbine APU ground/gate operation. The estimated baseline gas turbine APU CO emissions was ~0.60 to 0.75 kg operating for 1 hour on the ground, and ~0.10 to 0.12 kg operating for 10 minutes at the gate. The

estimated SOFC APU CO emissions was ~0.03 to 0.06 kg operating for 1 hour on the ground, and 0.005 to 0.010 kg operating for 10 minutes at the gate, achieving a possible 92 to 95 percent CO reduction for operation at the gate, if the thermal fatigue characteristic of the SOFC stack can be managed.

2.6.3.4 Landing and Takeoff (LTO) Cycle Emissions (Including 60 Minutes Gate Operation)

The data from Tables 45 and 46 are combined in Table 47, to evaluate the SOFC impact on LTO Cycle emissions including 60 minutes of APU operation at the terminal gate. The results show a possible 15 percent NO_x reduction (4.79 kg out of 5.64 kg), and 72.9 percent CO reduction (0.35 kg out of 1.29 kg) with main engine plus SOFC APU operation, compared to main engines plus baseline conventional APU operation.

Table 47. Landing and Takeoff (LTO) Cycle Emissions Including 60 Minutes Gate Operation.

Parameter	Units	Baseline	SOFC APU				
		Main Engines + Conv. APU	Case 1	Case 2	Case 5	Case 6	Case 7
Gate CO	kg	0.621	0.04	0.04	0.04	0.03	0.03
LTO + Gate CO	kg	1.29	0.35	0.35	0.35	0.34	0.34
Delta CO from Baseline	kg	---	-0.93	-0.93	-0.94	-0.95	-0.95
	%	---	-72.6%	-72.5%	-72.8%	-73.6%	-73.5%
Gate NO _x	kg	0.72	0.00	0.00	0.00	0.00	0.00
LTO + Gate NO _x	kg	5.64	4.96	4.79	4.91	4.93	4.85
Delta NO _x from Baseline	kg	---	-0.68	-0.85	-0.73	-0.71	-0.79
	%	---	-12.1%	-15.1%	-12.9%	-12.7%	-14.0%

2.7 Task 2.5 – Identification of Technology Gaps

This section of the report addresses the shortfalls and some of the possible aircraft level modifications for SOFC APU application in Regional Jet aircraft.

2.7.1 Desulfurization

Logistic fuels consumed by fuel cells need to be desulfurized at the refinery, onboard the aircraft, or at the airport. Onboard desulfurization adds considerable weight and complexity to the system and would require frequent maintenance. However, technologies are being developed which could make onboard desulfurization more practical. In addition, the development of more sulfur-tolerant reformers and anodes could significantly reduce the size of sulfur removal systems. The following paragraphs address some of the potential solutions to this issue.

Liquid Phase Sulfur Removal – Some notable low-temperature, low-pressure adsorbents are currently being developed by Song and coworkers at Penn State University^(11, 13, 14, 15) and by Yang and coworkers at the University of Michigan.^(29, 30) Cu(I)-exchanged zeolites developed by Yang and coworkers rely on selective thiophene π -complexation to the metals and have demonstrated one of the highest sulfur capacities of ~25 mg of S/g (~360 ppmw S jet fuel). However, Cu(I) disproportionates to Cu(0) and Cu(II) in the presence of air and/or high temperatures; therefore, high temperatures (~450°C) and long regeneration times (12 to 18 hrs) are required to promote autoreduction during regeneration. Ni(II)-

exchanged zeolites, which have lower sulfur capacities of ~9 mg S/g adsorbent, still require regeneration involving heating for 6 hrs at 350°C.

Unfortunately, the adsorbents that demonstrate relatively high capacities also tend to require long regeneration times. In addition, long residence times on the order of minutes to hours are required to reduce sulfur concentrations to acceptable levels (<10 ppm). To make onboard desulfurization more practical, the following issues need to be addressed:

- Long residence times
- Low sulfur capacities
- Long regeneration times
- Mass transfer limitations

Mesoscopic Devices, LLC has developed a continuously-regenerating sulfur removal system that overcomes problems associated with low sulfur capacity adsorbents.⁽³¹⁾ This system includes a liquid-phase adsorbent and compact hardware with a rotating valve mechanism that allows for frequent regeneration and constant fuel processing. Their ThioCycle-202™ adsorbent demonstrates low sulfur capacities (breakthrough capacity = 2.3 mg S/g, saturation capacity = 6.3 mg S/g) but has desirable regeneration properties (1 hr at 400°C in air). Mesoscopic claims that their system can treat 280 times more fuel (per system unit weight) when operated for ten hours a day over the course of a year in comparison to the best single-use adsorbents currently available. The development of a high-capacity *and* easily regenerable adsorbent would further reduce the weight and size of the system.

Gas Phase Sulfur Removal – Placing an H₂S adsorbent (at 250 to 600°C) onboard the aircraft would require heat exchangers for proper thermal integration with the reformer (~800°C) and the fuel stack (~800°C). Therefore, the development of high-temperature H₂S adsorbents which can eliminate the need for heavy heat exchangers would decrease the weight and complexity of the fuel processing system. Promising high-temperature H₂S adsorbents include metal oxides such as CeO_n and MnO; however, the technology needs to be further developed for commercial application.

Fractionation – The majority of sulfur contaminants in jet fuel are in the higher boiling point fractions.⁽³²⁾ Altex Technologies Corporation and Penn State University have developed a Logistic Fuel Preprocessor and Reformer (LFPPR), which includes a fractionator, organic sulfur trap, and pre-reformer.⁽³³⁾ They found that removing 30 percent of the heavy fractions from JP-8 reduced the sulfur level by 50 percent. In addition, a seven-fold increase in sulfur capacity was observed when desulfurizing the fractionated light JP-8 with a nickel-based adsorbent (in comparison with parent JP-8). The Altex processor includes a burner which consumes the high sulfur, heavy fractions to provide heat for the pre-reformer. Another option includes adding the heavy fractions back to the main fuel feed to be burned in the main engine. The effect of adding small amounts of high sulfur, high molecular weight fuel to the main engine feed will have to be investigated. In addition, it is uncertain whether the LFPPR designed by Altex to be used with a 20 W fuel cell system can be scaled up and how the system performs during transients.

Impact of Diesel Fuel Regulation on Jet Fuel Sulfur Level – While current EPA regulations require refiners to transition to ultra-low (<15 ppm) sulfur highway diesel fuels in 2006, there is currently no regulation that requires the reduction of jet fuel sulfur levels. Expectations are that jet fuel sulfur levels will be reduced in the future, and preliminary estimates indicate a corresponding 5 to 10 cents/gallon increase in fuel prices. The costs associated with desulfurization will need to be further investigated. In

addition, investigation of the potential impact that U.S. EPA and European Union (EU) diesel regulations will have on jet fuel sulfur levels is needed.

2.7.2 Reformer Technology

The size and weight of the reformer can be reduced by improving the catalyst and structured support. Reformation catalysts are typically supported on monolith structures; however, Precision Combustion, Inc. has developed a microlith-supported catalyst, which results in smaller reactors with increased power densities. In addition, catalysts with improved sulfur tolerance are being developed, so that sulfur-containing fuels, such as jet fuel, can be fed directly to the reformer.

2.7.3 Effects of Aircraft Attitude

It is known that various changes in aircraft attitude will be occurring during the times when the fuel cell APU system is required to operate. Taking typical APU specifications from the A330 and A340 commercial transport aircraft as a reference, each component of the fuel cell system can be evaluated individually. The baseline pitch (X) and roll (Y) values are defined as $X = +10$ to -23 degrees and $Y = \pm 15$ degrees, respectively.

In typical configurations, the fuel reformer itself will not be affected by changes in attitude, since the majority of the reformation reactions will occur in the vapor phase. However, it is possible that attitude changes may affect the fuel vaporization and/or reactions occurring at the inlet of the reformer. Fuel injection is being researched at the NASA Glenn Research Center to evaluate and improve injector/vaporizer performance.⁽³⁴⁾ Injector performance is crucial to obtaining proper fuel/H₂O vaporization and complete fuel/H₂/air mixing, which prevents coking and catalyst overheating (which can lead to sintering). The injector rig can also be used to investigate the effect(s) that spray characteristics may have on reformer performance. Similar experiments should be conducted under attitude changes to determine the effect(s) of pitch and roll on vaporization and/or reformation.

2.7.4 Combustion System Technology

Catalytic and non-catalytic combustors can provide the following benefits to a fuel cell system:

- Increase efficiencies by burning any unused hydrogen
- Provide heat during startup
- Reduce CO emissions.

During the present investigation, we investigated combustors which can oxidize both H₂ and CO while maintaining low NO_x emissions. One option involved feeding the combustor exit gases to a turbine and requires exit temperatures to be kept below 1,000°C. Process combustors with the following properties were investigated:

- Complete CO oxidation (with decreased size and weight)
- Complete H₂ oxidation (with decreased size and weight)
- Zero or minimal NO_x generation
- Temperature window of 800 to 1,000°C.

Investigation into the appropriate manner of addressing H₂/CO oxidation using a catalytic combustor with emphasis on the operating temperature, additional air input for maintaining combustor temperature and oxidant levels, and system specifics related to expected catalyst loading, cells per sq. inch and

monolith size and weight, were addressed. Technology gaps demonstrated by currently-available combustors were determined for further investigation.

2.7.5 Water Management and Utilization

The SOFC anode off-gas contains a steam/gas mixture at about 1,600°F. The amount of steam in the mixture is estimated to be 5 to 10 percent of the jet fuel mass flow rate. The steam or steam/gas mixture directly from the SOFC stack or further downstream, can be utilized for several purposes, depending on the need, preferences, and specific trade-off studies. However, lightweight, efficient water management technologies need to be further investigated to reduce the parasitic losses typically associated with water reclamation.⁽³⁵⁾ Potential water management technologies include adsorbent wheels, membrane humidifiers, porous metal foam humidifiers, and condensers.

Reformer Circulation – For aerospace applications, a CPOX reformer is desirable because of compactness and minimal water requirements. However, it is often beneficial to add water to the reformer feed to avoid coke formation and increase efficiencies (the heat generated by the exothermic CPOX reaction is used to drive endothermic steam reformation). Los Alamos National Laboratory and Delphi have investigated anode recycle gas as a method of providing water to the reformer.

Water/Steam Injection for Main Engine Emission Reduction – Steam exiting the SOFC anode can be mixed with jet fuel to reduce NO_x emission in the main engine combustion. A steam/fuel mixer would need to be designed to provide homogeneous steam/fuel mixture. The steam/fuel ratio and the mixture temperature would need to be further evaluated to avoid choking at the fuel nozzles. In case water is preferable over the use of steam, a condenser will be needed. The combustor fuel nozzles may also need to be redesigned for gas/liquid fuel atomization and vaporization. Although steam/fuel ratio may be small, sufficient margin from possible flameout should be evaluated and maintained.

Steam Injection for Main Engine Power Augmentation – Steam has a much higher density and specific heat than air (depending on temperature and pressure), and hence has much higher power density than air for thrust augmentation. Steam exiting the SOFC anode can be injected into the main engine, through the dilution zone of the combustor, for power/thrust augmentation. Improved steam manifold and injector designs will be needed to provide uniform injection through the combustor dilution holes. Injector stand-off distance from the dilution holes will need to be determined to also entrain sufficient dilution air into the dilution zone. The high-pressure (HP) turbine nozzle area will need to be adjusted to accommodate extra flow. The compressor will also need to be examined to ensure insignificant impact on stall margin.

ECS Heating – In an MEA architecture when the main engine bleed is not available, the steam exiting the SOFC anode can be used to augment the ECS heating system at altitude Cruise conditions. A steam/air heat exchanger will be needed.

Anti-Icing/De-Icing – Depending upon the amount of energy required, steam from the SOFC anode or steam/exhaust mixture from the SOFC APU system exhaust can be diverted to the aircraft empennage and vertical wing for anti-icing. The empennage and vertical wing will need to be designed as part of a heat exchanger. This design can also function as a condenser to recover water for drinking.

Drinking Water and Cleaning – Hydrogen-enriched water from SOFC through the empennage and vertical wing heat exchanger/condenser can pass through hydrogen separators, where a large percentage of the excess hydrogen can be removed. The hydrogen separators could consist of a matrix of silver-

palladium tubes, which have an affinity for hydrogen. The hydrogen could be directed into the catalytic burner, and the water passing through the hydrogen separators could then be stored in tanks for potable water. The water entering the tanks would be passed through a microbial filter that also adds iodine to the water. The water stored in the tanks can normally be used for drinking, but could also be used for flash evaporator cooling.

2.7.6 Stack Materials and Architectures

Significant research has been devoted to lowering SOFC stack operating temperatures in order to reduce the cost of materials and system components. However, the aerospace industry requires high power densities and optimized system integration, which might necessitate the use of high-temperature SOFCs. Therefore, while advances have been made towards low-temperature SOFCs, the aerospace industry may need to continue to focus on high-temperature SOFCs. This section highlights some developing technologies which have the potential to decrease stack weight, and/or improve stack performance and reliability. Of particular importance are stacks with compact, lightweight interconnects, seal materials which can tolerate the thermal stresses experienced during transient loads, and stacks which employ novel architectures and have the potential to increase power densities. In addition, technologies which improve system integration and reduce the weight of the balance-of-plant components should be further researched.

Direct Oxidation and Internal Reforming Solid Oxide Fuel Cells – Fuel cells that employ either direct oxidation or internal reforming have the potential to increase the power density of the system by eliminating or minimizing the need for a reformer. However, both technologies are still being developed and do not efficiently handle present logistic fuels.

Vohs and Gorte at the University of Pennsylvania have developed copper/ceria/YSZ anodes, which can be used for the direct oxidation of dry hydrocarbon fuels, and have licensed their technology to Franklin Fuel Cells.^(36, 37) Limited amounts of water may be available for an aircraft fuel cell APU; therefore, the fact that direct oxidation fuel cells can consume dry fuels is promising. Limited results have been reported for high molecular weight hydrocarbon fuels, and diffusion limitations are expected to be a problem with heavy hydrocarbon fuels. However, the technology is still being developed and should be further investigated for logistic fuels.

Significant research has been devoted to the development of anodes that can reform fuel internally; however, most of the research has been devoted to light hydrocarbon fuels, such as methane. Recently, Barnett and coworkers reported the development of an SOFC which can reform iso-octane and achieved single-cell power densities of 0.6 W/cm² at 770°C.⁽³⁸⁾ A porous ruthenium-ceramic (Ru-ceria)-based catalyst was layered on top of a conventional anode to reduce coking and produce stable cell operation. Problems with the system included diffusion-limited performance and stack cooling caused by endothermic steam reforming. This technology has not yet been proven with real fuel feeds.

Dynamic Shock and Low Cycle Fatigue (LCF)/Thermal Fatigue Characteristic – Current SOFC stack technology has low resilience to dynamic shock and has limited LCF life, estimated at <100 cycles. These characteristics of the SOFC stack may be applicable to land-based power plants delivering constant power for long durations, but would need much improvement for mobile/aircraft applications requiring shock resistance and LCF life on the order of 10,000 cycles minimum.

Interconnection Technology – Most fuel cell developers are focused on reducing the cost of fuel cell stacks to meet the DOE goals. Since high-temperature SOFCs require the use of expensive materials,

the trend has been towards developing medium-temperature SOFCs (650 to 800°C). At these lower temperatures, relatively inexpensive metallic alloy interconnects can be used. Unfortunately, these metal interconnects have so far been geared towards lowering costs rather than reducing size and weight.

Anode-supported SOFCs have thick Ni-YSZ anode layers to provide structural support and thick, heavy metal interconnects to deliver fuel and oxidant to the stack. The NASA Glenn Research Center has developed bi-electrode supported cells (BSCs), which use porous zirconia electrode scaffolds to direct the gas diffusion and permit the use of thin ceramic interconnects. This new BSC stack architecture has the potential to increase power densities by five-fold over anode-supported stacks, and allows for the rapid screening of new catalysts. Other technologies that minimize interconnect thickness and weight are also under investigation.

Seal Materials – Seal materials that can withstand the thermal fluctuations and vibration loads associated with transient operations, such as startup and shutdown, need to be investigated.

2.7.7 Air Management System Technology

Further studies into the air management systems for on-ground and in-flight operation should include the turbomachinery as well as positive-displacement blowers and compressors, most likely with variable geometric for a wider range of operations. In addition, interfacing and switching with existing aircraft air compression systems should be evaluated, which would include component designs for use of cabin air, air split from the ECS blower/compressor, as well as main engine bleed air sources.

Blower/Compressor Systems – Future research into aerospace quality turbomachinery or light-weight, positive-displacement-type blower and compressor designs should be considered. Mixed-flow, axial/centrifugal turbomachinery with variable geometry should be evaluated, capable of operating at long-range, sea level and in-flight conditions. Dual-spool or twin compressors in series may need to be considered. Certain advanced automotive-type design components may also be adopted and modified for aircraft applications.

Vehicle Compressed Air Interfaces – Air compression systems already existing in the aircraft should be utilized and/or re-designed to interface with the fuel cell air management system needs.

- **Cabin Air Re-Compression** – Cabin air feed to the SOFC should be carefully designed to avoid the possibility of back-flow. Re-compression of cabin air can increase SOFC stack and system performance, and can also reduce backflow uncertainty. A trade-off study should be conducted to balance the energy required to power the compressor, against the disadvantage of extra weight.
- **ECS Compressor** – Airflow from the ECS load compressor can be split to feed the SOFC system. However, Caution should be taken to ensure that sufficient air is retained for the cabin and passenger requirements. A separate blower will be needed to continue feeding the SOFC system while the aircraft is idling on ground with the ECS system shut off at night. Switching between the blower and ECS compressor should be scheduled.
- **Main Engine Bleed Air** – For a conventional, non-MEA architecture, the main engine bleed air can be directed to the SOFC system. Again, a separate blower will be needed to continue feeding the SOFC system while the aircraft is on ground, with the main engine(s) off. Switching between engine bleed air and the blower will need to be scheduled.

2.7.8 SOFC Technology Gaps and Road Map

The results of the present study have been combined to form a listing of Technology Gaps and a Technology Road Map, presented in Table 48.

Table 48. SOFC Technology Gaps and Technology Road Map.

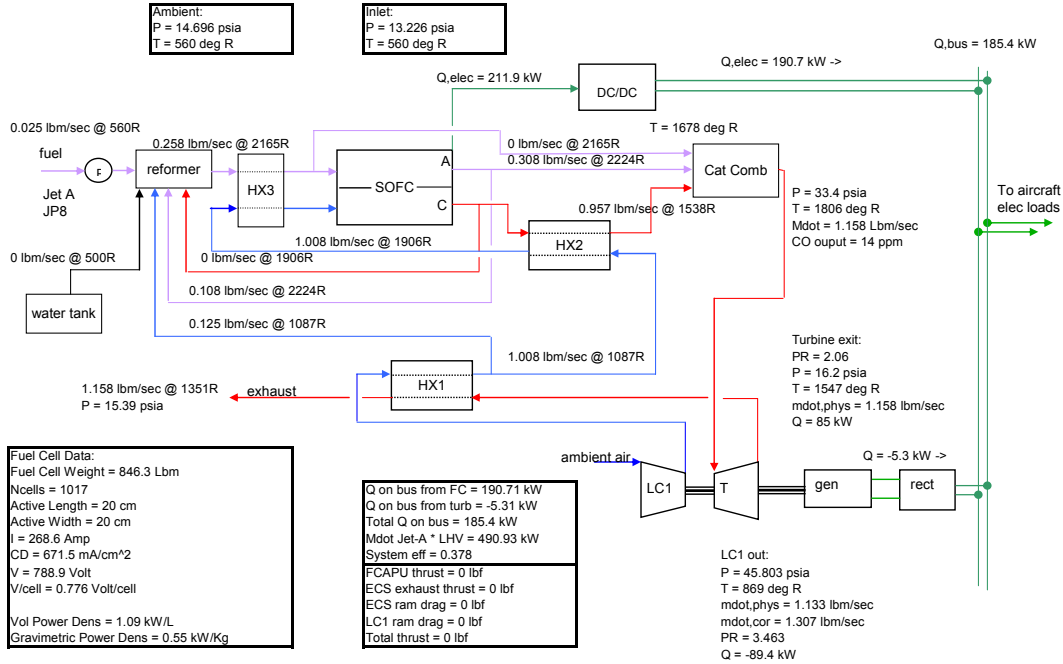
Technology	Shortfall	Mitigation	2010-2015 Requirement
Fuel Processing	Sulfur-laden fuels	Desulfurization	Sulfur levels <10 ppm
		Sulfur-tolerant reformer catalysts	Sulfur tolerance to 100 ppm Sulfur
	High Performance Reformer	Evolution of reformer catalysts	Low-temperature, high CO/H ₂ levels
	Water Recycle	Water separation technology development	Self-sustaining water feed
SOFC Stack	Interconnects	Development of stable, lightweight interconnects	2 W/L or 2 W/kg
	Direct Oxidation/Internal Reformation	Improved SOFC catalysts	Minimized or no reformer SOFC
	Sulfur Tolerance	Improved SOFC catalysts	100 ppm sulfur tolerant SOFC
	Sealing	Thermal stress tolerance	Sealing to handle thermal cycling
Water Management	Reformation Circulation	Improve circulation mechanism	Improved SOFC stack efficiency
	Main Engine Emission reduction	Develop water/steam injection technology	Lower NO _x from main engine
	Main Engine Power Augmentation	Develop steam injection technology	Higher main engine power
	ECS Heating	Integrate ECS with SOFC APU	Efficient ECS heating
	Anti-Icing	Develop aircraft empennage anti-icing and condenser technology	Anti-icing and water recovery
	Drinking and Cleaning	Develop aircraft empennage for steam condensing	Reduce water tank size and weight
Air Management	Low-flow high-pressure (HP) Compressor	Positive displacement type compressor at low power density	Low flow, HP, lightweight mixed-flow turbomachinery
	Main Engine/ECS Compression integration	Non-MEA with main engine bleed/ECS load compression	MEA with no main engine bleed/ECS load compression

APPENDIX A

SOFC APU CASE STUDY WITH INCREASED STACK FUEL UTILIZATION

In this additional case study, the assumed value for SOFC stack fuel utilization was increased from 70 to 85 percent to evaluate the impact of fuel utilization on system performance and weight. System 1, Case 2b was used for the sample study. Component performance parameters are shown in Figure 39.

System 1, Case 2b, Ambient Air, 5:1 Compr, Ground, 185.31 kW, MES Schematic



	Inlet			Exit		
	Mdot Lbm/sec	P psia	T R	Mdot Lbm/sec	P psia	T R
ambient	-	14.696	559.7	-	-	-
inlet	-	13.226	559.7	-	-	-
LC1	1.1326	13.226	559.7	1.1326	45.803	868.5
LC1 - bus power	-	-	-	-	-	-
LC2	0.0000	13.226	559.7	0.0000	57.270	931.6
LC2 - bus power	-	-	-	-	-	-
MES	1.6667	-	-	-	-	-
ECS	0.0000	-	-	-	-	-
HX1-cold side	1.1326	45.803	868.5	1.1326	43.513	1087.0
HX2-cold side	1.0081	43.513	1087.0	1.0081	41.337	1905.7
Jet A	0.0252	-	560.0	-	-	-
reformer	0.1245	41.337	1676.7	0.2577	41.007	2164.8
HX3-reformate	0.2577	41.007	2164.8	0.2577	38.956	1973.8
HX3-air	1.0081	41.337	1905.7	1.0081	39.270	1973.8
FC-anode	0.2577	38.956	1973.8	0.3084	37.008	2223.8
FC-cathode	1.0081	38.956	1973.8	0.9573	37.008	2223.8
FC -	-	-	2098.9	-	-	-
FC - bus power	-	-	-	-	-	-
HX2-hot side	0.9573	37.008	2223.8	0.9573	35.158	1538.5
cat comb	1.1578	35.158	1677.6	1.1578	33.400	1805.9
Turbine	1.1578	33.400	1805.9	1.1578	16.198	1547.3
LC1/Turbine Net	-	-	-	-	-	-
Gen/Motor bus power	-	-	-	-	-	-
HX1-hot side	1.1578	16.198	1547.3	1.1578	15.388	1351.0

(Note: Blocks shown with Blue or Brown highlighting indicate components nearing temperature limit.)

Figure 39. SOFC Performance Schematic with 0.85 Stack Fuel Utilization (System 1, Case 2b).

Table 49 shows the estimated SOFC APU system and component weight distribution based on the use of 85 percent fuel utilization and current technology 0.56 kW/kg SOFC stack power density. The results shown in Table 49 indicate that the stack-to-system weight ratio is increased from 68 percent with 70 percent fuel utilization to 70 percent with 85 percent fuel utilization.

Table 49. SOFC Mass and Volume With 0.85 Fuel Utilization for System 1, Case 2b.

Component	Volume (L)	Vol Fraction	Weight (Kg)	Wt Fraction
Compr./Turbine	129.63	0.313	35.83	0.065
HX1	3.87	0.009	13.61	0.025
HX2	12.00	0.029	22.06	0.040
Fuel pump	0.25	0.001	1.68	0.003
Reformer	20.58	0.050	6.86	0.012
HX3	3.61	0.009	7.37	0.013
Stack	195.04	0.471	383.81	0.697
DC/DC converter	20.48	0.049	15.36	0.028
Combustor	3.11	0.008	9.34	0.017
Generator/rectifier	3.03	0.007	10.50	0.019
Piping	22.30	0.054	44.10	0.080
Total	413.90	1.000	550.53	1.000

Table 50 compares the SOFC APU system performance with 85 percent fuel utilization vs. 70 percent fuel utilization, based on System 1, Case 2b. The results in the table show that the SOFC APU system performance is increased from 35 percent system efficiency with 70 percent fuel utilization to 38 percent system efficiency with 85 percent fuel utilization.

Table 51 compares the SOFC APU system weight, volume, power, and energy density with 85 percent fuel utilization versus 70 percent fuel utilization, based on System 1, Case 2b. The results in the table show that the total SOFC APU system power density stays essentially constant. The SOFC APU system weight increases by 3.7 to 5.4 percent, depending on the stack power density used.

Summary

The results of these comparisons show that an increase in SOFC stack fuel utilization from 70 to 85 percent could increase the SOFC APU system efficiency by ~3 percent (from 35 to 38 percent on the ground), but would also increase the SOFC APU system weight by 3.7 to 5.4 percent, depending on the stack power density.

Table 50. SOFC APU System Performance Comparison, 0.70 vs. 0.85 Fuel Utilization.

System 1, Case 2b, Ambient Air, 5:1 Compr, Ground, 185.31 kW, MES

Parameter Description	Uf = 0.85	Uf = 0.7
SOFC number of cells	1017	942
SOFC active area size (cm ²)	20 x 20	20 x 20
SOFC current demand (A)	268.6	268.6
SOFC volt/cell (V)	0.78	0.79
SOFC efficiency	0.69	0.69
SOFC power output on bus (kW)	190.7	179
SOFC operating temperature (°C)	892.9	915.4
SOFC inlet/exit dT (°C)	138.9	130.7
Reformer operating temperature (°C)	929.5	949.6
Anode recycle amount	0.35	0.35
Compressor PR	3.46	3.46
Compressor corrected flow (lbm/s)	1.31	1.23
Compressor efficiency	0.77	0.77
Turbine power output on bus (kW)	-5.31	6.34
Turbine PR	2.06	2.06
Turbine corrected flow (lbm/s)	0.95	0.96
Turbine efficiency	0.85	0.85
Total power on bus (kW)	185.4	185.4
Combustor operating temperature (°C)	730.1	872.4
Combustor CO output (ppm exhaust)	14	39
Combustor CO output (g/kg fuel)	0.60	1.54
Additional fuel to combustor	0.0	0
System efficiency	0.38	0.35
Net Thrust, aircraft basis (lbf)	0.0	0

Table 51. SOFC APU System Weight Comparison, 0.70 vs. 0.85 Fuel Utilization.

System 1, Case 2b, Ambient Air, 5:1 Compr, Ground, 185.31 kW, MES

SOFC Stack Anode Fuel Utilization, Uf	Uf = 0.85			Uf = 0.7		
	Std.	BSC-2	BSC-1	Std.	BSC-2	BSC-1
SOFC Stack Technology						
System total volume (L)	413.9	327.8	296.9	399.5	319.8	291.1
System total mass (kg)	550.5	381.1	320.2	522.2	365.3	308.9
SOFC volume (L)	195.0	109.0	78.0	180.7	100.9	72.3
SOFC mass (kg)	383.8	214.4	153.5	355.5	198.6	142.2
System volumetric energy density (kWh/L)	1.66	2.09	2.31	1.72	2.15	2.36
System gravimetric energy density (kWh/kg)	1.25	1.80	2.14	1.31	1.88	2.22
SOFC volumetric power density (kW/L)	1.09	1.94	2.72	1.1	1.97	2.75
SOFC gravimetric power density (kW/kg)	0.55	0.99	1.38	0.56	1	1.4
System volumetric power density (kW/L)	0.45	0.57	0.62	0.46	0.58	0.64
System gravimetric power density (kW/kg)	0.34	0.49	0.58	0.35	0.51	0.6

ABBREVIATIONS AND ACRONYMS

<u>Abbreviation</u>	<u>Definition</u>
A	Amperes
AC	Alternating Current
A/C	Aircraft
AFS	Honeywell Airframe Systems
APU	Auxiliary Power Unit
ATR	Auto Thermal Reforming
AZ	Arizona
BFL	Balanced Field Length (Runway Length Required for Takeoff)
BSC	Bi-Electrode Supported Cell
C	Carbon
CA	California
CAC	Cabin Air Conditioning
CACTCS	Cabin Air Conditioning and Thermal Control System
Cat	Catalyst
CEA	NASA Chemical Equilibrium Analysis Software
CH ₄	Hydrocarbons (Methane)
C/mol	Faraday's Number
cm ²	Centimeters Squared
CO	Carbon Monoxide
CO ₂	Carbon Dioxide
Comb	Combustor
Comp	Compressor
CPOX	Catalytic Partial Oxidation
CT	Connecticut
Cu	Copper
CuO	Copper Oxide
°C	Degrees Centigrade
DC	Direct Current
DC/DC	Direct Current to Direct Current Converter
degC	Degrees Centigrade
degF	Degrees Fahrenheit
deg R	Degrees Rankine
DOE	Department Of Energy
DOE-NETL	Department Of Energy – National Energy Technology Laboratory
dT	Differential Temperature

<u>Abbreviation</u>	<u>Definition</u>
ECS	Environmental Control System
Elec	Electrical
EMP	Electric Motor Pump
EPA	Environmental Protection Agency
Eq.	Equation
ESA	Honeywell Engine Systems & Accessories
ESS	Flight Essential
EU	European Union
Evap	Evaporator
FC	Fuel Cell
FCAPU	Fuel Cell Auxiliary Power Unit
FeO	Ferric Oxide
ft	Feet
ft/sec	Feet Per Second
°F	Degrees Fahrenheit
g	Grams
Gen	Generator
g/kg	Grams Per Kilogram
GRC	Glenn Research Center (Cleveland, Ohio)
GUI	Graphic User Interface
H ₂	Hydrogen
HDS	Hydrodesulfurization
H ₂ O	Water
HP	High Pressure
HPCA	High Pressure Cabin Air, High Pressure Compressor Axial
HPex	Horse Power Extraction
hrs	Hours
hrs:min	Hours and Minutes
H ₂ S	Hydrogen Sulfide
HX	Heat Exchanger
IFR	Instrument Flight Rules
IL	Illinois
Inv	Inverter
Jet-A	Aircraft Fuel
JP	Jet Petroleum
JP-8	Jet Petroleum Grade 8

Abbreviation**Definition**

K	Kelvin, Kilo, Knots
KCAS	Knots Compensated Air Speed
Kft	Thousands of Feet Altitude
kg	Kilograms
kJ	KiloJoules
KTAS	Knots True Air Speed
kVA	KiloVolt-Amperes
kW	KiloWatts
kWh	KiloWatt-Hours
kW-Hr	KiloWatt-Hours
kWh/kg	KiloWatt-Hours per Kilogram
kWh/L	KiloWatt-Hours per Liter
kW/kg	KiloWatts per Kilogram
kW/L	KiloWatts per Liter
L	Liters
lb	Pounds
lbf	Pounds of Force
lb-ft	Foot-Pounds (Torque)
lbm	Pounds Mass
lb/min	Pounds Per Minute
lbm/s	Pounds Mass Per Second
lbs	Pounds
lb/s, lb/sec	Pounds Per Second
LC	Load Compressor
LCF	Low Cycle Fatigue
L/D	Lift Over Drag
LFPPR	Logistic Fuel Preprocessor and Reformer
LHS	Left Hand Side
LHV	Lower Heating Value
L/kW	Liters per Kilowatt
LP	Low Pressure
LTO	Landing And Takeoff
L x W	Length Times Width
mA/cm ²	Current Density (milliAmperes per cubic centimeter)
max	Maximum
MCL	Maximum Climb Level
Mdot	Mass Flow Rate
MEA	More-Electric Aircraft
MES	Main Engine Start
mg	Milligrams

<u>Abbreviation</u>	<u>Definition</u>
min	Minutes, Minimum
Mn	Mach Number
MnO	Manganese Oxide
mol	Mole, Unit Measure of Molecular Weight
MTOGW	Maximum Takeoff Gross Weight
N ₂	Nitrogen
NASA	National Aeronautics and Space Administration
NASA-GRC	National Aeronautics and Space Administration – Glenn Research Center (Cleveland, Ohio)
NETL	Department Of Energy – National Energy Technology Laboratory
NFCRC	National Fuel Cell Research Center (Irvine, California)
Ni-YSZ	Nickel-Yttria-Stabilized Zirconia (Ceramic Material)
NJ	New Jersey
nmi	Nautical Miles
Non-ESS	Non-Flight Essential
NOx	Nitrogen Oxides
O ₂	Oxygen
OBIGG	On-Board Inert Gas Generator
OEM	Original Equipment Manufacturer
OH	Ohio
Ops	Operations
OWE	Overall Weight, Empty
P	Pressure
PADT	Phoenix Analysis and Design Technologies (Phoenix, Arizona)
Pamb	Ambient Pressure
PAX	Passengers
PCI	Precision Combustion, Inc. (North Haven, Connecticut)
Pd	Palladium
PEM	Proton Exchange Membrane
PEMFC	PEM Fuel Cell
ppb	Parts Per Billion
ppm	Parts Per Million
ppmw	Parts Per Million, Weight
poly	Polytropic
POX	Partial Oxidation

<u>Abbreviation</u>	<u>Definition</u>
PR	Pressure Ratio
PROX	Preferential Oxidation
PSE	Honeywell Propulsion Systems Enterprise (Phoenix, Arizona)
psia	Pounds Per Square Inch, Absolute (Pressure)
psig	Pounds Per Square Inch, Gage (Pressure)
Pt	Platinum
pwr	Power
P/W	Power-to-Weight Ratio
R	Rankine
RASER	Revolutionary Aero Space Engine Research
Rect	Rectifier
ref	Reference
req'd	Required
Rh	Rhenium
RHS	Right Hand Side
SAE	Society of Automotive Engineers
sec	Seconds
SFC	Specific Fuel Consumption
S/ads	Sulfur, Per Unit of Adsorbent
S/g	Sulfur, Per Gram
SL	Sea Level
SOFC	Solid Oxide Fuel Cell
SO _x	Sulfur Oxides
SR	Steam Reforming
SSPC	Solid State Power Control
STC	System Transfer Control
S-Zorb	ConocoPhillips Proprietary Desulfurization Process
T	Temperature
temp	Temperature
TIT	Turbine Inlet Temperature
TKO	TakeOff
TOGW	Takeoff Gross Weight
TSFC	Thrust Specific Fuel Consumption
TT2	Inlet Total Temperature
Turb	Turbine
T4.1	Turbine Rotor Inlet Temperature

<u>Abbreviation</u>	<u>Definition</u>
U.S.	United States
V	Volts
VAC	Volts Alternating Current
Vdc	Volts Direct Current
VI	Value Index
Vol	Volume
V/cell	Volts Per Cell
W	Watts
Wb	Bleed Flow
W/C	Steam-to-Carbon Ratio
WGS	Water Gas Shift
Wt	Weight
Wt%	Weight Percent
X	Pitch, Degrees
Y	Roll, Degrees
YSZ	Yttria-Stabilized Zirconia
ZnO	Zinc Oxide

REFERENCES

- 1) Brouwer, Jacob, Private communication, National Fuel Cell Research Center (NFCRC), University of California-Irvine, Irvine, CA.
- (2) Fuel Cell Handbook, E G & G Technical Services, Inc., 7th ed., 2004, p. 5. [Available on line from Dept. of Energy at URL: <http://www.osti.gov/bridge/servlets/purl/834188-H0AaAO/native/834188.pdf>]
- (3) *ibid*, pp. 7 to 9.
- (4) JANAF Thermochemical Tables, The Thermal Research Laboratory, Dow Chemical Company, 1971.
- (5) Incropera, Frank P., and Dewitt, David P., Fundamentals of Heat and Mass Transfer, Wiley NYC, 3rd Ed. (1990), pp. 543-548.
- (6) Kreith, Frank, Principles of Heat Transfer, Scranton Intl. Textbook Co. 2nd Ed., (1965) p.497.
- (7) Veyo, S.E., “Evaluation of Fuel Impurity Effects on Solid Oxide Fuel Cell Performance.” U.S. Department of Energy, Pittsburgh, PA. 1998.
- (8) Matsuzaki, Y.; and Yasuda, I., “The Poisoning Effect Of Sulfur-Containing Impurity Gas on a SOFC Anode: Part I. Dependence on Temperature, Time, And Impurity Concentration.” Solid State Ionics 2000, **132**, pp. 261-269.
- (9) Siriwardane, R.V.; Cicero, D.C.; Jain, S.; Gupta, R.P.; and Turk, B.S., “Durable ZincOxide-Based Regenerable Sorbents For Desulfurization of syngas in a Fixed-Bed Reactor.” Proceedings of the 5th International Symposium on Gas Cleaning at High Temperature, Morgantown, WV, September 17-20, 2002.
- (10) Edwards, T., “System Drivers for High Heat Sink Fuels.” Prepr. Pap. –Am. Chem. Soc., Div. Petro. Chem. 2000, **45**, pp. 436-439.
- (11) Velu, S.; Ma, X.; and Song, C., “Selective Adsorption for Removing Sulfur from Jet Fuel over Zeolite-Based Adsorbents.” Ind. Eng. Chem. Res. 2003, **42**, pp. 5293-5304.
- (12) Gislason, J., “Phillips Sulfur-Removal Process Nears Commercialization.” Oil Gas J. 2001, **72**.
- (13) Song, C., “Fuel Processing For Low-Temperature And High-Temperature Fuel Cells Challenges, And Opportunities For Sustainable Development In The 21st Century.” Catal. Today 2002, **77**, pp. 17-49.
- (14) Velu, S.; Ma, X.; and Song, C., “Selective Adsorption for Removing Sulfur from Jet Fuel over Zeolite-Based Adsorbents.” Ind. Eng. Chem. Res. 2003, **42**, pp. 5293-5304.
- (15) Watanabe, S.; Ma, X.; and Song, C., “Selective Sulfur Removal from Liquid Hydrocarbons over Regenerable CeOTiO₂ Adsorbents for Fuel Cell Applications.” Prepr. Pap. – Am. Chem. Soc., Div. Fuel Chem. 2004, **49**, pp. 511-513.

- (16) Slimane, R. B.; and Abbasian, J., "Copper-Based Sorbents for Coal Gas Desulfurization at Moderate Temperatures." Ind. Eng. Chem. Res. 2000, **39**, pp. 1338-1344.
- (17) Carnell, P. J. H., "Feedstock Purification." In Catalyst Handbook, 2; Twigg, M. V., Ed.; Manson Publishing Ltd: London, 1996; pp 191-224.
- (18) Myers, D.; Krause, T.; Bae, J. -M.; and Pereira, C., "Reducing The Volume And Weight Of The Fuel Post Processor For Polymer Electrolyte Fuel Cell Power Systems." Conference Paper 2000.
- (19) Babich, I. V.; and Moulijn, J. A., "Science And Technology Of Novel Processes For Deep Desulfurization Of Oil Refinery Streams: A Review." Fuel 2003, **82**, pp. 607-631.
- (20) Shore, L.; and Farrauto, L., U.S. Patent No. 6,541,419, "Process For Reduction Of Gaseous Sulfur Compounds." April 1, 2003.
- (21) Farrauto, R.; Hwang, S.; Shore, L.; Ruettinger, W.; Lampert, J.; Giroux, T.; Liu, Y.; and Ilinich, O., "New Material Needs for Hydrocarbon Fuel Processing: Generating Hydrogen for the PEM Fuel Cell." Annu. Rev. Mater. Res. 2003, **33**, pp. 1-27.
- (22) Slimane, R. B.; and Abbasian, J., "Copper-Based Sorbents for Coal Gas Desulfurization at Moderate Temperatures." Ind. Eng. Chem. Res. 2000, **39**, pp. 1338-1344.
- (23) Carnell, P. J. H., "Feedstock Purification." In Catalyst Handbook, 2; Twigg, M. V., Ed.; Manson Publishing Ltd: London, 1996; pp 191-224.
- (24) Borup, R.; Perry, L.; Inbody, M.; and Tafoya, J., "Fuel Processing For Fuel Cells: Fuel Effects On Fuel Processor Durability And Carbon Formation." Prepr. Pap. – Am. Chem. Soc., Div. Fuel Chem. 2002, **47**, pp. 547-548.
- (25) *ibid*, Ref. (2).
- (26) Tornabene, R.; Wang, W.-Y.; Steffen, C.J.; and Freeh, Joshua E., "Development of Parametric Mass and Volume Models for an Aerospace SOFC/Gas Turbine Hybrid System." Paper No. GT2005-68334, ASME TurboExpo 2005. NASA Glenn Research Center, Cleveland, OH, May 2004.
- (27) NASA Chemical Equilibrium Analysis (CEA) software program.
- (28) Quader, A. A.; Kirwan, J. E.; and Grieve, M. J., "Engine Performance and Emissions Near the Dilute Limit with Hydrogen Enrichment Using an On-Board Reforming Strategy." SAE Technical Paper Series (2003-01-1356) 2003.
- (29) Hernández-Maldonado, A. J.; and Yang, R. T., "Desulfurization of Diesel Fuels via π -Complexation with Ni(II)-Exchanged X- and Y- Zeolites." Ind. Eng. Chem. Res. 2004, **43**, pp. 1081-1089.
- (30) Hernández-Maldonado, A. J.; and Yang, R. T., "Desulfurization of Liquid Fuels by Adsorption via π Complexation with Cu(I)-Y and Ag-Y Zeolites." Ind. Eng. Chem. Res. 2003, **42**, pp. 123-129.
- (31) Poshusta, J.; Stevens, T.; Schneider, E.; and Kulprathipanja, A. "On-Board Desulfurization of High Sulfur Fuels." 2004 Fuel Cell Seminar Abstracts.

- (32) Samsun, R. C.; Pasel, J.; Peters, R.; Schmitt, D.; Tschauder, A.; and Stolten, D., “Autothermal Reforming of Kerosene for Application in Aviation.” 2004 Fuel Cell Seminar Abstracts.
- (33) Namazian, M.; Sethuraman, S.; Elder, W. E.; Venkataraman, G.; Wan, W.; Kelly, J.; Ma, X.; Subramani, V.; Strohm, J.; and Song, C., “Diesel and Jet Fuel Desulfurization and Reforming for Fuel Cell Applications.” 2004 Fuel Cell Seminar Abstracts.
- (34) Lee, C-M.; Tomsik, T. M.; Yen, C. H.; Tacina, R. R.; Hicks, Y. R. Hicks; and Surgenor, A. D., “Fuel Processing for Fuel Cell Applications in Air Vehicles.” 2004 Fuel Cell Seminar Abstracts.
- (35) Liu, C., “Development of Thermal and Water Management System for PEM Fuel Cells.” DOE Hydrogen Program Progress Report 2004, pp. 520-524.
- (36) Gorte, R. J.; and Vohs, J. M., “Novel SOFC Anodes For The Direct Electrochemical Oxidation Of Hydrocarbons.” J. Catal. 2003, **216**, pp. 477-486.
- (37) McIntosh, S.; and Gorte, R. J., “Direct Hydrocarbon Solid Oxide Fuel Cells.” Chem. Rev. 2004, **104**, pp. 4845-4865.
- (38) Zhan, Z.; and Barnett, S. A., “An Octane-Fueled Solid Oxide Fuel Cell.” Sciencexpress 2005.

REPORT DOCUMENTATION PAGE

Form Approved
OMB No. 0704-0188

Public reporting burden for this collection of information is estimated to average 1 hour per response, including the time for reviewing instructions, searching existing data sources, gathering and maintaining the data needed, and completing and reviewing the collection of information. Send comments regarding this burden estimate or any other aspect of this collection of information, including suggestions for reducing this burden, to Washington Headquarters Services, Directorate for Information Operations and Reports, 1215 Jefferson Davis Highway, Suite 1204, Arlington, VA 22202-4302, and to the Office of Management and Budget, Paperwork Reduction Project (0704-0188), Washington, DC 20503.

1. AGENCY USE ONLY (<i>Leave blank</i>)	2. REPORT DATE February 2007	3. REPORT TYPE AND DATES COVERED Final Contractor Report	
4. TITLE AND SUBTITLE Fuel Cell Auxiliary Power Study Volume 1: RASER Task Order 5		5. FUNDING NUMBERS WBS 561581.02.08.03.06.01 NAS3-01136	
6. AUTHOR(S) Audie Mak and John Meier			
7. PERFORMING ORGANIZATION NAME(S) AND ADDRESS(ES) Honeywell Engines, Systems & Services P.O. Box 52180 Phoenix, Arizona 85072		8. PERFORMING ORGANIZATION REPORT NUMBER E-15725	
9. SPONSORING/MONITORING AGENCY NAME(S) AND ADDRESS(ES) National Aeronautics and Space Administration Washington, DC 20546-0001		10. SPONSORING/MONITORING AGENCY REPORT NUMBER NASA CR-2007-214461-VOL1 21-13153	
11. SUPPLEMENTARY NOTES Project manager, Lisa Kohout, Power and Electrical Propulsion Division, NASA Glenn Research Center, organization code RPC, 216-433-8004.			
12a. DISTRIBUTION/AVAILABILITY STATEMENT Unclassified - Unlimited Subject Category: 07 Available electronically at http://gltrs.grc.nasa.gov This publication is available from the NASA Center for AeroSpace Information, 301-621-0390.		12b. DISTRIBUTION CODE	
13. ABSTRACT (<i>Maximum 200 words</i>) This study evaluated the feasibility of a hybrid solid oxide fuel cell (SOFC) auxiliary power unit (APU) and the impact in a 90-passenger More-Electric Regional Jet application. The study established realistic hybrid SOFC APU system weight and system efficiencies, and evaluated the impact on the aircraft total weight, fuel burn, and emissions from the main engine and the APU during cruise, landing and take-off (LTO) cycle, and at the gate. Although the SOFC APU may be heavier than the current conventional APU, its weight disadvantage can be offset by fuel savings in the higher SOFC APU system efficiencies against the main engine bleed and extraction during cruise. The higher SOFC APU system efficiency compared to the conventional APU on the ground can also provide considerable fuel saving and emissions reduction, particularly at the gate, but is limited by the fuel cell stack thermal fatigue characteristic.			
14. SUBJECT TERMS Auxiliary power unit; Auxiliary power system; Fuel cells; Hybrid fuel cell; Solid oxide fuel cell		15. NUMBER OF PAGES 159	
		16. PRICE CODE	
17. SECURITY CLASSIFICATION OF REPORT Unclassified	18. SECURITY CLASSIFICATION OF THIS PAGE Unclassified	19. SECURITY CLASSIFICATION OF ABSTRACT Unclassified	20. LIMITATION OF ABSTRACT

